University of Verona

Department of Biotechnology
School of Natural Science and Engineering
PhD in Biotechnology
XXXV cycle

PhD Thesis

Exploring the Genetic Determinants of Grapevine Phenology and QTL Identification in *Vitis vinifera* through Interval Mapping

SSD: AGR/03

Coordinator: Prof. Matteo Ballottari

Tutor: Prof. Giovanni Battista Tornielli

Doctoral Student: Tahir Mujtaba

Contents

ACKNOWLEDGMENT

I would like to express my warmest gratitude to my supervisor **Prof. Giovanni Battista Tornielli** for proposing and supervising me for this project, his support, timely guidance and helpful criticism concerning the setting up the project plan, phenological studies, results, presentations and the manuscript. I am very much thankful to him for his informative, enjoyable and fruitful discussions, also for the productive group meetings providing a nice platform for helpful discussions and sharing different ideas. Being a humble and kind person his contribution is highly obliged.

To **Prof. Diana Bellin**, for additional support and help as a co-supervisor, in understanding and applying the Bioinformatics tools for QTL analysis, for supporting me with setting the project targets, discussing strategies and results and for thoroughly reading and commenting the manuscript. Also, I would like to thank her for her patience, for enlightening explanations, interesting and amusing discussions, which encouraged me to complete this project.

To **Franco Rockel** for his valuable addition in making this work done and making a memorable work experience and stay at JKI, Germany.

To Martina Marini and Ron Shmuleviz for being wonderful coworkers, managing, updating and analyzing phenotypic data, making it available for everyone in the group.

To Salam, for informative discussions on R (statistical program language) related problems, solutions and all the motivation towards computational world.

To Mian and Faheem for providing valuable insights for understanding QTLs studies and insightful discussions.

To my grandparents and parents who passed their passion to me. Thank you all for always being there for me.

To my wife whose sacrifice and patience was immense during this journey, her support had a major contribution in achieving this milestone.

Finally, I would also like to pass my gratitude to the University of Verona for offering such a fantastic degree program and to all those who made a memorable stay at Verona.

Tahir Mujtaba
03-07-2023

SUMMARY

Grapevine (Vitis spp.) is a major crop, which has a worldwide high socioeconomic importance in viticulture, especially for its contribution in the production of high quality grape and wine. Grapevine production has greatly been influenced by changing climate. Recent research on grapevine phenology has revealed the adverse impact of environment on its phenology, in turn affecting the quality of wines. An alteration in grape berry composition due to annual anticipation in phenological growth is a clear display of such constraints. High temperature affects biochemical nature of the berries at harvest, ultimately altering the wine quality. Since yield and quality greatly depend on the GxE interaction, the development of effective strategies to introduce new characteristics and prevent negative environmental effects is thus indispensable. Although environmental effects on grapevine physiology have been studied over recent years, the genetic mechanism controlling such modifications is still unknown. Acclimatization of local grape varieties to the changing climates has attracted plant breeders to shift research focus to improve its adaptability in diverse environmental conditions. Corvina, a local (Verona's region, Italy) red grape berry variety, has been grown in a specific viticultural area called Valpolicella, famous for its wine brands viz., Amarone and Valpolicella. On account of annual losses and aiming at producing better wine quality, scientists have been trying to exploit Corvina to spell out genetic determinants controlling its phenology particularly the veraison time. Such attempts will highlight the possibilities to develop new cultivars with relatively improved traits, enhanced yield and better adaptability against diverse environment. Harboring genes from additive to complete dominance effects the genomic segments controlling phenology should however be studied to identify the effects expressed in phenological traits through QTL analysis. The current study has been aimed to identify such genes putatively involved in controlling grapevine phenological traits, the veraison time in particular. Such genes might then be utilized by plant breeders to develop local grape cultivar with improved traits under different climatic zones. In this study, a cross population (CP-F1), raised by a cross between local disease susceptible variety "Corvina" and a divergent disease resistant variety "Solaris", has been exploited by QTL analysis, to detect the candidate genes controlling grape phenology. The cross genotypes were analyzed by QTL mapping technique based on both phenotypic (data from phenological traits) and genotypic data (SNP markers) derived from the analysis of the bi-parental segregating population propagated in three replicates at two separate locations. Phenotypic data for four traits (budburst, flowering, veraison and

ripening) were collected for three years from 1st location (Verona) and for two years from 2nd location (Negrar). The genotypic data (SNPs) were collected from *Vitis*18KSNP ChiP hybridization assay. The consensus genetic maps were developed by using an R statistical programming software ("OneMap"). The statistical association between phenotypes and molecular marker's data was measured by anchoring the genomic data against grapevine genome assembly (12XV2), and analyzed through another software "MapQTL V5" to determine the genetic segments involved in variation of such complex traits.

In the current study, a QTL analysis conducted on CxS cross population revealed identification of a total number of 12 QTLs both for budburst and flowering, 22 QTLs for veraison and 13 QTLs for ripening stage. Moreover, putatively two new QTLs have been identified for veraison on chromosome 1 lying on position 48.71 cM with LOD threshold value of 3.59, consisting of 496 genes in the confidence interval and a QTL on chromosome 6 at a position 6.54 cM with 301 genes falling in the confidence interval.

ABSTRACT

Long-term studies on grapevine phenology have clearly demonstrated the anticipated phenological events due to gradual global warming, affecting the grape yield and wine quality. Adaptation of local grape varieties to changing climatic conditions is thus a major breeding target, which includes the selection of late ripening varieties/clones, whose bunches may escape the warmer summer condition by postponing the ripening period. However, assessment of the genetic basis of phenology and quality related traits is a prerequisite to develop effective breeding programs for grapevine varieties adapted for the cultivation in specific viticultural areas and to identify the candidate genes for the new breeding approaches. Grapevine phenological traits show complex quantitative inheritance. The potential genes with additive effects are mapped through QTL mapping approaches, to dissect the genomic regions harboring such QTLs to further explain the genetic basis of quantitative variation. For this purpose, we have evaluated a population from the cross between the locally (Verona province, Italy) grown grapevine variety "Corvina" and another variety viz. "Solaris", highly divergent for their phenology and fruit ripening traits. Seedlings were developed, propagated and grown in field conditions to be evaluated for mapping of genetic traits. High throughput SNP genotyping of the cross population was applied through hybridization to an Illumina *Vitis*18KSNP chip. The phenotypic data, collected over three seasons included the determination of the main phenological stages (budbreak, flowering, veraison) together with the assessment of some morphological and quality traits at harvest on all progenies with the final purpose of QTL mapping. The results from QTL analysis revealed genetic determinants putatively involved in controlling grapevine phenology. Derived markers, in future, will not only help grapevine breeders to further understand the genetic control of phenology and quality related traits but also guide to regulate /incorporate desired traits in future selections.

1 INTRODUCTION

1.1 Grapevine: A Brief History

Cultivation of wild plants in agriculture has been dated back to Neolithic Revolution. This period of domestication is characterized by the transition of various human cultures from a lifestyle of hunting to settlement, enabling the masses to a large population to live (Bocquet-Appel JP 2011). These settlements allowed humans to experiment with plants, leading to learn, grow, develop and initiate the process of plant domestication (Pollard et al., 2015; Lewin, 2009). Down the ages, nature has brought a huge plant diversity on account of genetic variability in plants, which has been improved by mutations and simultaneous selective breeding. Ultimately, selective crossing of wild species helped developing plant varieties with improved phenotypic traits as compared to their wild ancestors. Likewise, domestication of grapevine began with the birth of agriculture.

The first domestication of grapevine reportedly took place approximately 6000-5500 BCE in the area comprising the Caucasus (Iran and Anatolia) region, further spreading to Mesopotamia, Egypt, then to Italy and Iberian Peninsula and ultimately to the western areas (Limier et al., 2018). Genus *Vitis* has reportedly been originated form 3 different places viz., North America, Est Asia and Euro-Asian center of origin, however among various species from these origins, only *Vitis vinifera* has been truly domesticated. The grapevine (*Vitis vinifera L.*) is considered to be the most ancient and symptomatic perennial crops from the family *Vitaceae*. Its domestication has been attributed both with vine growing and wine making (Limier et al., 2018).

Grapevine (*Vitis vinifera*) has further been distinguished by two sub-species viz., the wild grape (*Vitis vinifera* L. subsp. *sylvestris*) and the cultivated-domesticated grapevine (*Vitis vinifera* L. subsp. *Vinifera*). The former grows occasionally over a large area spreading from south of Caspian sea to the Atlantic coast of Europe (Limier et al., 2018; Arnold et al., 1998). It is reproduced through vegetative and sexual reproduction however the wild grape is considered as vulnerable to pathogenic attack. The latter (*Vitis vinifera L. subsp. vinifera*) evolved through domesticating the wild grape species, and is highlighted by its phenotypes especially through seed, flower and fruit (Limier et al., 2018 and This et al., 2006). Roughly, more than 6000 grape varieties, both as table and wine grapes, are domesticated and roughly 400 out of 6000 domesticated grape varieties, are of economic importance (Galet, 2000). It is characterized by varying fruit shapes, color, flavor and the possibility of vegetative propagation. On the other hand

most of the American and Asian grapevine species are less suitable for winemaking, rather showing a particular aptitude for resistance to cold and diseases such as downy mildew, powdery mildew, botrytis and phylloxera. It is worth knowing that some of the wild species lost partial resistance during the course of domestication process, mainly due to their preferred selection for their appealing oenological characteristics while compromising their characteristics for harboring resistance.

1.2 Grapevine: Fruit Development and Ripening Process

Grapevine (*Vitis vinifera* L.), being one of the major woody perennial fruit crops, is cultivated worldwide, especially in central and southern Europe. Its economic importance is valued by many countries where, its fruit has been consumed as table grape, raisins and wine (Delfino et al., 2019). With the biennial reproductive cycle (bud formation in first and fruit formation in second year), the development of grapevine encompasses many phenological phases (described by the widely adopted BBCH and modified E-L classification systems), the most relevant being budburst (vegetative growth initiation), flowering (flower disclosure), veraison (onset of berry ripening) and full ripening (berry reaching final quality traits). Prior to the harvesting phase, grapevine berries develop from being smaller in size to large, become softer and less acidic and accumulate sugars and aroma compounds. These developmental changes are the key determinants of wine quality (Conde et al., 2007). The grapevine annual growth cycle is characterized by two phases, i.e., an active growth phase (spring to fall) and a dormant phase (winter). During fall, grapevine plants acclimatize to freezing temperature for their survival during winter time, whereas at the beginning of spring the dormancy is released as day length and temperature gradually increases, which initiates budbreak and shoot growth. Few weeks after the budbreak, the small inflorescences become visible, and flowers, initially grouped in clusters gradually develop and separate to individual flowers. Flower formation and blooming is followed by pollination and fertilization (cleistogamy can take place in most cultivated varieties) after which the fruit set occurs and the process of berry development is initiated.

Berry development completes in three phases. Phase I starts at bloom and last roughly for 60 days. During phase I the berries undergo the process of rapid cell division and enlargement. The volume of the berry is expanded with the accumulation of water, tartaric and malic acids and other solutes. Tartaric and malic provide acidity for winemaking. Other important components of

the first berry developmental phase include phenolic acids and pro-anthocyanidins, also known as tannins. Tannins accumulate in skin and seeds and contribute to important characteristic of red wine such as astringency, bitterness, body, color and stability (Keller et al., 2010; Eric, 2019).

Phase II, also called Lag phase, generally lasts a couple of weeks and is identified when berry growth is paused, the seed embryo develops and seed coat starts to lignify. At this stage berry reach approximately half of their final size. (Fig 1).

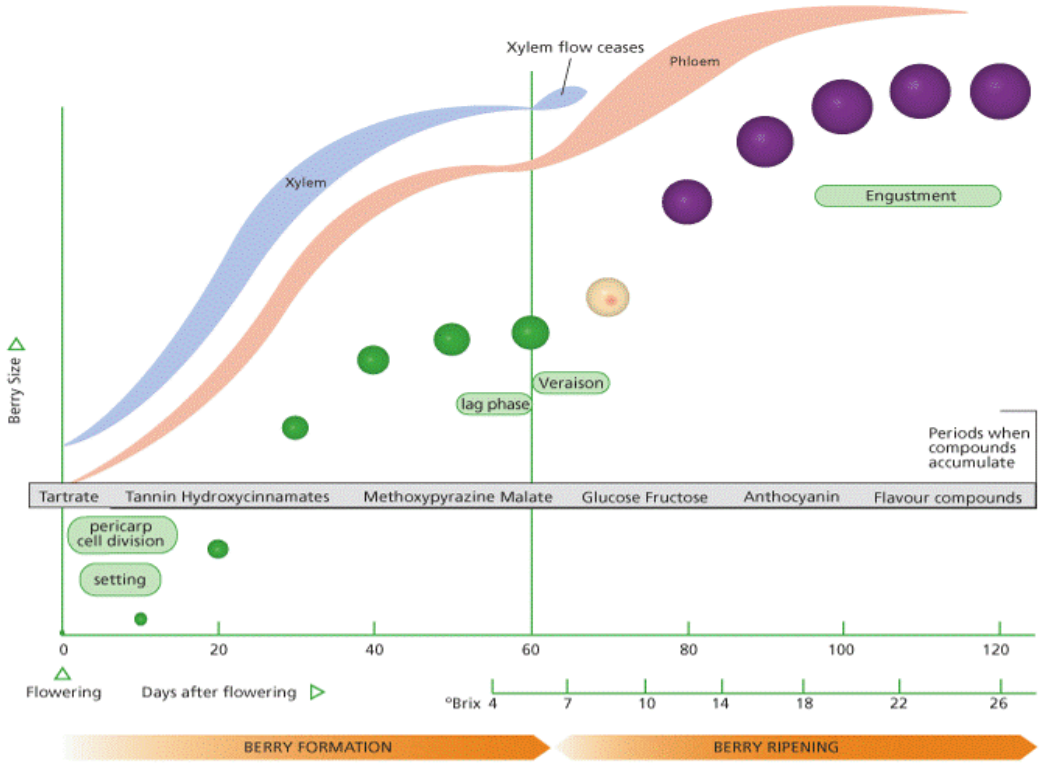

Figure 1: Growth and development of the grape berry with the indication of the period of the main compound accumulation through xylem and phloem inflow.

Finally, phase III starts with the onset of ripening (veraison), when berry soften, change its color, accumulates soluble sugars (mainly glucose and fructose), aroma precursors and anthocyanins (in red varieties). Veraison represents the transition from immature to mature berry development. Recently, genetic determinants controlling such transition at transcriptional level have been studied and a list of putative master regulators of the onset of ripening have been produced (Palumbo et al., 2014; Massonnet et al., 2017 and Fasoli et al., 2018). During ripening the berry enlarges, the amount of tannins and tartaric acid remain substantially unchanged and the amount

of malic acids is reduced thus increasing its palatability consumption and seed dispersal by birds and vertebrates. The grapes of warmer regions have less malic acid, seed tannins and different aroma compounds.

The most important changes that occur after veraison depend on various factors i.e., yield, crop load, hang time, canopy size, abiotic and biotic factors. Wine quality is also determined by other important secondary metabolites i.e., anthocyanins (in red grapes) and volatile flavor compounds (terpenoids) in red and white grapes (Stafne, 2019).

1.3 Characteristics of the varieties used in this study

Corvina is a red grape variety native to the Verona area. Its first reports are dated back to 1627 in the work of Alessandro Peccana i.e., “On the Problems of Cold Drinks”, and later in a poem by B. Lorenzi in 1778 and finally in the description of the botanist C. Pollini, dated back in 1824. It is also mentioned dating back to the early seventeenth century. Corvina Veronese is part of the large family of "Corbine" which differ from each other due to the slight differences in morphological characteristics. This variety, widespread in all areas around Verona (Valpolicella, Valdadige and Bardolino), is used for the production of fine wines. From an ampelographic point of view, Corvina has a medium-sized, pentagonal, five-lobed leaf with deep lateral sinuses, which often overlap, and with a lire-shaped petiolar sinus (Figure 2-A). The bunch is of medium size, pyramidal, winged, with one wing somewhat longer than the other, rather compact (Figure 2-B). The average weight is around 150 grams. The berries are spherical-ellipsoidal with a blue-violet, pruinose and firm skin. The pulp is melted with a simple flavor.

The vine has excellent vigor and good resistance to disease. It adapts well to both clayey-limestone and alluvial soils. The wine obtained has a brilliant ruby red color, with a winy smell and a contained fragrance. Corvina has a late budding and a medium-late ripening phase, between the mid of September and the beginning of October. With regard to cultivation characteristics and attitudes, the Corvina has a good vigor that requires multiple pruning during the vegetative season. The position of the first fruiting bud is placed at the height of the 2nd or 3rd node, with an average 1-2 inflorescences per bud. It exhibits normal behavior compared to propagation by grafting. It has normal pest resistance against diseases. Corvina is used only for winemaking. The product is a grape that is preserved quite well on both the plant and the fruit. From a nutritional point of view, it is clearly sensitive to the deficiencies of magnesium and potassium. It is very sensitive to water

stress and sunburn of berries. In particular, in the month of June, after the shoot trimming (edging and/or topping interventions) that unveil the clusters exposing them to the sun causing damage to the berries, manifesting widespread burns and wilting symptoms. These crop interventions should therefore be managed with great care and the clusters should be exposed in pre-harvest at complete flooding.

Figure 2. Leaf structure (A) of Corvina grape variety and berry cluster formation (B).

The Solaris vine, whose name means "belonging to the sun", was obtained in 1975 by Norbert Beker by crossing Merzling x (Zarya severa x Muscat Ottonel). Professor Vilem Kraus created Gm 6493 in Czechoslovakia in 1964. Kraus offered his crosses to Becker and he created Solaris by a cross between Merzling as mother plant and Gm 6493 as father plant at Geisenheim grape breeding institute, Germany. Solaris is considered as *Vitis vinifera* grape. It also contains traces of hybrid grapes in its pedigree. It is an approved as a *Vitis vinifera* grape by EU, to grow and to be used for making wine. It is formally listed as a *Vitis vinifera* cultivar (Vitis International Variety Catalogue: Solaris). It received varietal protection in 2001.

Merzling **X** **Gm6493**
(Seyve-villard 5276 x (Riesling x Pinot gris)) (Zarya Severa x Muscat Ottonel)

↓

Solaris

It is recognized as a variety resistant to the main fungal diseases. It is a fourth generation vine, obtained by hybridization, whose characteristics of resistance to the main fungal diseases derive from the use of *Vitis amurensis* as parental vine. In fact, the latter, originally from eastern areas such as China and Siberia, has a marked resistance to the main diseases, such as botrytis, downy mildew and powdery mildew. The Solaris variety is precocious in both budding and flowering. The bud is open in bronzed yellow and with high presence of creeping hairs. Early vine in both sprouting and flowering. (Fig 3-A). The cluster is of medium compactness (Fig 3-B). The grape is wide ellipse in shape, short-length, green-yellow with intensity of anthocyanin pigmentation of the pulp nothing or very weak, the yield in juice can be high or even very high, with no particular flavor. The bud has a complete opening of the apex. The intensity of anthocyanin pigmentation of crawling hair is low/medium and their density is medium/high. The young leaf takes on the top page of the flap (IV leaf) a green/bronzed color. The woody appearance is brownish in color. The sugar content of the must obtained from Solaris variety grapes is very high, showing a medium-low total acidity. This variety, obtained starting from the initial crossing of *Vitis vinifera* with *Vitis amurensis*, unlike the hybrids created by crossing with American vines, does not have a particularly unpleasant foxy flavor. The era of sprouting and flowering are both early. The vigour of the bud is medium/high. With regard to the physiological maturation of the berries, however, the age is very early. The grape yield is medium, with a very high sugar content of the must and total low/medium acidity. Solaris' characteristics and culture aptitudes relate to the degree of resistance. For cluster and leaf the degree of resistance to *Plasmopara* is high. While for the degree of resistance of the leaf to Botrytis is mean. The Laimburg Experiment Centre has contributed to the inclusion of five new varieties, including Solaris, on the list of grape varieties allowed for the production of wines with the protected geographical indication "Mitterberg". Solaris and other vines: Cabernet cortis N., Souvigniergris B., Muscaris B. and Johanniter are on the national list of vine varieties (G. U. 186 of 2013-08-09 and G. U. 258 of 2014-06-11) and belong to the so-called "Piwi" varieties, varieties resulting from repeated crosses between varieties that bear resistance against vine diseases and traditional varieties of wine grapes. All five varieties therefore have a high resistance against the two main fungal diseases of the vine, Oidio (Erysiphenecator) and Peronospora (*Plasmopara viticola*) and demand, for the production of perfectly healthy and mature grapes, with least plant protection treatments. The new generations of these partially resistant varieties reach a quality level of wines very close to that of traditional varieties. Due to the lower

need for plant protection treatments, they are especially suitable for sensitive areas such as in the vicinity of houses, schools, playgrounds, sports fields etc. and in steep slopes. The reason why this vine is mainly used by wineries in North Italy is to be found in the origin of this resistant vine. The creation of "Solaris" as mentioned above, was conceived and completed in 1975 at the University of Viticulture in Freiburg, in central Germany, an area with an average temperature much lower than the seasonal averages of Italian temperature. This variety is also characterized by very early occurring of all phenological stages.

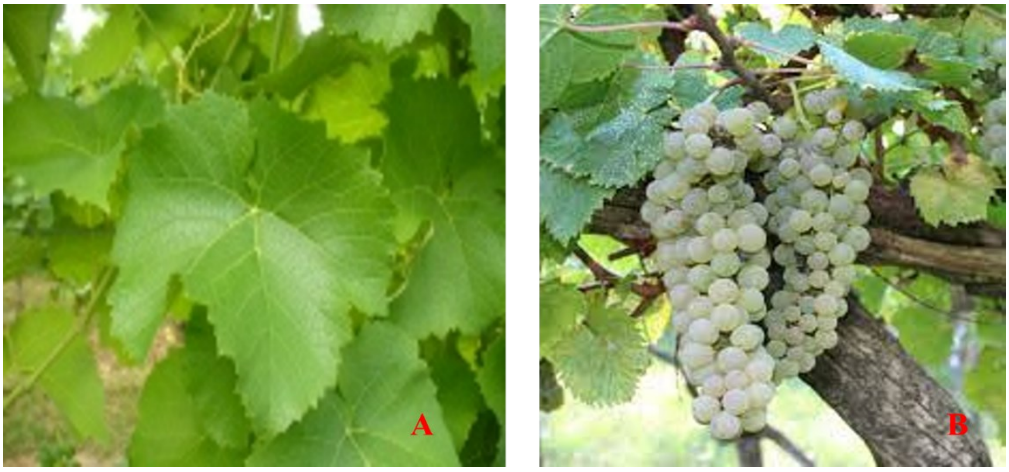

Figure 3. Leaf structure (A) of Solaris grape variety and berry cluster morphology (B).

1.4 Climate Impact on Wine Quality

For several centuries, grapevine cultivation has been a remunerative fruit crop for wine production. The optimum production, usually requires a temperature ranging from 12°C to 22°C with a rainfall range, falling approximately between 600 mm and 800 mm (Arias et al., 2022). Intergovernmental Panel on Climate Change (IPCC) has mentioned in its assessment reported that the temperature has sequentially been increased since 1850, particularly in the last four decades. The land surface temperature of the first two decades of the twenty-first century has been observed as 1.59 °C higher than the temperature since 1850-1900 (Arias et al., 2022). Likewise a huge share to the climate by carbon dioxide production has also been added. Intergovernmental Panel on Climate Change (IPCC) has speculated an increase in surface temperature huge shift in climates due to higher surface temperature and continuous CO_2 emission.

Long-term studies on grapevine phenology have clearly demonstrated that global warming is affecting phenological events, leading to an anticipation in their timing and increasing the impacts

of temperature on grape quality. Imbalanced division for adaptation of wine regions would compromise the identity and distinctiveness of particular wines of a specific region.

Different cultivars of grapevine have specific range of optimum temperature to produce high quality wine grapes (Keller, 2010). Falling vine growth out of such ranges deteriorate wine quality, therefore a better adaptation of prime cultivars, to these dynamic shifts is needed to maintain both the fruit and wine quality (Van Leeuwen et al., 2019). Thus, an optimum threshold is necessary for quality wine production (Coombe, 1987). Low temperature enhances the accumulation of necessary soluble berry contents whereas high temperature negatively affect berry ripening by lowering berry weight, total soluble solids and polyphenols (Kuhn et al., 2014).

Good quality grape parameters include sufficient sugar concentration and secondary metabolites that improve the wine's overall profile with appropriate alcohol, color, aroma and flavor (Coombe, 1987), since these metabolites have strong correlation with sugar levels during the ripening process which is however also affected by specific environmental factors (Torres et al., 2021). The cultivar-specific temperature ranges are believed to be the most important standard for suitable environment features (Morales-Castilla et al., 2020 and Parker et al., 2020). Since most of the vineyards are planted in the regions of warm to hot climate, the impact of climate on wine in entrenched regions is still intuitive. It is suggested that cool climate region would more likely to produce high quality wines in near future despite of lower level of CO_2 emissions (Mosedale et al., 2015). Assessment of different climate models (RCMs) using bioclimatic indices also resulted in negative impact on wine quality on account of accumulation of heat in central and southern Europe (Lorenzo et al., 2016). Thermal interventions in such regions also suggest no longer suitability of wine production by the end of 21st century, however Northwestern European part could escape such risks and enjoy predicted fluctuation in warming.

Adaptation of the change in temperature might change the altitude and latitude of suitable areas to ensure desired wine quality and production (Cabre and Nunez, 2020). This displacement bring huge challenges to practice improved viticulture. Likewise, the climate models like RCP4.5 and RCP8.5 scenarios, might enhance grape production and fruit quality in an Italian region Emilia-Romagna for the period 2011-2040, whereas, this rise might fall between 2071-2100 (Teslic et al., 2019). Winemaking process might get affected if continuously exposed to the increased temperature if adaptive measures were not taken. The climate regions with relatively colder ground

temperature such as Belgium, Germany and South England, might be benefited with suitable temperature threshold in next few decades (Cardell et al., 2019). Naulleau et al. (2021) reported that local requirements of soil and irrigation water for usual crop production are not coherent with suitable mapping studies. Differences in land utilization, crop preference and conservation policies are the major constraints in setting up new wine growing enclaves (Naulleau et al., 2021), however the temperature forecast for other colder regions will not affect wine production at the cost of associated increase in precipitation in wet lands (Dunn et al., 2019).

The rise in temperature related to climate change has sometimes resulted in improved potential of high quality wine production in the viticultural regions of higher altitude (Arias et al., 2022). This potential has motivated farmers to increase grapevine production and scientists to research at advanced level the potential of high altitude agricultural areas. Some countries including Italy, China and Turkey have been reported to extend the vine cultivation at relatively higher altitudes (350 m a.s.l. to 2,900 m a.s.l.) as compared to the average areas for wine growing (Gladstones, 2011).

1.5 Climate Impact on Grapevine Phenology and Berry Ripening

The process of berry development is greatly affected by various internal and external factors i.e., environment (temperature, relative humidity, sunlight, nutrient and water supply) and hormones (Kuhn et al., 2014). Certain growth hormones e.g., auxins were reported to affect the ripening process by delaying the berry softening and enlargement, and the evolution of the main technological ripening parameters (i.e., anthocyanin, sugar and organic acid content) (Kuhn et al., 2014). The grape berry is a non-climacteric fruit and its ripening onset is independent from ethylene production. However, ethylene may have a role in the ripening progression because treatments of berries with this hormone has been reported to enhance the ripening process, similarly to the treatment with brassinosteroids and ABA (Fortes et al., 2015). Likewise, ABA is also involved in the accumulation of sugar and phenolic compounds (Fortes et al., 2015) and brassinosteroids are reported to be found in higher quantity during the onset of ripening, suggesting their role in ripening process (Kuhn et al., 2014).

Among environmental parameters, temperature is undoubtedly a very important factor for grapevine and fruit development (Rogiers et al., 2022). The Mediterranean climate is one of the best suitable climates to practice viticulture. Interplay between warm dry summers, cool wet

winters, optimum temperature, effective light and sufficient water availability enable desirable evolution of berry development for its aroma, color and flavor in hundreds of grape cultivars (Rogiers et al., 2022). Because of the raise in temperature associated with global climate change, the grapevine phenology is continuously anticipating in flowering veraison and some maturity parameters in several viticultural regions (Rogiers et al., 2022). Increase in temperature over last 3 decades in EU has brought new challenges to mitigate such effects to ensure the maximum production and quality. However, the magnitude of such effects is variable due to different climate and environmental variation (Rogiers et al., 2022). Plant research is generally aimed to explore both normal vegetative and reproductive growth in coordination with environmental stresses. In grapevine production, the phenology is anticipated, thus increasing bud frost, at early budburst stage due to early endodormancy and increased temperature (Fig 4).

Such negative effects could possibly be aggravated in relatively warmer regions like as in South of Italy. Early budburst exposes young plants organs to early freeze events which may destroy primary shoots, and delayed frost events which may deteriorate flower development. The negative impact of frost not only affect the current growth process but also destroy the yield in the following years (Friend et al., 2011). Vineyard management techniques such as delayed winter pruning might help delaying budburst (Friend et al., 2011). However excessive delay in pruning adversely affect the yield and may negatively affect the must quality (Brighenti et al., 2017 and Van Leeuwen et al., 2019). Similarly, other vineyard management techniques such as late defoliation, treatments with anti-transpirants or auxins have been proposed to delay the phenology and push the ripening process towards less warm periods of the season (Dinu et al., 2021). Moreover, the selection of regional climate specific cultivars, either by exploring the existing biodiversity in grapevine cultivars and clones or by developing tailored breeding programs, could be the best way to adapt viticulture to the changing environment, minimize the management cost and avoid risks of poor yield and quality.

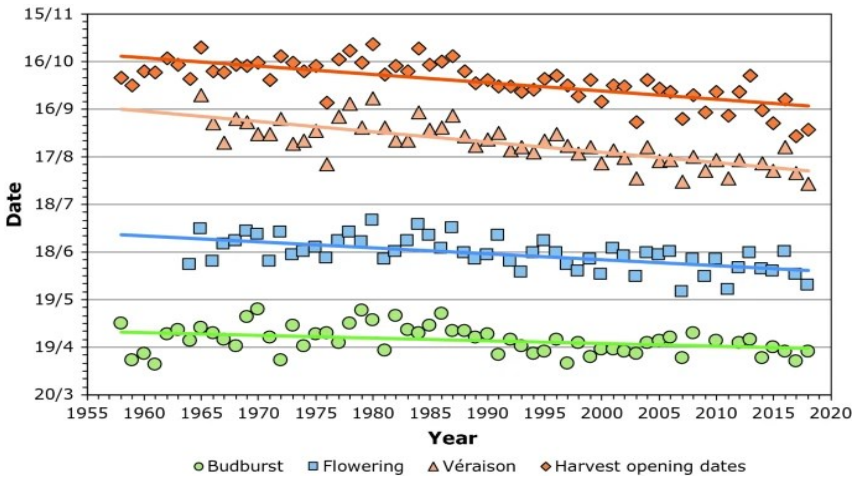

Figure 4. Anticipation in grapevine phenology over past.

1.6 Grapevine Breeding

Worldwide grape production during the marketing year 2021/2022 has been amounted to about 25.62 million metric tons (US Department of Agriculture; National Agricultural Statistics Service). Grapevine has widely been exploited under breeding programs to ensure high yields and quality in cultivated grapevines region through studying its phenology and genetics under diverse climatic conditions (Duchene et al., 2020). A deep understanding of grapevine genetic architecture is required for better adaptation to the changing climate and for its consistent performance over the future years. However, a sustained quality of wine has been a big challenge for breeders, especially under fluctuating seasonal climatic conditions. Therefore, assessment of genetic basis of phenology and quality related traits is needed to develop breeding programs to develop grapevine varieties adapted for the cultivation in specific viticulture areas and to identify the candidate genes for the new breeding technology approaches. Improved agronomic practices and advanced breeding strategies are the vital options for future improvements (Jones and Davis, 2000 and Duchene et al., 2010). The segregation pattern of phenological traits in grapevine biparental population helps to identify the genomic regions responsible for their genetic control.

Breeding in grapevine for resistance started in 1960 in the State Institute for Viticulture in Freiburg in Germany. These crossings led to the birth of two white grape varieties, progenitors of resistant varieties: Johannitter (created in 1968) and Solaris (1975), whose cultivation was only allowed in

Italy in 2013. In 1999, again in Germany, an international working group "PIWI International" was built, with the aim to of promote fungi-resistant vines.

The most famous PIWI grape varieties developed by PIWI include Bronner (created by Norbert Becker as a cross between Merzling and “GM 6494” in 1975), Solaris, which is a cross selected by Norbert Becker at the State Institute of Viticulture in Freiburg. The aim of this selection was to obtain a red variety suitable for colder climates in the German wine-growing regions with a variety of aromas, extracts and tannic structure equal to the classic international vines, Muscaris, the resistant variety Solaris and the aromatic variety Muskateller (white Muscat) are the parents of this variety, selected in 1987 by Nobert Becker and Souvignier Gris, obtained from a cross between Cabernet Sauvignon and Bronner.

The first Italian center for the propagation and distribution in Italy of certified cuttings of the German PIWI varieties was born with the collaboration of Vitis Rauscedo and the State Institute of Viticulture of Freiburg (WBI-FR) and with the German nursery Rebschule Freytag (https://www.vitisrauscedo.com/en/grafted-vines-vitis-rauscedo). These resistant varieties selected in Germany, a country with a characteristic continental climate, have a short vegetative cycle and early ripening. Enabling these varieties particularly suitable for cultivation in wine-growing areas of northern Italy, and not suitable for regions with a Mediterranean climate. In fact, in Italy, these new varieties are registered in the national register of vine varieties and in some northern regions, such as Friuli Venezia Giulia, Lombardy, Trentino-Alto Adige, Veneto, they are allowed to be cultivated for the production of varietal wines with Geographical Indication.

Since 2006, the Institute of Applied Genetics (IGA) and the University of Udine have been collaborating, together with the Vivai Cooperativi Rauscedo, in the creation of vine varieties resistant to downy mildew and powdery mildew and suitable for the Italian pedoclimatic/enological needs. In 2015, 10 new vines were registered in the Italian National Register of vine varieties and protected by patent, of which 5 with white grapes and 5 with red grapes: Fleurtai, Soreli, Sauvignon Kretos, Sauvignon Nepis, Sauvignon Rytos, Cabernet Eidos, Cabernet Volos, Merlot Khorus, Merlot Kanthus and Julius. These new varieties show resistance to downy mildew, powdery mildew and in some cases even low temperatures, down to -24°C, utilizing introgression of resistance genes present in the non-vinifera parentals Bianca and 20/3, used in the hybridization. These new varieties contain one or two main genes for resistance to

downy mildew and one to powdery mildew, so they can be effectively protected against fungal diseases with just 2-3 treatments a year based on cupric and sulfur products. They would therefore guarantee the reduction of the incidence of viticulture on environmental pollution.

The Edmund Mach Foundation of San Michele all'Adige also played a fundamental role in the same area of research. The research program developed by this organization has the objective of selecting new varieties, developing new techniques for the promotion and dissemination of Trentino viticulture that is sustainable from an environmental, economic and social point of view. The Vine Genetics and Genetic Improvement Unit of the E. Mach Foundation is engaged in the development of new varietals for sustainable viticulture, through the study of the genetic control of resistance to downy mildew and powdery mildew present in the genus *Vitis*. Crossbreeding, selection and agro-enological evaluation of seedlings in greenhouses and fields are also carried out in parallel. In 2014, the Foundation was able to include in the Italian National Register the first four vines created through traditional genetic improvement, with particular characteristics of resistance to Botrytis cinerea: Iasma Eco 1, Iasma Eco 2, Iasma Eco 3, Iasma Eco 4.

A breeding program aimed to the creation and study of resistant vines is also active in CREA - Council for agricultural research and analysis of the agricultural economy. The Center for Viticulture and Enology, which is part of this research institution, deals with genetic improvement plans aimed at the creation of new table and wine grape varieties. The program "Breeding Vite da Vino (Arezzo, Conegliano, Turi and Velletri)" aims to obtain and select quickly, through the use of molecular markers, varieties resistant to the pathogens that affect the vine, so to guarantee the drastic reduction of the use of plant protection products while maintaining high quality. Likewise, France is also actively engaged in the development of resistant vines, especially the research body INRAE - National Research Institute for Agriculture, Food and the Environment. In 2018, it obtained the possibility of registering four new resistant varieties in the French National Catalogue, selected for sustainable viticulture. The research program had been undertaken in the 2000s, through the implementation of repeated crossings between two INRA varieties, selected by Alain Bouquet, and two specimens obtained from the Julius Kuhn Institute (Germany). The development of specific molecular markers for each resistance gene has made it possible to select individuals with the desired characteristics at an early stage. The four new varieties, two with red grapes, Artaban and Vidoc, and two with white grapes, Floreal and Voltis, have natural resistance to

downy mildew and powdery mildew. In fact, two downy mildew resistance genes and two powdery mildew resistance genes were combined, originating from the species *Vitis rotundifolia* and from a group of species dominated by *Vitis rupestris*.

1.7 Genetic Maps and QTL Mapping

A genetic map is the linear arrangements of genes on respective chromosomes based on recombination among several genetic markers. Construction of genetic maps is an important tool to identify the genomic regions controlling specific phenotypic variation, helping plant breeders to develop economically important crops. Construction of high resolution genetic maps and QTL maps are based on molecular markers. Over the course of development in plant biotechnology, use of co-dominant molecular markers such as Single Nucleotide Polymorphism (SNP) has increased largely. Crop improvement has become highly successful by utilization of molecular markers for QTL identification. Genetic mapping utilizes the Mendelian principles of allele assortment and recombination to identify the potential proximity of molecular markers along the chromosomes. Genetic recombination frequencies help estimating the distance between two adjacent loci, thus creating linkage maps.

Plant breeding programs provide new strategies to deliver new cultivars with sustainable yield and improved quality under fluctuating climate conditions, through identification of stable genetic determinants controlling specific phenological traits. Exploring its phenological characteristics like budburst, flowering and ripening help understanding the climate impact on its quality and quantity of yield. Anticipation in budburst and flowering, for instance, may face yield loss when exposed to the spring frost. Increased temperature negatively impact berry ripening and its composition (Houel et al., 2015). Genetic studies have provided information on the regulation of grapevine reproductive development, including flowering, berry growth, anthocyanin accumulation and sugar uploading. Houel et al. (2015) reported identification of ten stable QTLs controlling berry development and wine quality in parental maps, a single QTL for berry weight, berry acids and seed number on chromosome 7, and a minor QTL for leaf area on chromosome 4.

Modern plant breeding programs have greatly involved the use of DNA markers for effective genomic selection to provide insight for productive use of genetic diversity, since genetic markers are closely linked with the target genes controlling desired phenotypic trait (Begna and Yesuf, 2021). High density genetic linkage maps has become an essential tool for research at genomic

level. The QTL analysis is a powerful tool in breeding research to identify genetic regions contributing to the manifestation of a trait. Grapevine breeding has widely been aided for identification of underlying marker-trait association, Quantitative Trait Loci (QTL) mapping, genome-wide association studies and comparative genetic studies, by such linkage maps. QTL mapping greatly extend our knowledge in harnessing grapevine genetic resources. Role of transcription factors controlling veraison time is another aspect to harness the transcriptomic data of genes involved in the process of berry development. Grapevine genome sequence harbors immense opportunity to exploit the sequence data to evaluate the gene functions and to identify candidate genes controlling flowering and ripening processes that yet needs to be explored (Jaillon et. Al., 2007).

Grapevine genome sequence shelter several traits which follow complex quantitative inheritance. These traits under QTL mapping, are studied to explore potential determinants of typical grape phenotypic characteristics (Vezzuli et al 2019). Likewise, until now 33 resistance loci (Rpv1-Rpv33) against grapevine downy mildew have been detected on chromosomes 4, 5, 6, 7, 8, 9, 11, 12, 14, 17 and 18 (Merdinoglu et al., 2003; Fischer et al., 2004; Welter et al,. 2007; Bellin et al., 2009; Marguerit et al., 2009; Moreira et al., 2011; Schwander et al., 2012; Venuti et al., 2013; Ochssner et al., 2016; Zyprian et al., 2016; Divilov et al., 2018) in grapevine of different genetic information (Surya Sapkota et al 2019 and Possamai and Wiedemann-Merdinoglu 2022). Another major QTL (Resistance to Plasmopara viticola 8 (Rpv8)) for resistance to downy mildew has been detected in *V. amurensis* explaining 86% phenotypic variance (Blasi et al., 2011). He et al., 2022 reported an important reference for grapevine breeding program with identification of genomic elements of QTLs for ripening process, where grapevine varieties with superior haplotype expressed early start of berry development, also VvFTB was found to be highly expressed during veraison onset (He et al., 2022). Another study on grapevine (*Vitis vinifera L.*) reported identification of five new QTLs for berry weight on linkage group 1, 8, 11, 17 and 18, showing 31% of total variance whereas four QTLs were detected for seed traits on linkage group 4, 5, 12 and 14, with 51% variance, however the QTLs for both traits lacked colocalization (Doligez et al., 2013). Likewise, Lukasz Grzeskowiak reported nine QTLs for budburst, flowering initiation and onset of ripening with 44 % of total variance. Chromosome number 15 harbors QTLs for budburst and veraison (Grzeskowiak et al., 2013). Malate is one of the important organic acids in grapevine which determines the fruit acidity and pH. Reshef et al. (2022) reported identification of three

major QTLs for malate on chromosome 1, 7 and 17 expressing a total of 41 % phenotypic variance (Reshef et al., 2022). Previous reports have been trying to identify the genetic determinants of these traits through classical QTL analysis, with an ultimate goal of developing information to breed grapevine varieties that are best adapted to the changing climate. By exploring the genomic locations (Bigard A 2018) a huge number of genes, potentially controlling veraison, linked with relevant QTLs have been reported (Delfino et al., 2019, Fig 5).

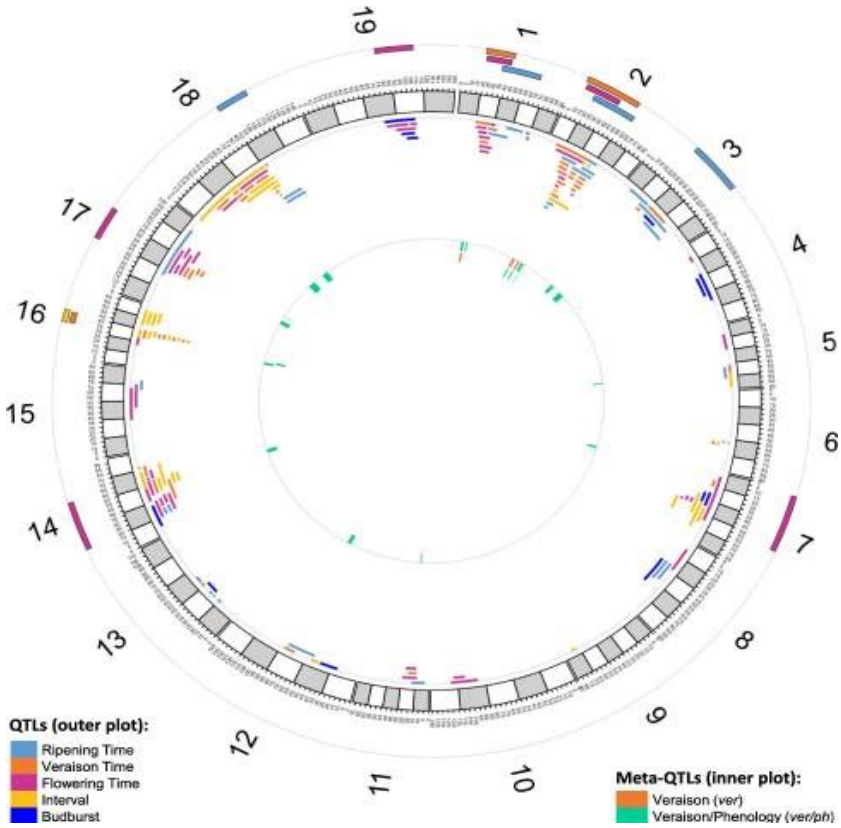

Figure 5. Meta-QTL analysis for phenology related QTLs in literature (from Defino et al., 2019).

Various QTLs have been identified in grapevine, controlling size of the berry (Duchene E et al., 2020 and Costantini L et al., 2008), yield, phenology, flavor, anthocyanin components, fruitfulness, cluster architecture and resistance against diseases (Doligez A 2013), however the whole genetic determinism regulating plant phenology remained largely unanswered. Developmental stages have been characterized by their relevant QTLs e.g., flowering time QTLs (Kamal N et al., 2019 and Duchene E et al., 2012) on different chromosomes i.e., chr. 1, 4, 8, 14, 17, 18 and 19 in different mapping populations. The finding of MADS-box flowering time genes i.e., *VvFL*, *VvFUL-L* and *VvAP1,* within *FTC* QTL regions, encourages to further exploring the

role of these transcription factors in the control of flowering phenology impact on flowering time (Duchene E et al 2012).

1.8 Aims of the project

Corvina, being an Italian wine grape variety, mainly grown in Veneto region, is used with several other grapes to create the light red regional wines. Likewise, the divergent variety of grape, Solaris on the other hand, is used for white wine. Both these varieties are very divergent in their phenology. To explore this divergence further we aim to determine the potential QTLs harboring at genomic locations for the phenology under studies.

Quantitative Trait Loci (QTLs) mapping have been studied, in changing climates, in grapevine since many years. The previous reports provided the evidence for identification of QTLs for berry size and seedlessness (Costantini et al., 2008; Doligez et al., 2013), phenology (Duchene et al., 2012 and Grzeskowiak et al., 2013), anthocyanin composition (Fournier-Level et al., 2009), tannin composition (Huang et al., 2012), cluster architecture (Correa et al., 2014) and disease resistance (Venuti et al., 2013; Barba et al., 2014). However, stable QTLs identification controlling phenology in changing temperature is still unanswered. Adaptation of local grape varieties to changing climatic conditions is therefore a major breeding strategy including the selection of late ripening varieties/clones, whose bunches may escape the warmer summer condition by postponing the ripening period. However, assessment of the genetic basis of phenology and quality related traits is a prerequisite to design breeding programs for grapevine varieties adapted for the cultivation in specific viticultural areas and to identify the candidate genes for the advanced breeding technology approaches.

Rapid fluctuations in global climate change has highlighted the role of temperature on grapevine phenology and trait characterization both at phenotypic and molecular level. The overall grapevine (*Vitis vinifera*) composition and yield has been affected on account of diverse effect of high temperature in recent past. Development of stable varieties with persistent yield, under changing environmental conditions, has been the need of current era. Exploring advanced methods in plant breeding has posted a new challenge for breeders across the world. Grapevine breeding propose huge potential to identify the novel genetic determinants, ensuring stable yield with desired traits. The current study focus on exploring phenological and molecular factors determining grapevine quality for wine production. Assessment of correlation between phenology and genetic data, based

on molecular markers (SNPs) will help in developing a quantitative trait loci (QTL) map with improved resolution to locate the position of candidate gene and to understand the potential role of genes involved in grapevine flowering, ripening time and disease resistance. Role of transcription factors controlling veraison time, is another aspect to harness the transcriptomic data of genes involved in berry development process. Gradual advancement in grapevine phenology urge plant breeders to develop novel strategies to combat early onset of general phenology of grapevine to ensure persistent yield, wine quality and perseverance against plant disease. Although the grapevine varieties are well adapted to their respective territorial climates, their phenological development is strictly dependent on heat summation (Carmona et al., 2008), the warmer climates result in early onset of bud burst, flowering, veraison and ripening process (Kamal et al., 2019), This in turn has an impact on fruit quality, yield and sensitivity to pests. Ultimately increasing the input cost of grapevine farmers to control ripening and fungal infections. Considering the diverse effects of global climate change, the current research project is aimed to achieve the following goals as an outcome of the project.

1. To develop a consensus genetic map to support the mapping of QTLs for veraison time and other phenological stages by studying a cross population derived from parents divergent for these traits. A consensus map for CxS progeny has been generated, for a subsequent comparison with an integrated genetic map.
2. Identification of candidate genes through QTL mapping / analysis. The segregation data will be analyzed to discover the putative genes controlling phenological anticipation in targeted grapevine cultivars.

2 MATERIALS AND METHODS

2.1 Mapping population

The mapping population was raised after crossing between two grapevine varieties i.e., Corvina and Solaris. This cross mapping population was propagated locally at two different locations, started in 2018 in the City of Verona. Corvina (C) belongs to genus *Vitis* (grown at an area of 7495 hectares (2010) in the Northern part of Italy called Veneto) an autochthonous variety, which is black in color. Corvina is a disease susceptible and late ripening variety with high yield and producing low quality red wine. Whereas Solaris (S) is a white and early ripening variety used for wine production for its fruity and perfumed aroma and medium acidity. It is relatively a disease resistant variety against pests. The grafted plants of CxS were propagated, grafted on SO4 rootstock and grown in 2 different locations i.e., "Negrar", which is an experimental site located in a very famous region of grapevine production called Volpollicella in San Floriano and "Vivai Gozzo" in the locality of Porto San Pancrazio, Verona. The whole set of plants was propagated in two rows (named as left and right) to make two replicates at Verona to evaluate the growth comparison whereas, only one replicate was propagated at Negrar. The plants were grown at a distance of a few centimeters (approx. 40 cm) apart. The parental plants each for Corvina and Solaris were grown in the beginning (before the first cross genotype) and at the end of the population (after the last cross genotype). Initially 120 plant genotypes were grown in all 3 replicates at both locations however, missing/dead plants were replaced with more genotypes in each successive year to make a set of 150 genotypes for phenotypic evaluation. A brief description of the project scheme has been shown in Fig 6.

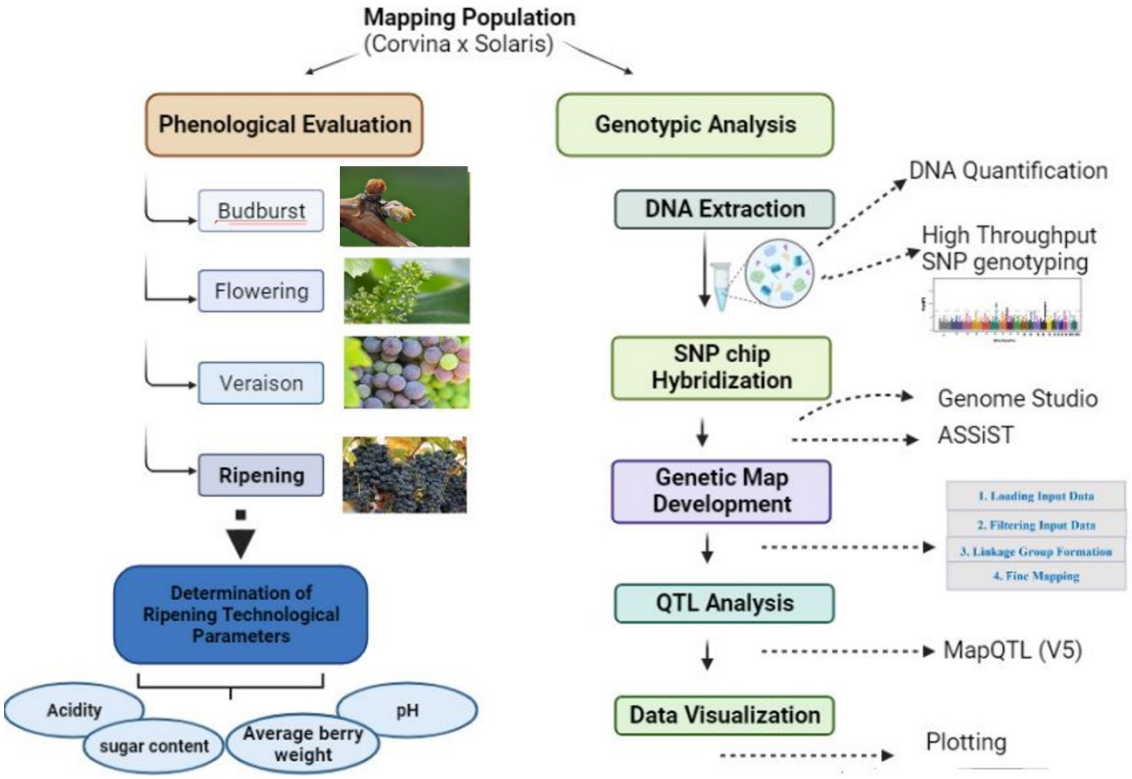

Figure 6. Work flow for the steps taken to accomplish the project.

2.2 Phenological evaluation in the field.

The collection of phenotypic data for segregating population derived from a cross between Corvina and Solaris started in 2018 in Verona region, however the phenotypic data for 2018 and 2019 has not been shown. Phenotypic data for the three years (2020, 2021 and 2022) have been shown and analyzed. Phenotypic characterization was carried out on three basic traits i.e., budburst, flowering and veraison. However, the maturity traits after harvesting have also been observed and evaluated in the laboratory. The post-harvest evaluation was conducted for the quality traits such as, Brix^{o} (total sugar contents), average berry weight, total acidity, pH, color of berry clusters, compactness of the berry clusters and polyphenols (Appendix Table 5-7). The phenotypic measurements in the field for three traits (budburst, flowering and veraison) were observed for all three replicates at both locations (Negrar and Verona) and described for each successive year 2020-2022.

2.2.1 Budburst

Budburst is defined as when air temperature in spring reaches at optimum levels, the swollen buds become fuzzy and turned into new green leaf tissues, which are pushed out of the protective scales,

and turn the tissues into bud opening. Budburst is generally observed when 50 % of the grapevine shoots express bud opening. This is an arbitrary value since the determinants of budburst percentage is rarely provided. A traditional descriptive system “Eichorn-Lorenz system” for the measurement of various stages of budburst has been reported by Coombe (1988 and 1995), however some modifications are possible in this measurement system according to the needs of vineyard and specific time period when the field observations are made. Various stages of budburst start from the dormant bud (winter bud) which is usually covered by two brown protective scales, which are then converted to the first visible form of budburst called “budswell” followed by cottony bud. The buds start progress gradually and turn the cottony surface into green tip which is highlighted when the buds further turn into the tip of young shoot. Finally, the buds emerge into a rosette of young leaves (Coombe 1988 and 1995). Coombe introduced a modified system (Eichorn-Lorenz) to identify the grapevine growth stages. He proposed 2-5 stages to describe the budburst growth period (Signorelli et al., 2020).

In order to observe the budburst, four lateral bud opening spots were selected on the main shoot exposing maximum to the sunlight. The initial phenotypic measurements started in the month of April, approximately twice a week. A measuring scale 1-5 phenological stages (proposed by Coombe) was used for the budburst observations. On average 5 observations were made to record the budburst date for all three years (2020-2022) with 2 observations per week. The date of budburst observations were recorded when 50 % of the buds (2/4) reach the growth stage of 5 (Fig 7) for each plant.

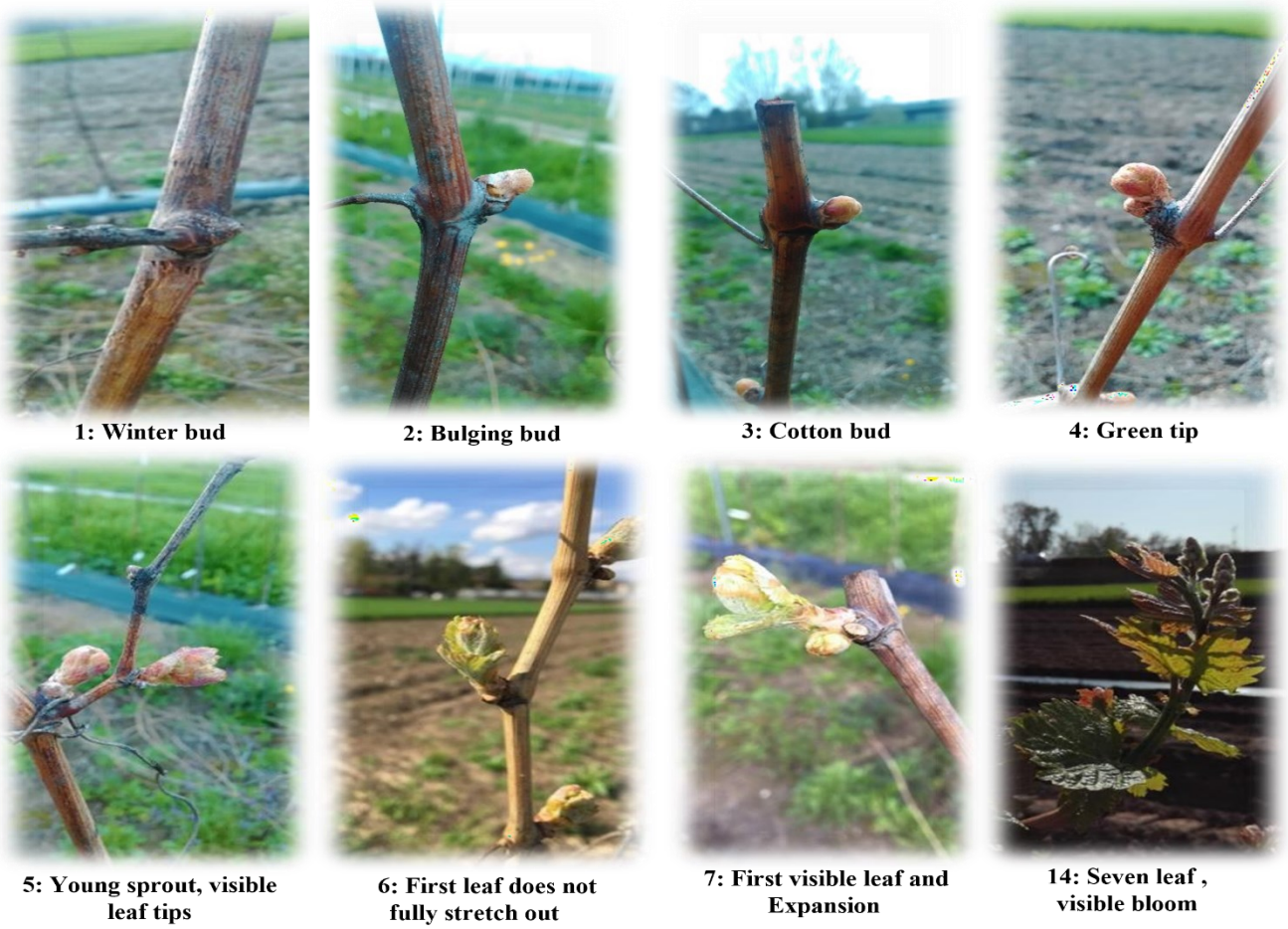

Figure 7: Phenological Stages of Budburst growth

2.2.2 Flowering

Flowering stage is defined as the bloom of available buds, however some buds do not flower at all during the growth period. Flowering stages for fertile buds (same 4 lateral buds as used for budburst) were measured based on the growth scale i.e., (0%, 25%, 50%, 75%, 100% of the inflorescences (Fig 8). In case of any missing buds, the next underlying bud was observed for flowering date, to get the usable data for each plant. Flowering stage was measured and the respective dates were noted when each bud expressed flower initiation stage at both locations, usually during the months of May and June in all three years (2020-2022).

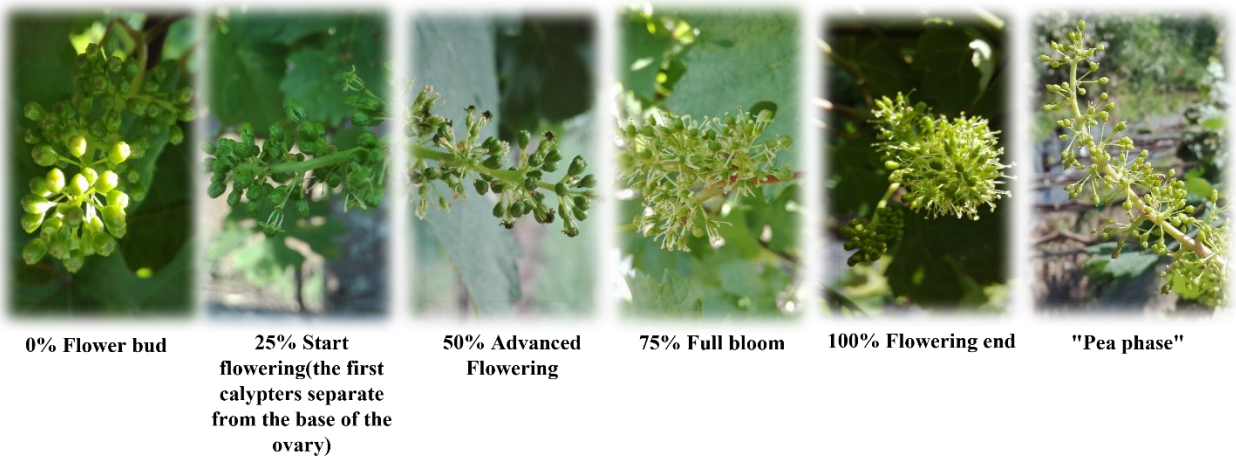

Figure 8: Phenological Stages of Flowering growth

2.2.3 Veraison

The veraison phase is recognized with the beginning of growth by cellular distension of the berry, with the phenomenon of the decrease in chlorophyll and the assumption of a translucent appearance of the berry itself. This phase initially involves only a few berries of the cluster, then progressively extends to all the others. The berries gradually take on the typical color of the cultivar, i.e. from green to yellow in the white grapes, and to more or less intense red in the black ones. In this phase the berry reduces and cancels chlorophyll photosynthesis, but the synthesis of aromas, polyphenols and other components begins which chemically modify the composition of the berry.

The presence of Solaris (a white grape variety) in the crossing population, made it difficult to note the veraison for plants with a dominance of the white color, but through the tactile and visual sensation against the light, it was possible to indicate the researched data. Veraison being the indicator of ripening process, the ripening period was established by examining all the clusters on a weekly basis. The examination was performed by touch (softening) of the berries, randomly choosing 10 berries, at three different heights of the cluster to assign the veraison percentage of the cluster since the CxS progeny included both red and white berry genotypes. The cluster bunch was determined to have color change when 50% of the berries were soft. The overall veraison status of the plant was calculated by averaging the veraison status of all its clusters.

The scale used to determine the veraison period is as follows: 0% bunches with veraison = 0, 0-25% bunches turning dark = 1, 25% bunches turning dark = 2, 50% bunches turning dark = 3, 75% bunches turning dark = 4 and 100% bunches turning color = 5 (Fig 9). The veraison date is defined as the day on which the total veraison of the plant has reached 50%. On average, 8 measurements were recorded for veraison stage for each plant at both locations, usually during the months of August and September in all three years (2020-2022).

Figure 9: Phenological Stages of Veraison phase

2.2.4 Ripening

The ripening stage was arbitrarily set when the grapes reached the soluble solid level of 19 °Brix, assessed by an using a portable refractometer. To determine the progress of the accumulation of sugar content in the berries, periodic analyzes were carried out in the field, starting from the veraison date of the individual plants. The unit of measurement that has been used is the Brix degree (°Brix), indicating the quantity of solid substances dissolved in a liquid substance; usually a sugar content in the berry equal to 8 grams coincides with 1° Brix (Fig 10).

To determine the sugar contents of the grapes of a single plant, three berries from three different bunches were taken for each sampling day, defining the sugar contents by averaging the three individual data obtained. The berries were harvested when an average sugar content of 19° Brix was obtained per single plant, consequently the harvesting was staggered.

2.3 Ripening technological parameters

Once the overall sugar level of the plant reached 19° Brix, the grapes were harvested and taken to the laboratory, in order to proceed with the analysis of the main ripening parameters, such as the average weight of a single berry, the pH, the total acidity and the total polyphenol contents (only the plants that presented clusters with an accentuated coloring of the berries) were analyzed at Villa Lebrecht, the Faculty of Viticultural and Oenological Sciences and Technologies. These observations have been described as below.

2.3.1 Determination of average berry weight

To determine the average weight of a berry, of each single genotype, three biological replicates were taken, each consisting of 30 berries removed from the cluster without the pedicel, randomly selected from the clusters that had been harvested (Figure 10-A). Once the 30 berries were weighed, using a technical balance, the average weight of a berry was calculated for each sample and then the average of the three replicates was made, obtaining a single value equal to the average weight of a berry of that sample.

2.3.2 Determination of Total Acidity

Generally, approximate saline weak acids are found in the Must and therefore in the wine. Taking this aspect into consideration, from a chemical point of view, musts and wines are buffer solutions. Therefore, upon the addition of a smaller quantity of strong base equivalents, the latter are immediately neutralized by an equal number of acid equivalents, and the pH variation is limited. On the other hand, when the quantity of base and acid equivalents is equal, the solution indicates pH 7. On the basis of this phenomenon we can trace the number of equivalents of weak acids present in the must or wine, knowing the quantity of equivalents of a strong base that we add during a titration. As a rule, weak acids are expressed by considering the equivalent weight of tartaric acid, the main acid in must and wine. Using a solution of the strong base NaOH, at 0.1N the acidity is expressed in g/L according to the following formula.

$$\mathrm{TA}\left(\frac{\mathrm{g}}{\mathrm{L}}\right) = \frac{(\mathrm{NaOH\ mL}) \cdot\ 0{,}1\,\frac{\mathrm{eq}}{\mathrm{L}} \cdot 75\ \mathrm{g/eq}}{7{,}5\ \mathrm{mL}}$$

To determine the total acidity of the samples, titration was carried out, with the indicator bromothymol blue, and with the aid of the pH-meter, to ensure the desired level of neutrality. The

total acidity was evaluated in three biological replicates for each sample in order to obtain an accurate and as precise result as possible. 7.5 mL of must were taken and placed in three small glass beakers. After calibrating the pH-meter, the electrode was immersed in the beaker containing the must and placed on the stirrer with the stir bar. The titration was done with NaOH (0.1 N), after the addition of 3 drops of bromothymol blue, when the solution reached pH 7 and at the same time the color change to blue, confirming the completion of titration.

2.3.3 Determination of pH

Knowledge of pH allows precise production decisions to be made, it directly affects microbiological stability and color. The pH of wine is usually between 2.8 and 4. The measurement was carried out for each of the three biological replicates obtained from each sample. The pH was measured using a benchtop digital pH meter. The latter consists of a measuring system composed of an electronic instrument and a glass electrode. The heart of the electrode is a glass membrane sensitive to the concentration of hydrogen ions. This probe measures the electric potential generated by the concentration of hydrogen ions H^+ outside the membrane, with reference to a potential of hydrogen ions inside the membrane, and with respect to a standard reference potential.

2.3.4 Determination of Sugar Content

Once the three replicates of 30 berries were weighed, each one was decanted into a beaker and the berries were manually mashed. Once the must was obtained, a small quantity was taken with a disposable pipette and the Brix degree (°Brix) was measured using a laboratory digital refractometer (Figure 10-B). The latter, through the evaluation of the refractive index, determines the concentration of a substance within a liquid sample. The refractive index was used to determine the °Brix i.e. the sugar content in an aqueous solution, in this case the must, obtained by pressing the grapes. The digital refractometer has been calibrated with each use by measuring the °Brix of a sample of deionized water, always reporting a measurement equal to zero.

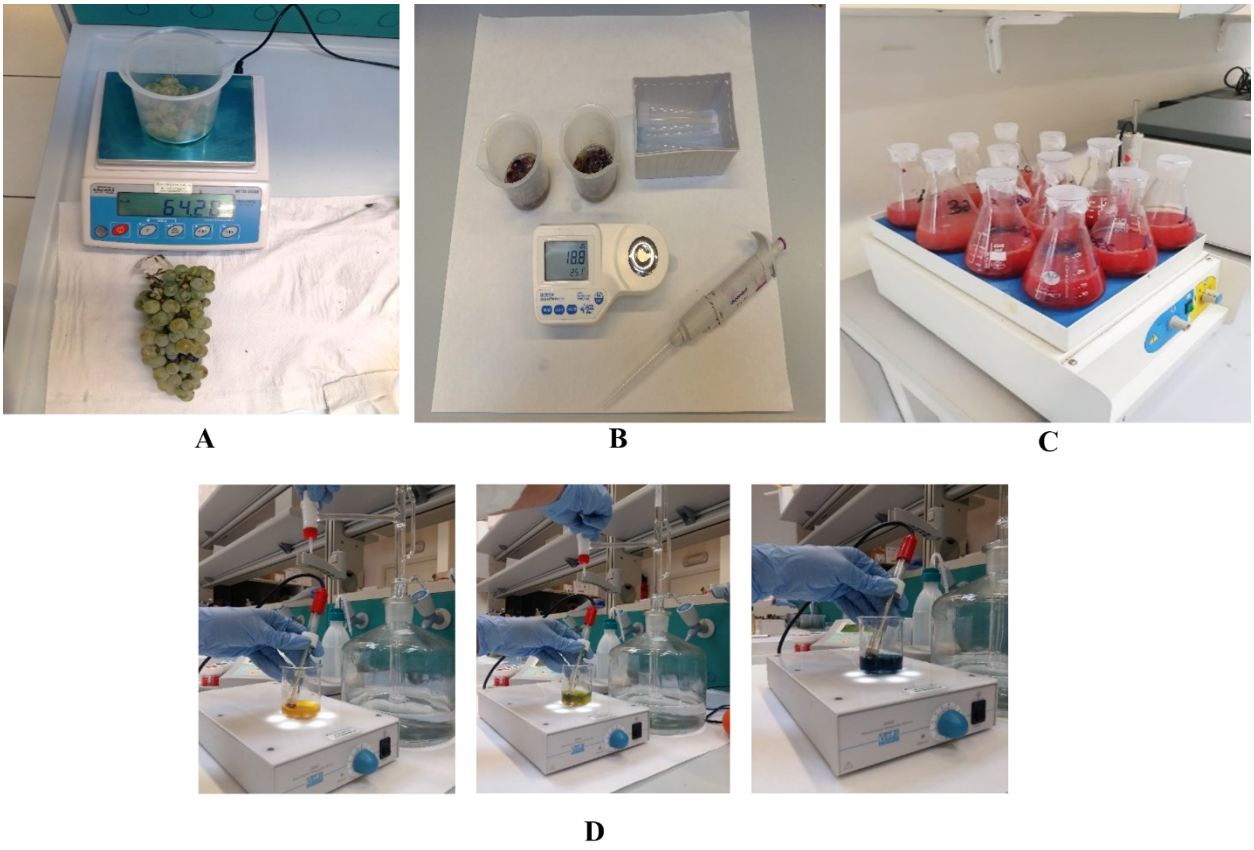

Figure 10: Laboratory analysis for different maturity related traits, average berry weight (A), Brix measurement through digital refractometer (B), polyphenol determination (C) and titration process for measuring total acidity (D).

2.4 Genotyping

Genotypic evaluation was carried out to reveal the position of single nucleotide polymorphic markers (SNP) in the cross population. The observed SNPs were then projected on all 19 chromosomes for each individual and respective genetic maps were built. The raw genetic maps were then utilized for QTL analysis to identify the putative candidate genes controlling phenotypic traits under study (Fig 11 - workflow).

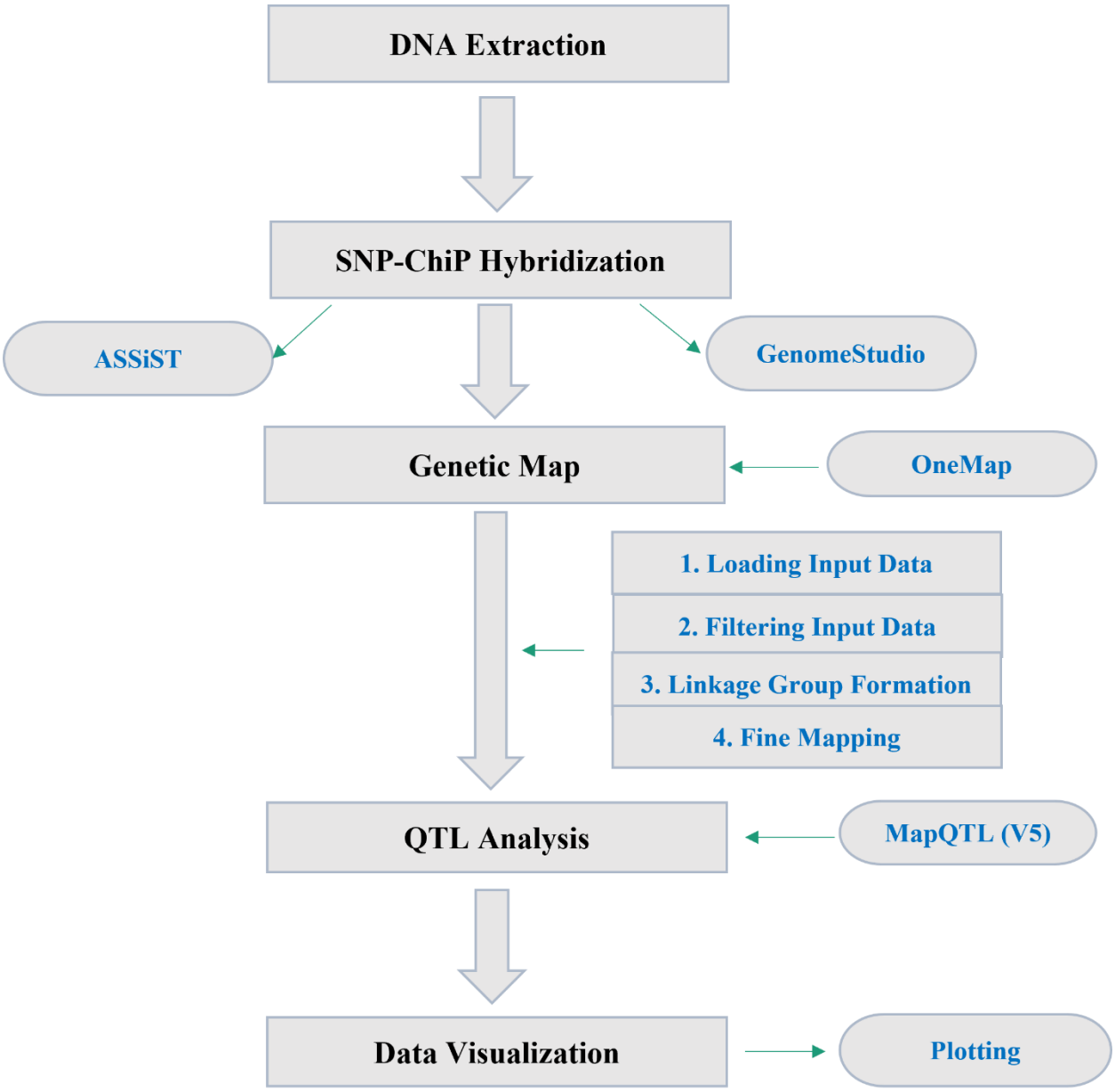

Figure 11: The workflow followed to carry out genotypic evaluation.

2.4.1 Plant Material

In order to generate genotypic data, fresh leaves of 100 grams from each plant were selected from one location i.e., Verona. The fresh leaves from the aerial part of each plant were selected before sun rise to ensure the maximum quantity of sugar in leaves. The leaves were collected in plastic bags and immediately stored in ice filled bags to ensure the minimum loss of sugars from harvested leaves due to intense sunlight. Moreover the leaves were then stored in -80 freezer for subsequent DNA extraction.

2.4.2 DNA Extraction

The frozen leaf samples were then used in order to get genomic DNA. The process of DNA extraction was performed by using a protocol from QIAGEN DNA extraction kit according to manufacturer's instruction (DNeasy Plant Mini DNA extraction kit, cat. Nos. 69104). The extraction buffers required for DNA extraction were supplied with the extraction kit. Prior to start DNA extraction process, some initial steps were carried out e.g., water bath was preheated at 65° C and ethanol was added to buffer AW-I and buffer AW-2 concentrates.

Fresh leaf samples (100 mg) were stored in liquid nitrogen. Small glass beads were added into the labelled 1.5 eppendorf tubes. A 500 ul of AP-1 buffer in 1.5 eppendorf tube and was kept in a preheated water bath. The frozen leaf samples were mashed to powder form by using an electric beater, in beaded 1.5 eppendorf tubes. The mashed samples were then stored in liquid nitrogen again. After adding AP-1 buffer, a 5 ul of RNase was added in each sample and they were placed in pre-heated water bath for 10 minutes. The samples were treated with 163 ul of P-3 buffer and incubated on ice for 5 minutes. The eppendorf tubes were centrifugated for 5 minutes at 14000 rpm. The lysate were pipetted into QIA shredder spin column placed in a 2 ml collection tube and centrifugated for 2 minutes at 14000 rpm. the flow-through were transferred into new tubes without disturbing the pellet and 1.5 volumes (600 ul) of AW-1 buffer was added and samples were mixed well until the oily layer disappeared. A 650 ul of the mixture was transferred into a DNeasy mini spin column placed in a 2 ml collection tube, centrifugated for 1 minute at 8000 rpm twice after discarding the flow-through. The spin column were placed into new 2 ml collection tube and 500 ul of buffer AW-2 was added and centrifugated for 1 minute at 8000 rpm the step was repeated with centrifugation for 2 minutes at 14000 rpm. The spin columns were then removed from the collection tube and placed into new 1.5 eppendorf tubes. Sterilized water (100 ul) was used for elution, the samples were incubated for 5 minutes at room temperature on ice and centrifugated for 1 minute at 8000 rpm. Finally, the samples were centrifugated again for 1 minute at 8000 rpm and the eppendorf tubes with DNA extracted were stored in -20° C refrigerator (Fig 12-A). DNA extraction was performed twice to remove artifacts and genetic relationships of the genotypes were verified by using a set of four microsatellite (SSRs) molecular markers (GF15-28, GF09-46, UDV-737 and VCHR-05C).

2.4.3 Quantification of Nuclei Acid (DNA)

The quantity and quality of extracted DNA was assessed through NanoDrop (ThermoFisher) with three different wavelengths: 230 nm, 260 nm and 280 nm. The quantification was measured out by placing sterilized water as blank and with 1-2 ul of the extracted DNA on NanoDrop sensor. The concentration of nucleic acids were expressed in ug/ul. The absorption peak for proteins is expressed at 280 nm, whereas, the peak for sugar is expressed at 230 nm. The criteria for desired quantity were set as if 260/280 ratio > 1.8, the samples were free of protein contamination and if 260/230 > 1.8, the samples were free of sugar contamination.

The integrity of DNA samples was then determined through agarose gel electrophoresis using TAE 1X buffer followed by staining through ethidium bromide staining dye (Fig 12-B).

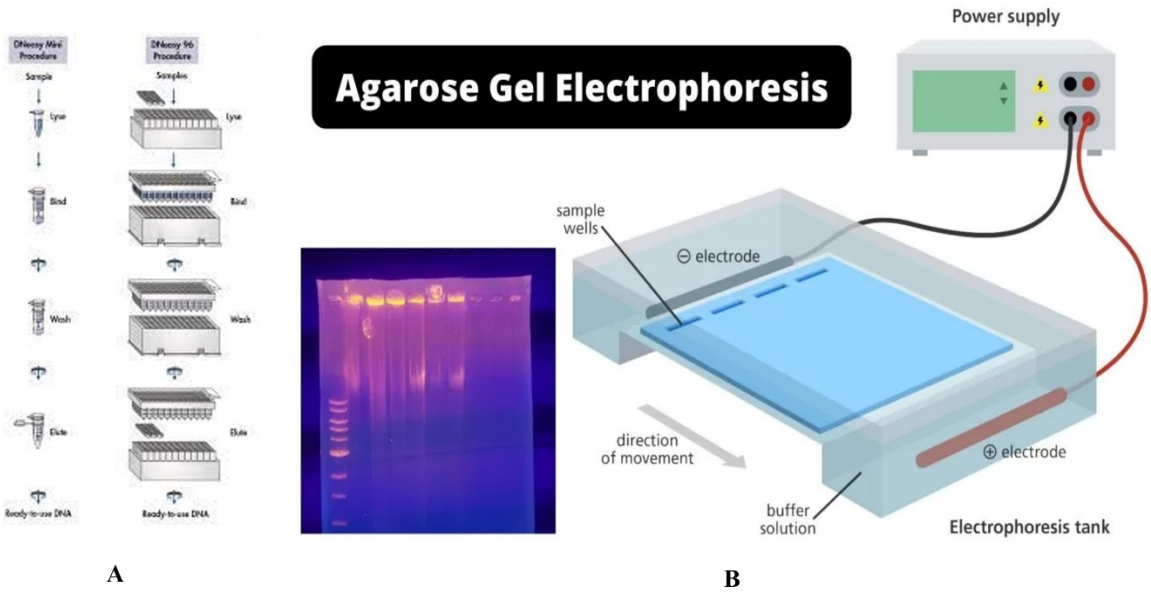

Figure 12: DNA extraction workflow (A) and agarose gel electrophoresis set up for the verification of desired quality of DNA (B).

2.4.4 SNP-ChiP Hybridization

After verification of sample's quality and integrity the DNA, samples were used for high-throughput SNP genotyping.

Genotypic characterization was performed by using an Illumina Vitis18KSNP-ChiP hybridization kit (Laucou et al., 2018) according to several benchmarks i.e., no variation in 60 bp both in 3' and 5' directions (Illumina standard), repetitive and SNPs responsible for structural variation were

removed and a final set of SNPs was selected based on their physical distribution through the 12X.V0 version of grapevine genome (FN597015-FN597047). DNA Samples were placed in 96 well SNP-Chip hybridization assay to get raw SNPs data. Initially, we got approximately 8000 SNPs from SNP-Chip assay (Table 2). The short sequence reads were mapped against PN40024 reference genome to detect polymorphism.

Initially, the raw genetic data were scored and validated through GrapeReSeq *Vitis*18K genotyping chip by using a software "GenomeStudio" with its v2011.1 version (Di Guardo et al., 2014) and later were further analyzed with another software called "ASSiST". GenomeStudio is only used to convert (makes SNP clusters) the raw imaging data of the SNP chip to quantitative values.

GenomeStudio requires three input files which were prepared in three separate folders as described below.

1. **Intensity data folder:** It contains all the intensity data in folders labelled with their barcodes.
2. **Manifest folder:** It contains the manifest file (.bpm) from Illumina which is the SNP index.
3. **Sample sheet folder:** It contains the sample sheets (.csv) for all GS projects, can be prepared with the sample sheet template. In case of multiple sample sheets, the basic information is kept same at the end of the sheet, and the "Sample_Plate" column is edited. It is important to make sure that the Sentrix Barcode_A column is placed correctly and contains the barcodes along with the scientific notation.

GenomeStudio finally prepares the input datafiles that are required for ASSiST, which is used to filter out monomorphic, failed (bad clustering or low hybridization) SNPs, and to re-cluster SNPs that shows null alleles or new mutations within the sequence which will result in different cluster profiles.

The ASSiST software requires three input files:

1. **DNA Report:** created in GenomeStudio
2. **Final Report:** created in GenomeStudio
3. **Pedigree file:** It includes the sample names, Parent-1 and Parent-2.

The grapevine genome assembly "PN40024" was used as control reference for allele similarity. During this process the monomorphic, low quality and SNPs with missing data were discarded. Theoretical Illumina SNP positions were recalculated by re-mapping the flanking regions (2x60 bp) with NCBI/BLAST1 v2.2.31.

2.5 Genetic Map development

The process of consensus genetic linkage map construction was started the projection of initial set of SNP markers on 19 chromosomes. SNP polymorphic makers between both parents (CxS) were used for genetic linkage map construction by using an R package OneMap.

2.5.1 OneMap

OneMap is an open source R package used for the construction of linkage maps for various species. The analysis for a cross population derived from a cross between Corvina and Solaris, were performed by using a novel methodology based on maximum likelihood approach for simultaneous estimation of linkage and linkage phases (Wu et al., 2002). It works based on various functions that handle pairwise marker analysis, appropriate marker order and map refinement process (Garcia et al., 2007). The algorithms in OneMap are developed in C language whereas, the data manipulation functions are coded in R language. This simultaneous estimation of linkage and linkage phases encourages the analysis of different marker types in various segregation patterns i.e., 1:1:1:1 (fully informative markers), 1:2:1, 3:1 (partially informative markers) and 1:1 (less informative markers). OneMap also allows to study all possible cross types, hence any dataset is easy to analyze except more complicated F1 populations derived from a cross between two outbred parents.

The basic steps followed to develop linkage maps for all 19 chromosomes include, loading data in to R environment (RStudio), filtering raw marker data (quality control/QC), linkage group formation, refined mapping and plotting (data visualization) given below. The consensus dataset for OneMap was prepared from the output files (JoinMap format) of GenomeStudio and ASSiST. The output files from both software were then cleaned, processed and formatted for subsequent use in R program. After formatting and cleaning the SNP data we got 6786 SNPS for 137 individuals for the further analyses. Initially, a consensus map was built for all 19 chromosomes.

The OneMap input dataset was formatted and prepared according to the OneMap requirements and finally consisting of 130 individuals (genotypes) and 6790 SNP markers (including 4 SSR markers). Dataset for the consensus map includes five different types of segregating markers i.e., “ab x cd”, “ef x eg”, “hk x hk”, “lm x ll” and “nn x np”. The genotypes (allele pairs) for each marker were converted according to the conversion scheme to make it readable in R program, in order to run an R package “OneMap” for the construction of genetic maps (Table 1).

Table 1. Notation used to identify markers and genotypes

		crosstype	Parent Cross			Observed bands			Offspring Observed bands	Segregation
A		1	ab	×	cd	ab	×	cd	ac, ad, bc, bd	1:1:1:1
		2	ab	×	ac	ab	×	ac	a, ac, ba, bc	1:1:1:1
		3	ab	×	co	ab	×	c	ac, a, bc, b	1:1:1:1
		4	ao	×	bo	a	×	b	ab, a, b, o	1:1:1:1
B	B_1	5	ab	×	ao	ab	×	a	$ab, 2a, b$	1:2:1
	B_2	6	ao	×	ab	a	×	ab	$ab, 2a, b$	1:2:1
	B_3	7	ab	×	ab	ab	×	ab	$a, 2ab, b$	1:2:1
C		8	ao	×	ao	a	×	a	$3a, o$	3:1
D	D_1	9	ab	×	cc	ab	×	c	ac, bc	1:1
		10	ab	×	aa	ab	×	a	a, ab	1:1
		11	ab	×	oo	ab	×	o	a, b	1:1
		12	bo	×	aa	b	×	a	ab, a	1:1
		13	ao	×	oo	a	×	o	a, o	1:1
	D_2	14	cc	×	ab	c	×	ab	ac, bc	1:1
		15	aa	×	ab	a	×	ab	a, ab	1:1
		16	oo	×	ab	o	×	ab	a, b	1:1
		17	aa	×	bo	a	×	b	ab, a	1:1
		18	oo	×	ao	o	×	a	a, o	1:1

Parents	Cross Type	Segregation	Observed bands	Type of markers
<ab x cd>	ab x cd	ac, ad, bc, bd	a = a, b = b, c = c, d = d	A1
<ef x eg>	ab x ac	ee, eg, ef, fg	e = a, f = b, g = c	A2
<hk x hk>	ab x ab	h-, kk	h = a, k =b	B3.7
<hk x hk>	ab x ab	hh, hk, kk	h = a, k =b	B3.7
<lm x ll>	ab x aa	ll, lm	l = a, m = b	D1.10
<nn x np>	aa x ab	nn, np	n = a, p = b	D2.15

Since, OneMap requires a specific file format, the allele combinations were converted as “aa = homozygous =a”, “ab = heterozygous = ab”, “bb = homozygous= b” and “null Allele = -“ etc.

The linkage groups were formulated for all 19 chromosomes, based on the final set of markers after multiple trials of using different LOD score. A combination of different LOD scores and recombination fractions were used until we get the final 19 linkage groups with most appropriate number of markers in each group. The threshold likelihood of odds (LOD) value was determined with 1,000 permutations at a $P = 0.05$ level (Churchill and Doerge, 1994).

Generally, OneMap uses four different ordering algorithms (Seriation (SER), Recombination Counting and Ordering (rec), Rapid Chain Delineation (rcd) and Unidirectional Growth (ug)) to order the markers in different way, a relatively best correct order is considered for the final map construction.. Combinations of different LOD scores and recombination fractions and algorithms were also used wherever required. Finally, parental and progeny haplotypes were found for all 130 individuals to assess the allelic contribution from each parent to the progeny.

2.6 QTL Analysis

2.6.1 MapQTL

Linkage map data were analyzed through a software "MapQTL" (licensed from Diana Bellin group), which is a computer program used to calculate the QTL position on genetic maps in different types of mapping populations. We used MapQTL version 5 which is based on previous version V-4.0 (Van Ooigen et al., 2002). It provides an improved and user friendly interface with good quality maps and easy export. It also allows to analyze multiple populations and maps at the same time. Final results are stored in files called "sessions", which can be accessed for any further inspection after needed computation. Another improved parameter is the creation of quality QTL charts and can easily be exported to files, windows and MS-Office etc. MapQTL 5.0 stores various settings in the directory MapQTL 5.0, which is created in y Documents directory while running the program (Van Ooigen et al., 2002). MapQTL also provides no built in limits and storage memory for needed amount of data is allocated dynamically besides the length of names (maximum of 20 characters for population, locus trait and linkage group names) and a RAM memory of 256 MB is recommended for reasonably sized projects (MapQTL manual 5).

MapQTL accepts text files as input dataset aided with the necessary instructions required to guide the program to conduct the analysis. For the population like CP the type of segregation may vary across the loci with four different segregating alleles (Table 2). The first two characters e.g., (a and b) in the given codes represent the alleles of the first parent and last two characters represent alleles of second parent and each distinct allele is represented with a different character. Two characters must be used for coding the genotypes of a CP population, representing two alleles for a single individual. Coding for genotypes depends on the segregation type (Table 3).

Table 2. Segregation type codes for population type cross pollinated (CP)

Code	Description
<abxcd>	locus heterozygous in both parents, four alleles
<efxeg>	locus heterozygous in both parents, three alleles
<hkxhk>	locus heterozygous in both parents, two alleles
<lmxll>	locus heterozygous in one parent
<nnxnp>	locus heterozygous in other parent

Table 3. Genotype codes for a CP population, depending on the locus segregation type

Seg. type	Possible genotypes
<abxcd>	ac, ad, bc, bd, -- (no dominance allowed)
<efxeg>	ee, ef, eg, fg, -- (no dominance allowed)
<hkxhk>	hh, hk, kk, h-, k-, --
<lmxll>	ll, lm, --
<nnxnp>	nn, np, --

Remarks:

1. each character a to p represents a distinct allele; "–"means unknown allele
2. h– and k– are dominant genotypes:
   h– means hh or hk, and
   k– means kk or hk
3. "." and u are treated equivalent to "–"

Three input data files were prepared, a) a locus genotype file (*loc-file*), which contains the genotype codes for all the loci of the segregating population. It has a specific sequential structure. The header of the file contains four instructions on the contents of the data body. The data body contains the actual genotype information for each locus and for all individuals. The four instructions define the nameof the population (which is for administrative use only), the type of the population, the number of loci, and the number of individuals. These instructions can be given in any order within the header. The syntax of the four instructions is:

```
name = NAME (name of population)
popt = POPT (population type)
nloc = NLOC (number of loci)
nind = NIND (number of individuals)
```

Likewise, a (*map-file*) consisting of map positions of all loci. The loci are examined individually by nonparametric mapping and the map positions are used just to sort the loci. The *map-file* is very line-structured and contains no header. Finally, the quantitative file (*qua-file*) which consists of phenotypic (quantitative) traits data of all individuals. It follows a sequential structure, with the header containing three instructions followed by name so the traits. The file data contains the actual information for each trait and individual. The three instructions define the numbers of traits and individuals and the text that indicates a missing value. The syntax of the three instructions is given below.

```
ntrt = NTRT (number of traits)
nind = NIND (number of individuals)
miss = MISS (missing values)
```

In the data body all traits values are mentioned and grouped for each individual whereas, in the loc-file the data are grouped for each locus.). Although the layout is completely sequential.

2.6.2 Interval Mapping (IM)

After formatting the three input files, a significant LOD threshold value was found by launching the computation for permutation test in order to detect the genomic regions for each trait and individual chromosome. The QTL analysis was conducted with IM, which calculated a QTL likelihood map at each centimorgan (cM) position to determine presence and subsequent genetic effect of any segregating QTL. IM analysis produced its output in the form a list of genomic regions putatively involved in controlling the phenological traits under study. After determining the LOD threshold level, the genomic regions with significant LOD peaks more than the LOD threshold were scored and their respective confidence interval, involving putative QTL region, was scored.

2.6.3 LOD Score and Permutation Test (PT)

The principle of IM includes the testing of null hypothesis (H_o) for likelihood of having QTLs with zero genetic effect to the alternative hypothesis (H_1) with likelihood of having QTLs with significant segregating effect by using the likelihood ratio ($\log_{10}$) of LOD score. When LOD score exceeds the significant threshold of any linkage group, a segregating QTL is likely to be present at that specific peak. The level of peak also indicates the estimated position (cM) of QTL in the respective LG. This requires the correct scoring of LOD value with specific algorithm (Van Ooijen et al., 1999), which depends on the genome size, number of markers and number of chromosome

pairs. The permutation test (PT) is a statistical test used to calculate the significant threshold for each LG along the whole genome. PT also enables to customize the number of PT i.e. 1000 (current study) to rearrange the quantitative values at random. Once PT is completed, IM is done based on maximum LOD value, resulting in distribution frequency of the maximum LOD values under the H_o hypothesis (with no QTL). The further results in a table with absolute and cumulative frequencies of each LG. For the current study, a LOD threshold value i.e., "*P-value* = 0.05" was considered based on a selection from LOD values wrt 1- 0.05 (0.95) in order to score a QTL.

2.7 Gene Annotation

The three instructions define the numbers of traits and individuals and the text that indicates a missing value. The syntax of the three instructions is given below.

2.8 Data Analysis

The phenotypic data (phenology and maturity traits) from three replicates at both vineyards over three years, were observed, measured, recorded in excel sheets, analyzed through one way ANOVA and presented through distribution graphs and tables, generated both in excel and R statistical software. Correlation graphs for both vineyards for the years 2021 and 2022 were generated in excel, whereas correlation coefficient (spearman rank correlation) was measured in R statistical software. The genotypic data (SNP genotyping) was done through hybridization of DNA samples from plant population on GrapeReSeq *Vitis*18KSNP chip, including GenomeStudio and ASSiST software. Finally, QTL analysis was conducted through Interval Mapping (IM) in mapping software MapQTL 5.0.

3 RESULTS

The main aim of the project was to explore the genetic determinants controlling phenology in grapevine and since the project was developed within the Verona province viticultural area, a locally raised cross mapping population derived from the local grape cultivar Corvina, was used to identify and map the putative QTLs and underlying candidate genes controlling phenological stages. The plant genotypes studied in the current research project belong to the segregating population (CP-F1) derived from the cross between Corvina (C) and Solaris (S). The segregating population (CxS) was evaluated both phenotypically and genetically. The crossing between these two varieties was made in 2016, with Solaris used as pollinator and Corvina as seed carrier.

3.1 Phenotypic evaluation in the field

The phenotypic evaluation for the three phenological traits i.e., budburst, flowering and veraison along with the berry juice soluble solid content (°Brix) as a maturity measure were made in the field for three years (2020-2022) at Verona site and for 2 years (2021 and 2022) at Negrar vineyard. To gain information about other technological maturity parameters of each genotype, the analysis of average berry weight, pH, acidity and phenolic content was also carried out in laboratory. The field observations were recorded in the form of Julian days based on the respective date for each field survey and respective year of observation. Both vineyards initially included 120 different individuals but some plants did not survive or were not possible to observe, in each replicate at both vineyards. Afterwards few additional genotypes were added to the existing population in order to make a considerable population size (150 genotypes) for genotyping (Appendix Table 1). When necessary (i.e., in case of missing values) the precise date (Julian days) for a specific phenological determination for each year and location have been interpolated through an R script. The correlation (spearman rank) have also been found through an R script and excel for the 4 traits (Budburst, flowering, veraison and brix) between both replicates at Verona's vineyard and Negrar's vineyard for the years 2021 and 2022.

The graphic representation with mediated distribution curve, for each trait, for the two replicates of Verona's vineyard (Left and Right) with average and for Negrar's vineyard is presented (Fig. 13-16). Number of plants are shown on Y-axis whereas the date in Julian days, at which the phenological stage occurred is shown on X-axis of the histogram. The parental distributions have been marked with arrow head with respective name viz., C and S respectively.

3.1.1 Budburst data

In order to observe the budburst, the four distal buds of a cane were selected on the main shoot well exposed to the sunlight. The initial phenotypic measurements started in the month of April and were performed approximately twice a week. The bud opening time was measured according to the criteria shown in Figure 13 of Materials and methods. The distribution of gradual bud opening time of the population is shown in Fig 13-A, B and C for each replicate (left and right row) and for the average value at Verona's vineyard for the year 2020, 2021 and 2022.

The graphical presentation of budburst data show mediated distribution for three replicates at both vineyards (Verona and Negrar). Each replicate consisted of 150 individuals however, due to the young age of some of the plants, it was not possible to collect the data from all plants. The parental growth behavior is indicated as C (Corvina) and S (Solaris) with respective arrows. The graphs 13 A-C shows the data distribution over three years for left replicate, right replicate and average of both replicates from Verona vineyard whereas in graph 13-D, the data is shown from Negrar's vineyard for two years.

The average budburst data for parental lines and progeny individuals show reproducible behavior over three years from Verona's vineyard (Fig 13 A-C). A similar reproducible behavior is shown also from Negrar's vineyard for parental lines and slightly transgressive behavior from progeny individuals (Fig 13-D). There is also an indication of anticipation in budburst data for progeny individuals in each proceeding year from Verona's vineyard however, a slightly opposite behavior from Negrar's vineyard, as there is a slight delay in budding period in 2022 as compared to 2021. Moreover, a slight anticipation is observed in Negrar's vineyard as compared to Verona's vineyard in 2022 both for parental and progeny individuals.

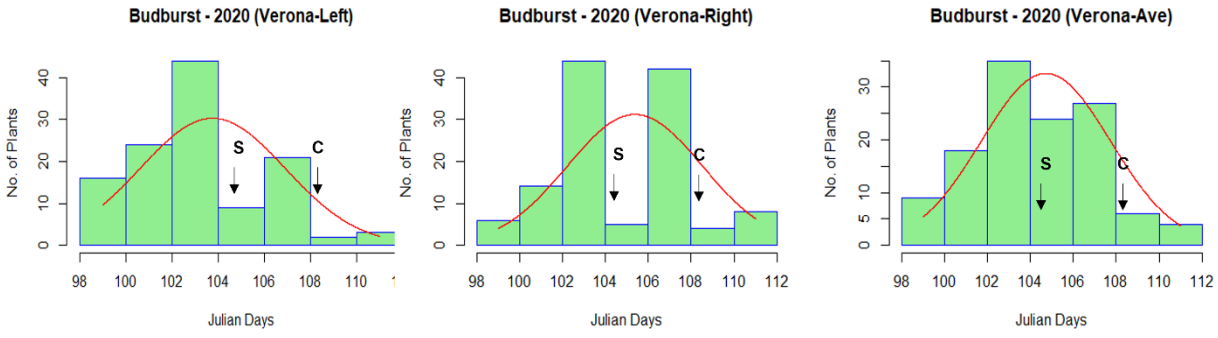

Figure 13-A: Distribution data for budburst time for both replicates (left and right) and averaged budbreak time (left-right) in CxS population at Verona's vineyard for 2020.

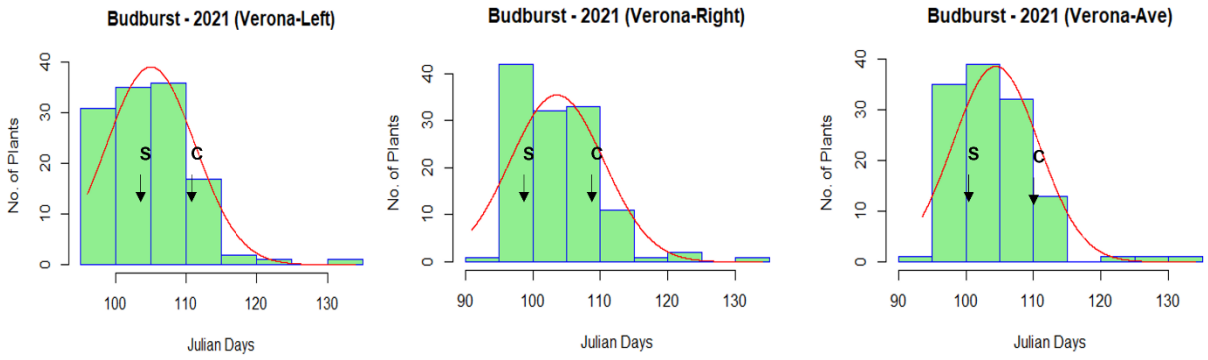

Figure 13-B: Distribution data for budburst time for both replicates (left and right) and averaged budbreak time (left-right) in CxS population at Verona's vineyard for 2021.

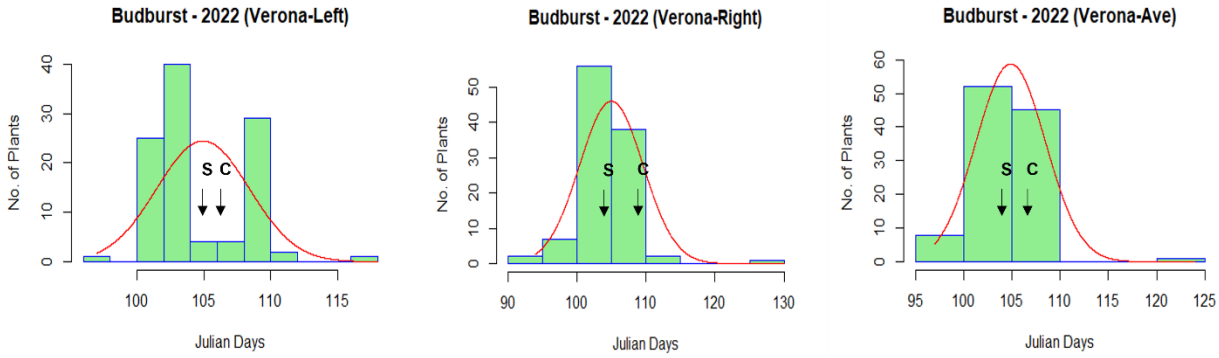

Figure 13-C: Distribution data for budburst time for both replicates (left and right) and averaged budbreak time (left-right) in CxS population at Verona's vineyard for 2022.

Likewise the budburst distribution for the Negrar's vineyard is shown for the year 2021 and 2022 (Fig 13-D).

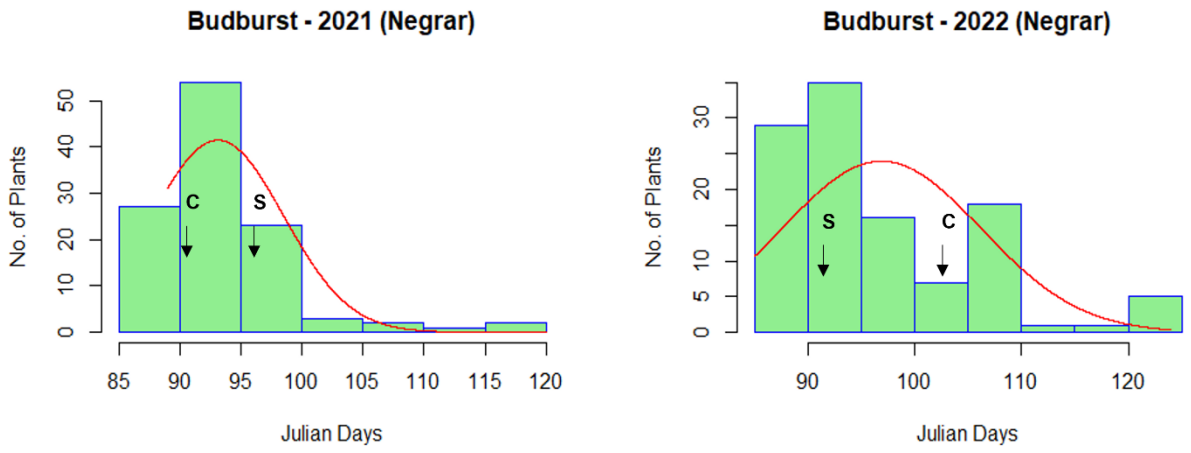

Figure 13-D: Distribution data for budburst time for Negrar's vineyard in CxS population for 2021 and 2022.

3.1.2 Flowering

Following budburst measurements, the data for flowering time was measured for both locations. The flowering date for fertile buds (same four distal buds used for budburst) was defined as the stage when inflorescences had 50% of open flowers (Fig 14). The graphical representation of flowering time data distribution is shown for Verona's vineyard over three years (Fig 14 A-C). Flowering time data is shown in the graphs (Fig 14 A-D). The average flowering data for the year 2020 and 2021 show somewhat normally distributed reproducible data whereas a slightly transgressive distribution for the year 2022 from Verona's vineyard (Fig 14 A-C). Likewise, the flowering data express transgressive behavior for both years (2021 and 2022) from Negrar's vineyard (Fig 14-D). Flowering time data both for parental and progeny individuals is clearly anticipated with each successive year from Verona's vineyard, however a slightly opposite behavior has been observed at Negrar's vineyard where flowering initiation was slightly late in 2022 as compared to 2021 (Fig 14 B-D). The same behavior is observed while comparing both locations for both 2021 and 2022 (Fig 14 C-D). A slight transgressive behavior was observed at Negrar's vineyard for both years. In general, the flowering data has been observed more difficult to interpret due to fewer number of surveys.

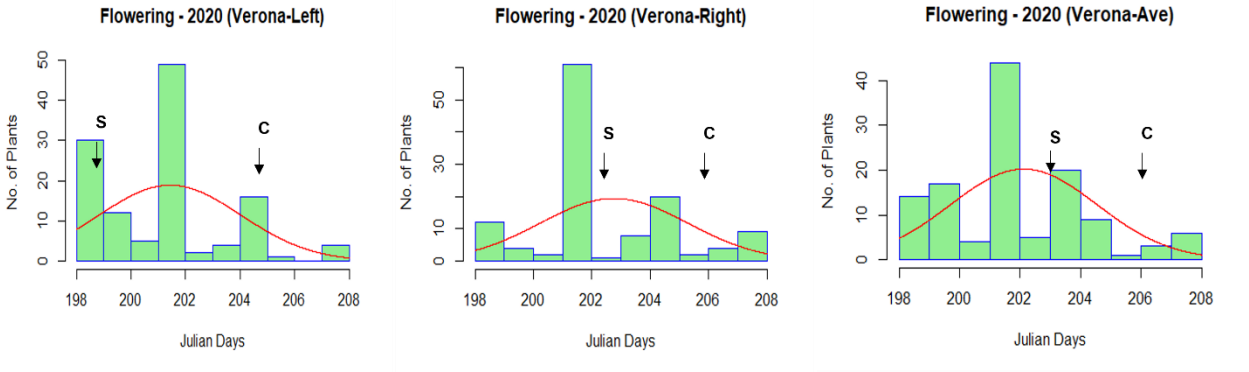

Figure 14-A: Distribution of flowering time at Verona's vineyard in CxS population for the year 2020.

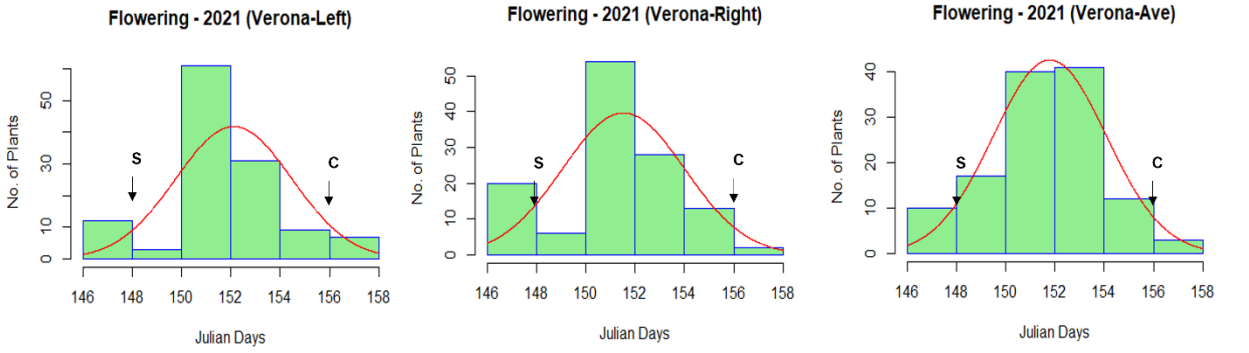

Figure 14-B: Distribution of flowering time at Verona's vineyard in CxS population for the year 2021.

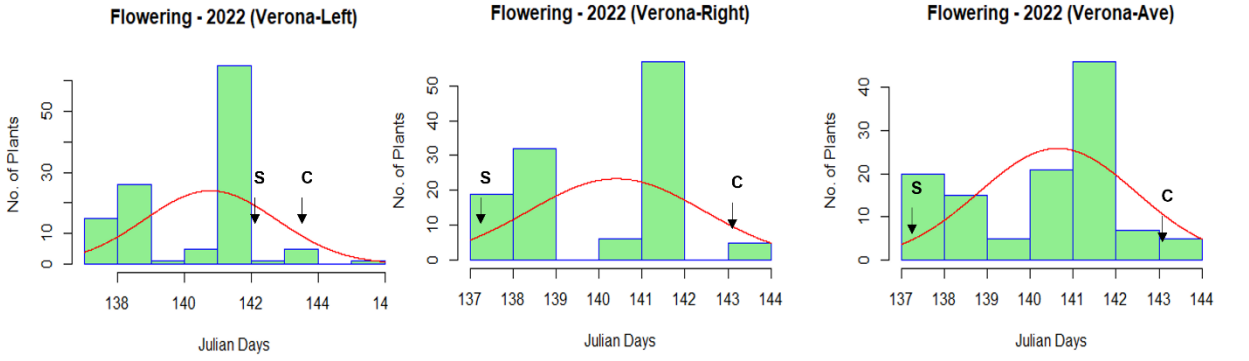

Figure 14-C: Distribution of flowering time at Verona's vineyard in CxS population for the year 2022.

Similarly, data for flowering time at Negrar vineyard has been shown for the years 2021 and 2022 (Fig 14-D).

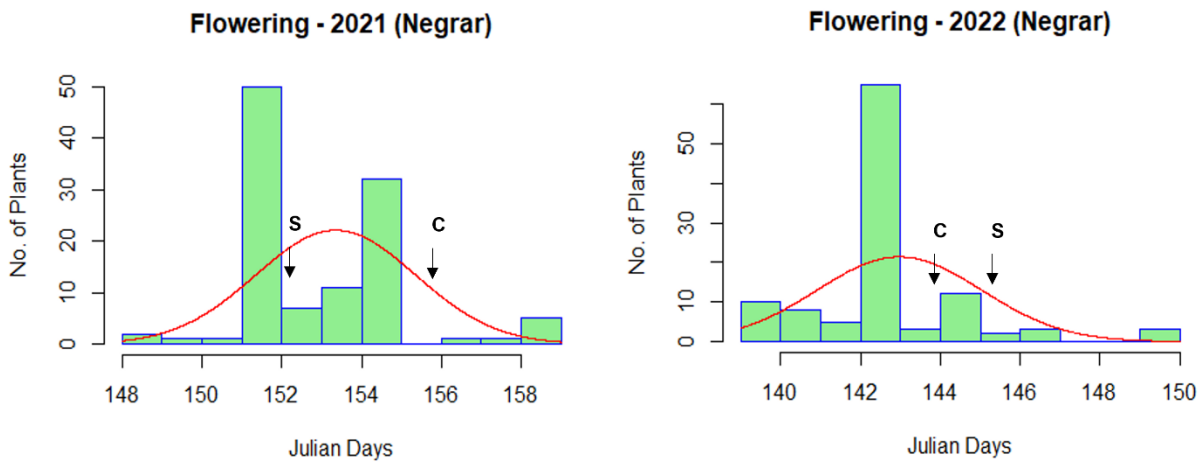

Figure 14-D: Distribution of flowering time at Verona's vineyard in CxS population for the year 2022.

3.1.3 Veraison

The veraison phase (onset of ripening) defines the beginning of the second berry growth phase, with the phenomenon of the decrease in chlorophyll and the assumption of a translucent appearance (in white varieties) or red pigmentation (in red varieties) of the berry. The distribution of veraison lasted for more than a month, and is shown in Fig 15 A-C for Verona's vineyard over three years. The veraison time was recorded on the same clusters used for budburst and flowering time measurements. Graphs 15 A-C highlights the anticipated average veraison data for all three years at Verona's vineyard, both for parental and progeny individuals. Majority of the plants in case of 2020 at Verona's vineyard are little skewed towards left side but this behavior is seemed to be overcome in successive years with majority of the plants falling in normally distributed curve area (Fig 15 A-C). The distribution data from Negra's vineyard express reproducibility in case of progeny individuals but in case of parental individuals, there is slight delay in veraison time in 2022 as compared to 2021. The similar delayed behavior is evident at both locations when data for 2022 is compared to 2021 between both vineyards (Fig 15 B-D and C-D).

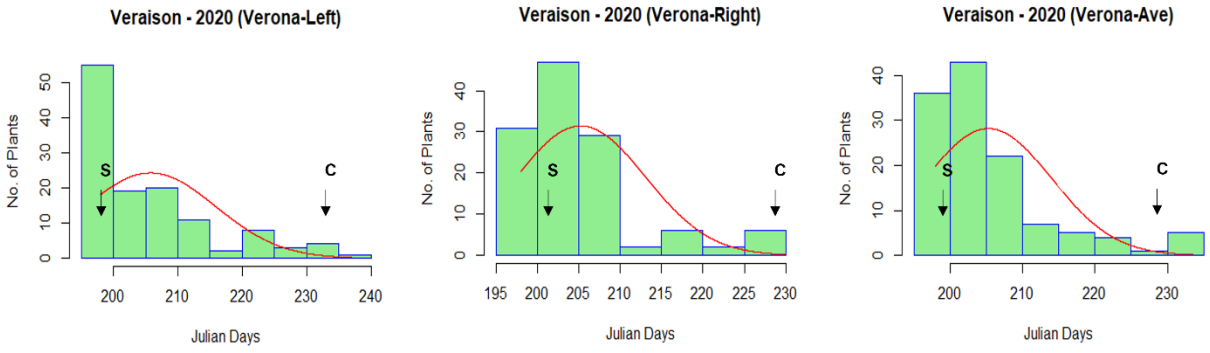

Figure 15-A: Distribution of Veraison time at Verona's vineyard in CxS population for the year 2022.

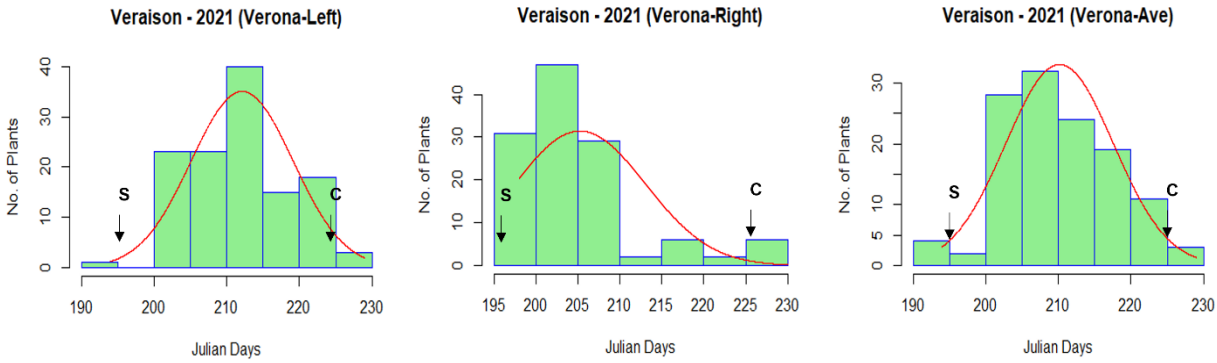

Figure 15-B: Distribution of Veraison time at Verona's vineyard in CxS population for the year 2021.

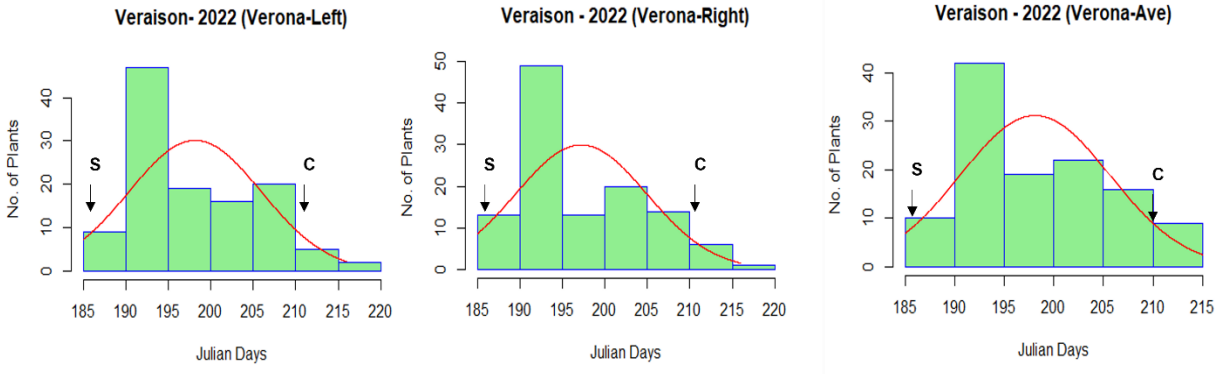

Figure 15-C: Distribution of Veraison time at Verona's vineyard in CxS population for the year 2022.

Similarly, veraison time data were observed with same method at Negrar's vineyard and expressed as below (Fig 15-D).

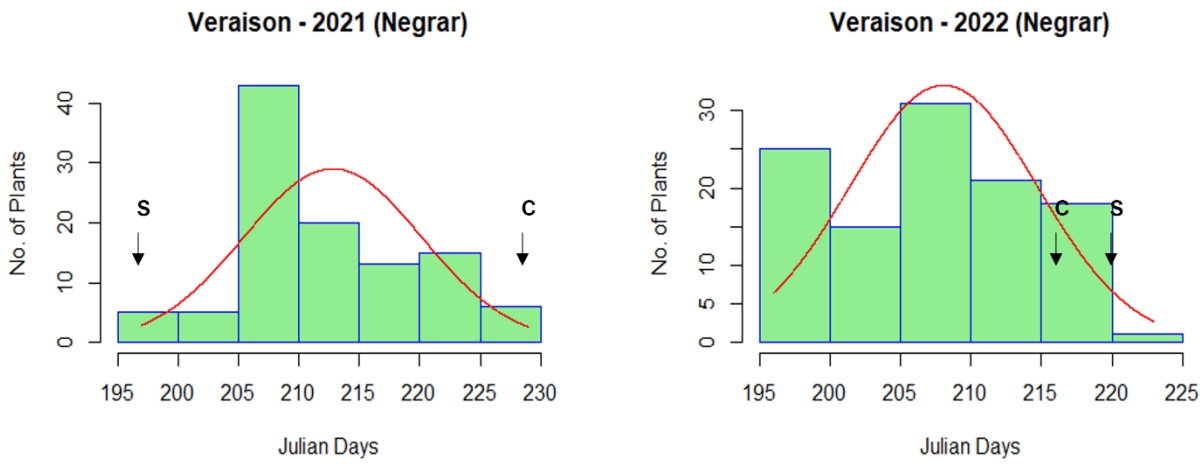

Figure 15-D: Distribution of Veraison time at Negrar's vineyard in CxS population for the year 2021 and 2022.

3.1.4 Ripening

Ripening of berries was defined by the measurement of total soluble sugars (°Brix) according to the method described in the section "Materials and methods". Some plant genotypes did not produce any grape clusters due to their young age. °Brix level was recorded by examining the three berries from three different bunches as the average berries for each plant reach the level of 19 °Brix on portable refractometer 2-3 times a week. Furthermore, observing the trend of the populations in the graphs, a clear difference in the ripening intervals could be observed (Fig 16 A-D). A reproducible behavior is expressed with a slight delay in the year 2021 at Verona's vineyard. Parental behavior is also reproducible and anticipated over three years (Fig 16 A-C). Similarly, reproducibility is observed at Negrar's vineyard in case of progeny individuals only and a slightly opposite behavior was observed in case of parental lines for the year 2022 (Fig 16-D). Almost similar behavior in observed when both vineyards were compared for the year 2021 and 2022.

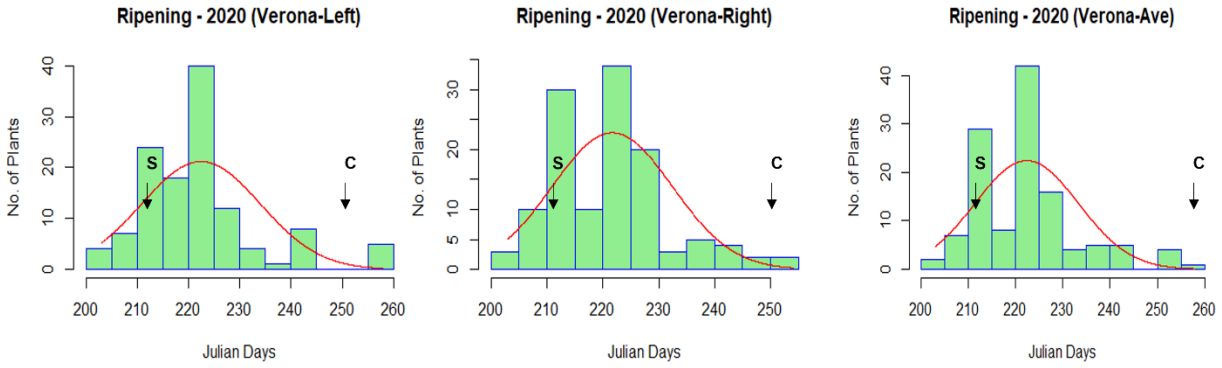

Figure 16-A: Distribution of Brix level at Verona's vineyard in CxS population for the year 2020.

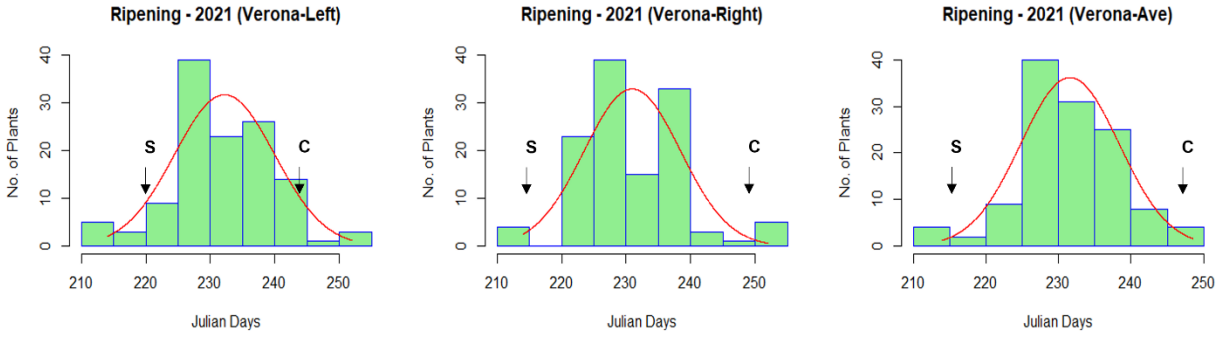

Figure 16-B: Distribution of Brix level at Verona's vineyard in CxS population for the year 2021.

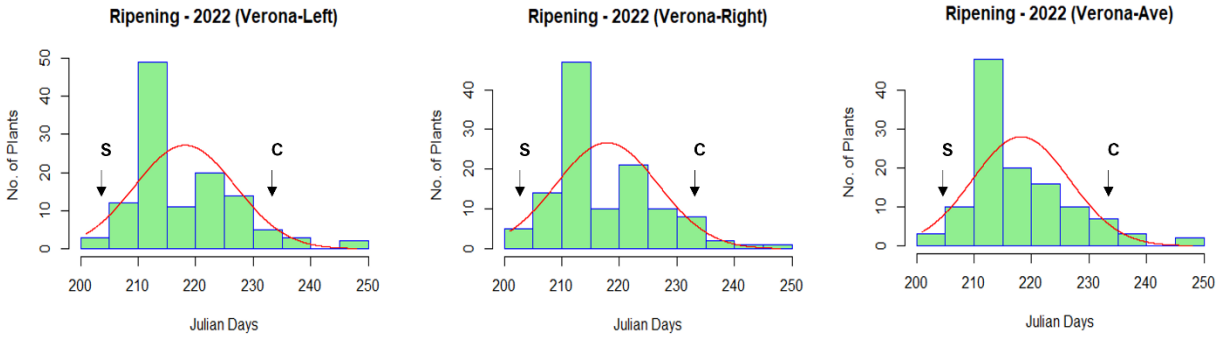

Figure 16-C: Distribution of Brix level at Verona's vineyard in CxS population for the year 2022.

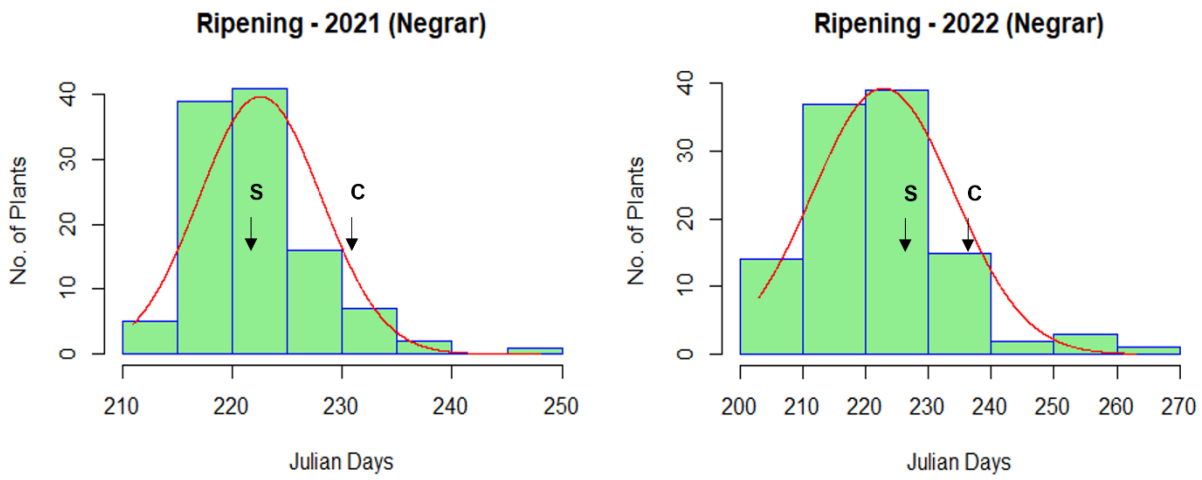

Figure 16-D: Distribution of Brix level at Negrar's vineyard in CxS population for the years 2021 and 2022.

3.2 Correlation analysis

3.2.1 Correlation between CxS genotypes at Verona's vineyard between two adjacent replicates (left and right side).

To assess the consistency of the phenological behavior of the populations grown in the two nearby replicates, the correlation between the two data sets has been measured. The spearman rank correlation for each phenology trait was calculated and results are presented below for both replicates (Table 4-A). The dead plants or non-available data were removed from the analysis. Flowering, veraison and ripening showed relatively higher correlation as compared to budburst.

3.2.2 Correlation between CxS genotypes grown at Negrar's vineyard.

Likewise, correlation analysis has also been performed between phenological data collected in the two experimental years (2021 and 2022) at Negrar's vineyard. Moreover the comparison between data collected in Verona and Negrar was also performed (Table 4-A and Figure 1 in Appendix). In general, a quite low correlation was observed for the phenological traits budburst and flowering for the years 2021 and 2022 at Negrar's vineyard and at Verona's vineyard for the year 2021. However, a stronger correlation was observed for veraison and ripening in different years.

	Verona's vineyard			Negrar's vineyard	Verona's vineyard	Verona x Negrar	Verona x Negrar
	L+R (2020)	L+R (2021)	L+R (2022)	(2021 x 2022)	(2021 x 2022)	(2021 x 2021)	2022 x 2022
Budburst	0.57	0.46	0.44	0.25	0.53	0.31	0.39
Flowering	0.41	0.54	0.58	0.27	0.66	0.34	0.48
Veraison	0.84	0.72	0.78	0.70	0.79	0.72	0.67
Ripening	0.77	0.63	0.32	0.48	0.59	0.45	0.33

Table 4-A: Spearman rank correlation for both vineyards among different years of propagation.

The components of variance (analysis of variance) have been analyzed through one way ANOVA in excel. All four phenological traits were observed to be significantly different over three years (2020-2022) at both vineyards (Tables 4 B and C) as *F-stat* values were observed higher than *F-critical* value, whereas a non-significant differences have been observed, as *F-stat* values were observed lower than *F-critical* value in two cases i.e., budburst only at Verona vineyard over three years and ripening at Negrar vineyard over two years (2021-2022) (Table 4-D).

ANOVA Budburst (Verona + Negrar)

Source of Variation	*SS*	*df*	*MS*	*F*	*P-value*	*F crit*
Between Groups	9477.69	4	2369.423	58.133	7.89E-39	2.393755
Within Groups	16670.29	409	40.75865			
Total	26147.98	413				

A

ANOVA Flowering (Verona + Negrar)

Source of Variation	*SS*	*df*	*MS*	*F*	*P-value*	*F crit*
Between Groups	204980.5	4	51245.11	11066.8	0	2.395184
Within Groups	1778.122	384	4.630525			
Total	206758.6	388				

B

Table 4-B: ANOVA showing significant differences for budburst (A) and flowering (B) at both vineyards over three years.

ANOVA Veraison (Verona + Negrar)

Source of Variation	SS	df	MS	F	P-value	F crit
Between Groups	10891.75	4	2722.937	48.4367	7.3E-33	2.39561
Within Groups	21193.58	377	56.21639			
Total	32085.33	381				

A

ANOVA Ripening (Verona + Negrar)

Source of Variation	SS	df	MS	F	P-value	F crit
Between Groups	8833.275	4	2208.32	32.4576	3.79E-23	2.39646
Within Groups	24765.44	364	68.0370			
Total	33598.72	368				

B

Table 4-C: ANOVA showing significant differences for veraison (A) and ripening (B) at both vineyards over three years.

ANOVA Budburst (Verona)

Source of Variation	*SS*	*df*	*MS*	*F*	*P-value*	*F crit*
Between Groups	17.59606	2	8.798032	0.339085	0.712746	3.031629
Within Groups	6538.488	252	25.94638			
Total	6556.084	254				

A

ANOVA Ripening (Negrar)

Source of Variation	*SS*	*df*	*MS*	*F*	*P-value*	*F crit*
Between Groups	8.910519	1	8.910519	0.106882	0.744256	3.915138
Within Groups	10671.06	128	83.36765			
Total	10679.97	129				

B

Table 4-D: ANOVA showing non-significant differences for budburst (A) and ripening (B) at Verona and Negrar respectively.

3.3 Analysis of ripening technological parameters

3.3.1 Determination of Average Berry Weight

Average berry weight for the both vineyards (Negrar and Verona) is shown for the years 2021 and 2022 in Table 5-7 (Appendix). Graphical data for average berry weight shows that most of the progeny individuals have average berry weight ranging between 0.99 g and 0.66 g for the year 2021 and 2022 for Negrar's vineyard, respectively (Fig 17-A). The average berry weight for both parental lines (C and S) seems to decreased in equal ration for the year 2022 as compared to 2021. In case of Verona's vineyard, the average single berry weight for most of the progeny individuals has been observed as 1.2-1.8 g for the year 2021 and 1.3-2.1 g for the year 2022. The parental lines expressed approximately similar measurements for both years (Fig 17-B).

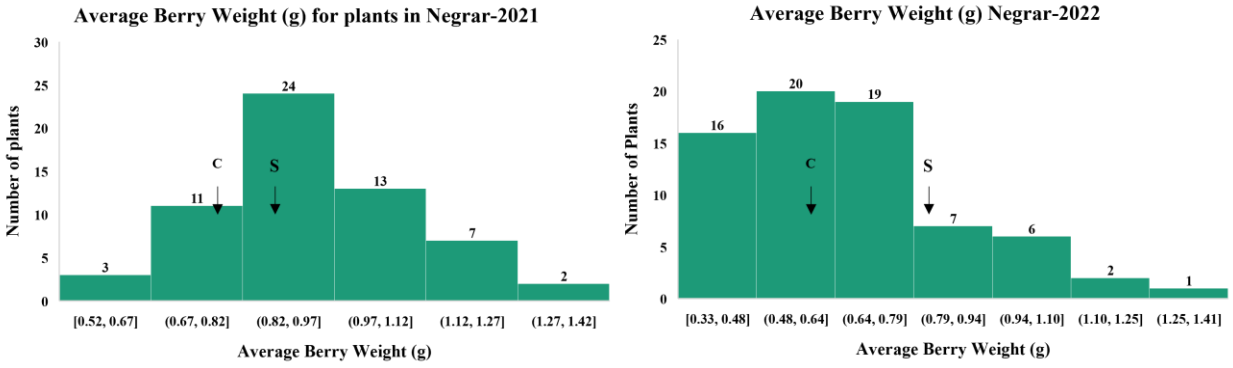

Figure 17-A. Average berry weight (gram) for the Negrar vineyard for 2021 and 2022

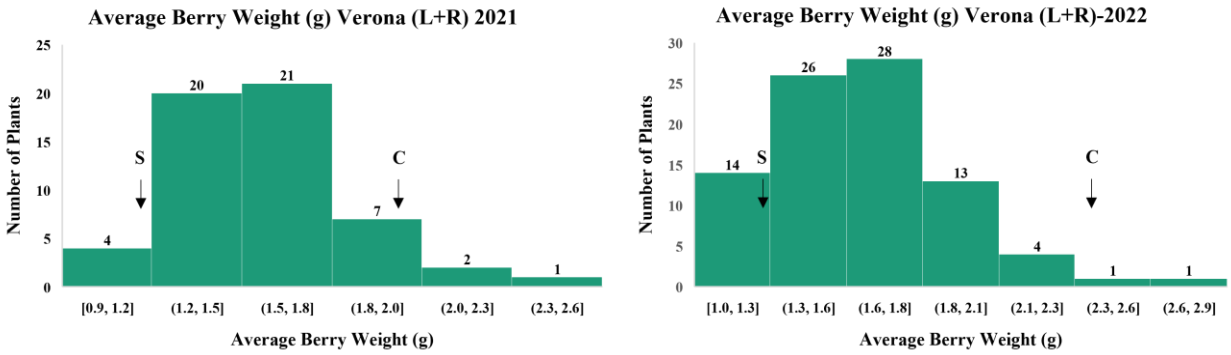

Figure 17-B. Average berry weight (gram) for the Verona vineyard for 2021 and 2022

3.3.2 Determination of Total Acidity

The graphical distribution of plants with their relative acidity in g/L for both locations and for two years (2021 and 2022) is shown in Figure 17. The graphical data for total acidity highlights most of the progeny individuals falling under normally distributed curve in case of 2021, with total acidity ranging between 5-13 g/L and with slightly transgressive behavior with 4.5-19 g/L for Negrar's vineyard. The parent C expressed reproducibility (closer to 7 g/L) across both years whereas S expressed slightly higher level of acidity in 2022 as compared to 2021 (Fig 17-A). Conversely, the progeny data for total acidity for Verona's vineyard in 2022, has been observed with majority of individuals falling under normal distribution curve with 6.5-12.5 g/L of acidity (Fig 18-B), whereas in 2021, the data seems relatively more transgressive showing the acidity level from 3-11 g/L. likewise, the parental data expresses approximately similar behavior for both years in Verona's vineyard (Fig 18-B).

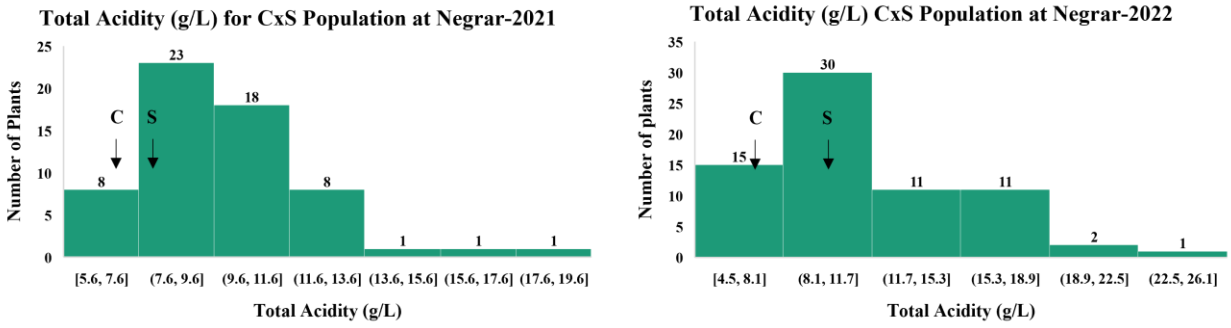

Figure 18-A. Total Acidity for the CxS population at Negrar vineyard for 2021 and 2022.

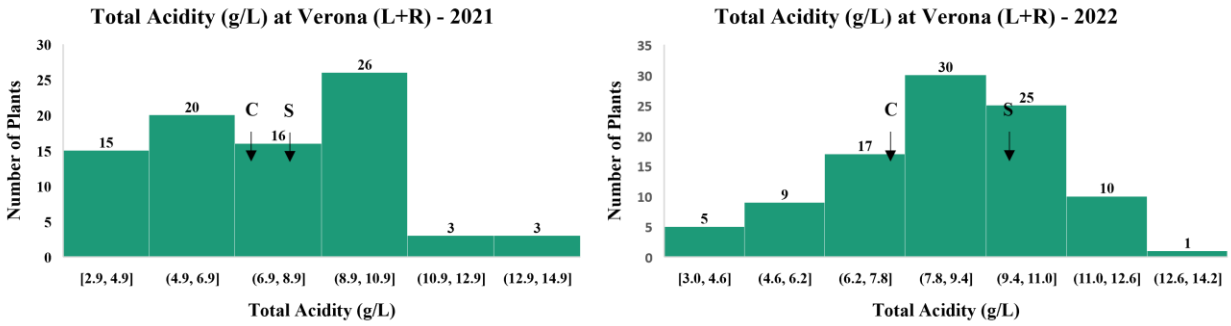

Figure 18-B. Total Acidity for the CxS population at Verona vineyard for 2021 and 2022.

3.3.3 Determination of pH

The pH for three biological replicates from both locations was observed to be falling between 2.4 to 3.3 for most of the plants propagated in 2021 and 2022, however some plants were also found be falling out of this range (Fig 19 A, B). The pH for three biological replicates from both locations was observed. The graphs express the pH values in the range between 2.4-3.3 for most of the plants propagated in 2021 and 3-3.5 in 2022 in Negrar's vineyard. Both parental lines show a pH value slightly less than 3 in 2021 and slightly higher than 3 in 2022 (Fig 19-A). On the other hand, the pH values, showing normal distribution, for most of the progeny individuals and parental lines fall between 3-3.3 in 2021. Likewise, most of the progeny individuals and parental lines fall in the range of 3-3.2 (Fig 19-B).

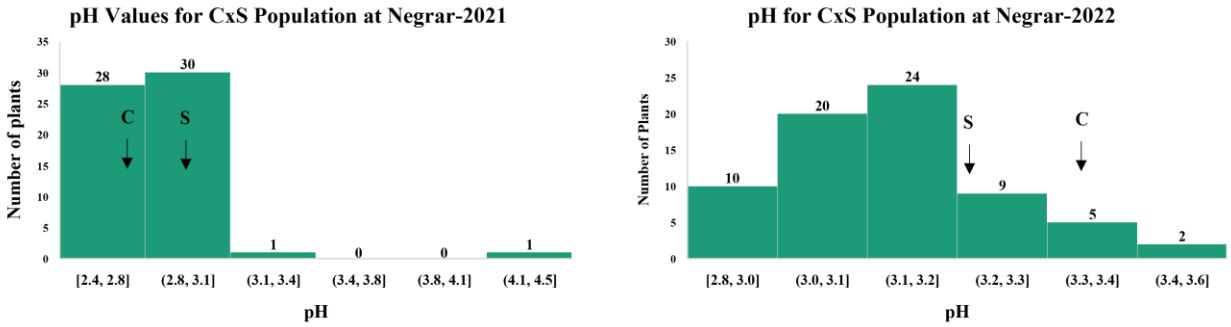

Figure 19-A. pH values for the CxS population at Negrar vineyard for 2021 and 2022.

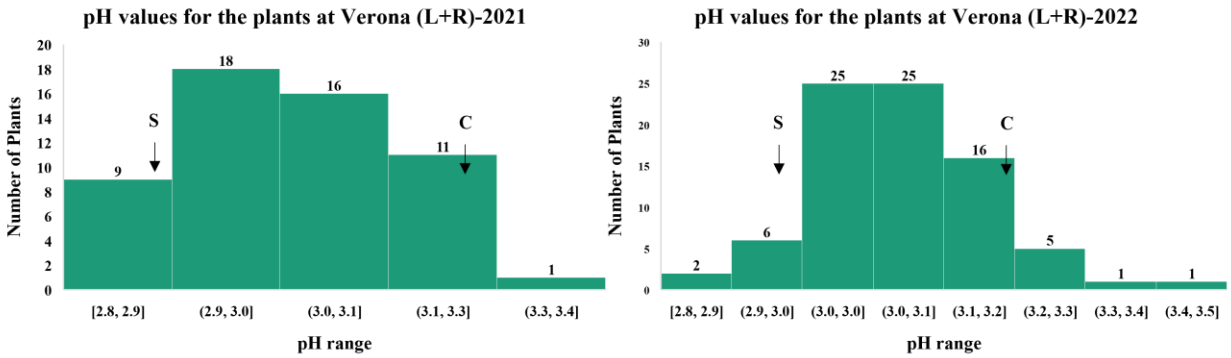

Figure 19-B. pH values for the CxS population at Verona vineyard for 2021 and 2022.

3.3.4 Determination of ºBrix level (Laboratory)

Once the ripening process was assumed to be completed based on reaching the sugar level corresponding to 19 ºBrix for each genotype, the grape clusters were harvested, and a sub-sample of 30 berries was weighted and mashed, and a small quantity of juice was taken with a disposable pipette to measure the Brix degree to confirm the correct measure made in the field. The observed level of 19 ºBrix for most of the plants was confirmed: the presented graphs show a clearly defined of about 19 ºBrix level for most of the plants at both locations (Fig 20 A, B). However there were also some samples that were clearly at an earlier or at a more advanced ripening stage. This is probably related to the heterogeneity of the ripening stage reached by the berries of the same plants that is reflected by the different °Brix of the field sample compared to the sample measured in laboratory.

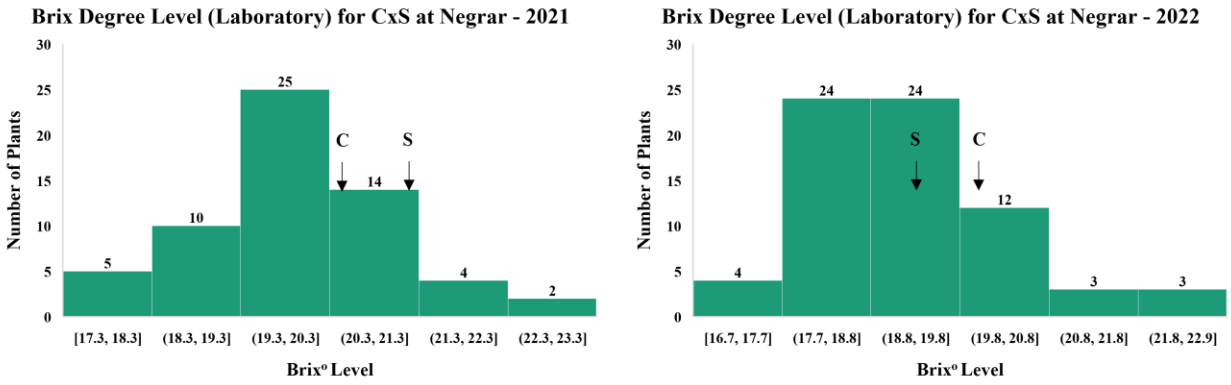

Figure 20-A. Brix level for the CxS population at Negrar vineyard for 2021 and 2022.

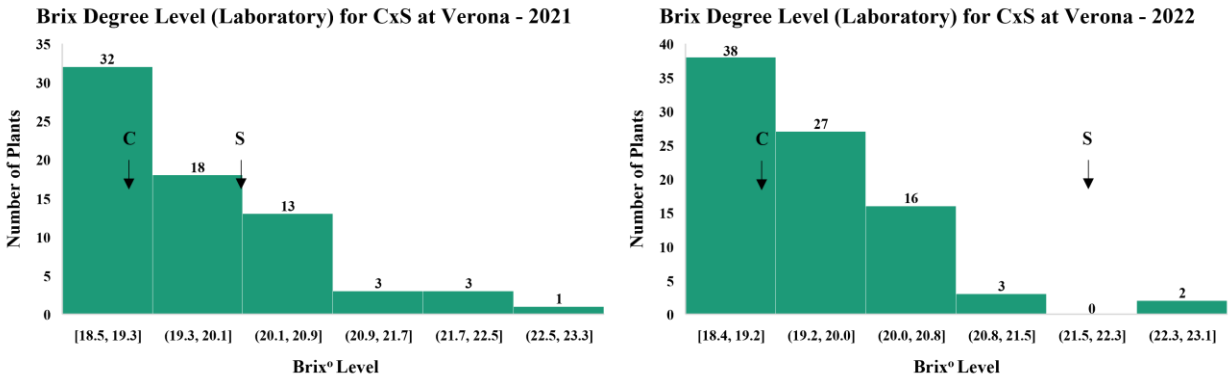

Figure 20-B. Brix level for the CxS population at Verona vineyard for 2021 and 2022.

3.4 Genotyping

The major aim of this project was to explore the genetic determinants controlling grapevine phenology. For this purpose the F1 progeny (appendix table 1) of CP population from the genetic cross between Corvina and Solaris (CxS) was developed and analyzed and subsequently under genetic evaluation, linkage maps were developed ultimately a QTL analysis study was performed.

3.4.1 DNA Extraction and Quantification

The extracted genomic DNA was quantified through NanoDrop (ThermoFisher) and the integrity of DNA was validated through agarose gel electrophoresis (an example Table 5, Fig 21).

Plant no.	DNA(ng/µl)	A260/A280	A260/A230
C	131.2	1.84	2.09
S	140.5	1.72	1.42
132	137	1.8	171
133	184	1.83	2.04
134	199	1.82	1.95
135	109.2	1.82	1.94
136	207	1.85	2.09
137	423.7	1.84	2.02
138	41.5	1.88	1.98
132	137	1.8	1.71

Table 5: Quantification of extracted DNA through nanodrop.

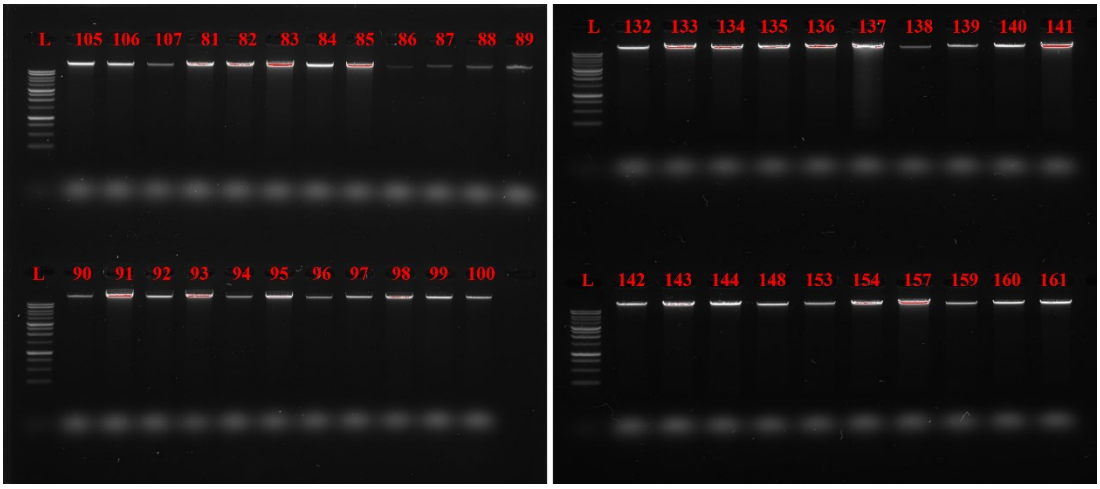

Figure 21: Verification of DNA integrity through gel electrophoresis.

The kinship of plant genotypes was verified with already designed SSR primer (UDV737) through Sanger Sequencer. Initially, DNA from 120 individuals were extracted from Verona's vineyard (Verona), however in order to complement the standard 96 well assay lay out, for SNP-ChiP hybridization few additional genotypes were added (appendix table 2) afterwards to make a total size of 144 for.

3.4.2 High throughput SNP Genotyping

Genotypic characterization was performed by using an Illumina *Vitis*18KSNP-ChiP hybridization kit (Laucou et al., 2018). Theoretical Illumina SNP positions were recalculated by re-mapping the flanking regions (2x60 bp) with NCBI/BLAST1 v2.2.31. Initially, we got approximately 18071 SNPs from SNP-Chip assay (Table 6) and 11285 SNP markers were discarded as monomorphic, polymorphic, distorted and null-allelic SNP markers. finally a set of 6786 SNP markers were approved for subsequent steps.

SNP-ChiP Hybridization Summary	
Approved	6786
Discarded	11285
Monomorphic	8270
Failed	2244
Distorted / Unexpected Segregation	746
Null-Allelic / Failed	25
Total	**18071**

Table 6: Output from SNP-ChiP assay revealing different types of SNPs.

3.5 Genetic Maps development

The process of consensus genetic linkage map construction was performed following the workflow mentioned on page 33 under section "Genetic evaluation" of Materials and methods. An initial dataset of total 6790 SNP makers (6786 SNPs+4 SSRs=6790 total markers) was prepared and formatted according to formatting criteria of an R package "OneMap", to construct the genetic maps. The SNP-ChiP output files were converted into JoinMap input file format by the software "ASSiST". The segregating markers were distributed between both parental lines (Corvina as ♀ and Solaris as ♂) into five segregation types of markers (Table 1 & 2, Materials and Methods).

Initially 17 linkage groups with 3231 SNPs, were formulated where one big LG was found consisting of huge number of markers from 2 different LGs, which later on was split into 2 respective LGs, thus making it a total number of 19 LGs (Table 7-A).

LGs	No. Of Markers
1	237
2	172
3	184
4	152
5	109
6	178
7	242
8	169
9	104
10	170
11	143
12	154
13	116
14	205
15	166
16	182
17	164
18	218
19	166
Total	3231

A

Chromosome No.	No. of Markers	Length (cM)
1	224	63.72
2	166	76.69
3	179	57.12
4	150	69.6
5	98	57.58
6	167	62.45
7	230	76.48
8	169	60.25
9	101	55.36
10	156	58.95
11	136	60.41
12	148	65.77
13	103	58.51
14	185	56.38
15	157	54.7
16	177	66.33
17	159	68.82
18	202	81.13
19	160	65.41
Mean	**161.421053**	**63.9821053**
Total	**3067**	**1215.66**

B

Chr	Coverage.PN12x.v.2.
1	94.8
2	95.46
3	92.81
4	94.97
5	94.36
6	93.51
7	74.78
8	98.95
9	61.41
10	75.48
11	96.97
12	92.28
13	81.77
14	99.04
15	98.76
16	92.82
17	87.56
18	83.07
19	96.83

C

Table 7: Number of markers for each LG (A), map summary: showing the total length of genetic map with individual chr. Map size and markers (B) and coverage of all chromosome's maps against reference genome assembly (C).

The 3231 SNPs were then processed for quality control (QC) and after filtering redundant, null-allelic and distorted SNPs, a final set of 3067 SNPs were projected by using different ordering algorithms. At initial stage, raw genetic maps for 19 chromosomes were observed, with huge gaps between the adjacent markers and two different maps on single chromosome, which were then removed through different ordering algorithms (ser, rec, rcd and ug), force mapping functions through R scripting (OneMap) and manually fine ordering of the SNP markers based on their physical position in the reference genome. Finally, a consensus map of high density linkage data was built, projecting 3067 final SNPs on 19 linkage groups (Fig 22 and Figure 2 individual 19 maps in appendix).

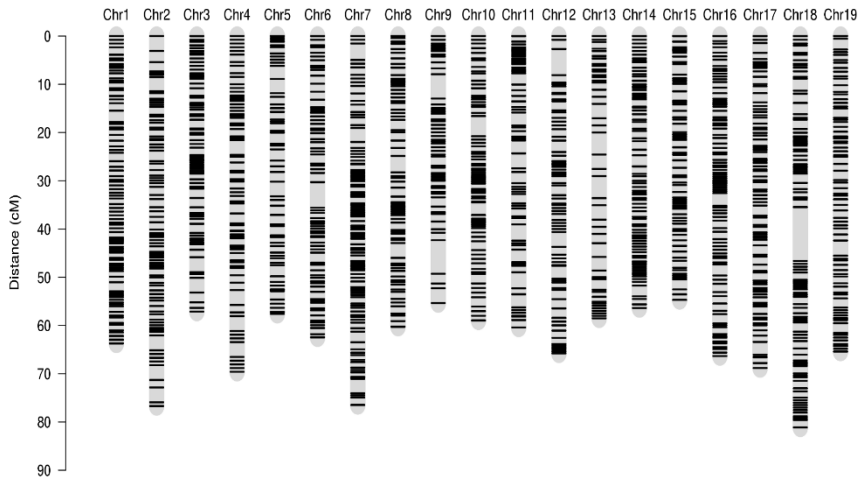

Figure 22: Final view of consensus map for 19 chromosomes.

The map had a total length of 1215.66 CM (Table 7-B) with an average number of 161 markers and 64 CM size for each linkage group. The Genome coverage, estimated by mapping the first and last marker on each chromosome to the PN40024 12X.v2 assembly and determining the percentage of the physical sequence covered by the mapped markers (Tello et al., 2019), was found as 90 % on average with 61.41 % as the lowest for chromosome no. 9 and 99 % as the highest for chromosome no. 14 against the reference genome assembly (Table 7-C). The genetic distances of the markers were derived from the genetic map developed for 19 chromosomes and physical distances are from version 12X.2 of the PN40024 reference genome. The analysis of progeny haplotypes gave an idea of the allelic contribution to the progeny individuals, from each parent (Fig 23-A). Similarly, the relationship between the genetic and physical maps for the nineteen chromosomes was derived through a collinearity plot (Fig 23-B).

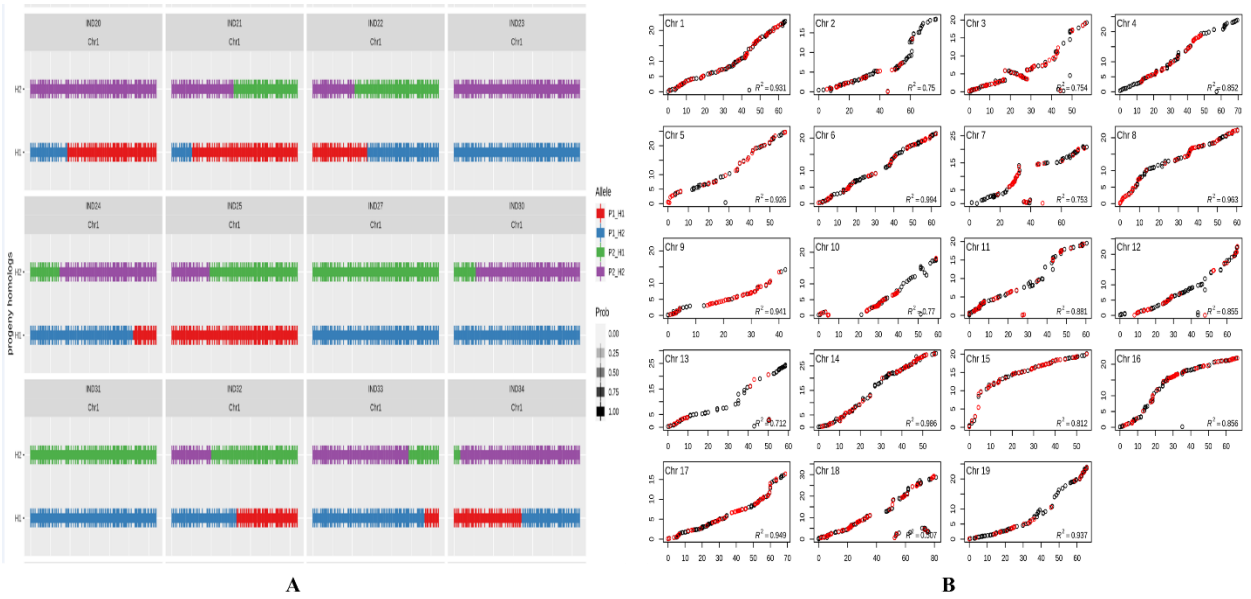

Figure 23: Progeny haplotype showing parental contribution in genetic structure (A) and collinearity plot showing relationship between the genetic and physical maps for the nineteen chromosomes (B).

3.6 QTL Analysis

Quantitative trait loci (QTL) analysis was performed to find the statistical correlation between phenotypic (phenology) and genetic (SNPs markers) data, collected over three years at 2 locations. The data was analyzed to identify the putative chromosomal regions involved in controlling phenology in segregating population of grapevine (*Vitis vinifera*). The genotypic data was used to build a consensus genetic map for the CP progeny derived by a CxS cross, aiming to harness the contribution from Corvina genetic structure, involved in phenology. Phenotypic data for 2 years from Negrar vineyard and for 3 years from Verona vineyard helped finding the reproducible results. Primarily, after loading the data in MapQTL-V5, the permutation tests (PT) were launched to find the LOD threshold, required to find the QTLs region's significance once found. For the subsequent QTL analysis, interval mapping (IM) method was used to find the genomic regions putatively associated with respective phenotypic traits.

3.6.1 Interval Mapping (IM)

The interval mapping was performed for 4 traits (budburst, flowering, veraison and ripening) from 3 different years (2020, 2021 and 2022) from Verona vineyard and for 2 years (2021 and 2022) from Negrar vineyard, thus making a total number of 10 input files, each for PT and IM. The three input files (*loc, map* and *qua*) were prepared according to the MapQTL file format requirements

(Materials and Methods). The phenology data was averaged between left and right replicates, from Verona vineyard for all three years.

The QTLs identified through IM for four phenology traits in successive years over two locations have been scored based on LOD threshold calculated by PT. For each scored QTL, level of significance peak, chromosome number, map position (cM), underlying marker, LOD score, percentage of variance and a range of confidence interval has been mentioned (Table 8-12). The criteria of reproducibility for any QTL includes its repetition in at least 2 years falling within the confidence interval.

The identified QTLs have been observed as QTLs found reproducible within each trait and QTLs found reproducible across the traits. The QTLs identified within the trait for budburst, include 12 QTLs scored on LGs 1, 4, 7, 9, 10 and 11 (4 QTLs on LG 9, 3 QTLs on LG 10, 2 QTLs on LG 7 and 1 QTL each for LG 1, 4 and 11), with maximum LOD peak scores of 8.23 and 7.17 on LG 9 with 37 % and 44.4 % of variance, from Negrar's vineyard-2021 and Verona's vineyard-22 respectively. The overall confidence interval for these 12 QTLs for budburst was ranging from 0.70 cM to 60.40 cM. The QTL with LOD 7.17 identified on LG 9, was fund at a position 12.95 cM position and QTL identified again on LG 9 with LOD 8.23 was found on 20.81 cM position of on chromosome. The reproducibility of QTLs was observed in case of LG 7 and 9 where ≥ 2 QTLs were detected. Moreover, no QTLs were identified from Verona's vineyard and Negrar's vineyard for the years 2020 and 2021 respectively (Table 8).

List of QTLs regions observed through IM for Budburst.

		Peak Position					Confidence Interval		Misc. Information	
Trait	Dataset	LG	Position (cM)	Marker	LOD Score	% Variance	LOD	Position (cM)	Flanking Markers	
Budburst	bbgoz20	-	-	-	-	-	-	-	-	-
	bbgoz21	9	12.95	9_30277635	7.17	44.4	5.68 -7.17- 4.34	7.9 - 14.182	9_2909561	9_3115478
		11	57.96	11_19350926	3.4	16.3	2.2 - 3.4 - 4.85	56.80 - 60.406	11_18848178	11_19559507
	bbgoz22	10	7.3	Un_31022123	4.42	21.8	3.7 - 4.42 - 3.23	0 - 12.34	10_157322	Un_31396095
		10	13.114	Un_30911496	4.31	21.3	3.23 - 4.31 - 3.22	12.72 - 14.27	Un_30664097	Un_25602155
		4	20.26	4_5758095*	3.57	18.8	2.5 - 3.57 - 2.25	16.56 - 24.66	4_5108722	4_7034738
		10	16.588	Un_25187741	3.33	16.8	3.7 - 3.33 - 1.78	0 - 20.76	10_157322	Un_7917520
		7	11.883	7_2241711	3.11	16.3	1.46 - 3.11 - 1.74	6.49 - 16.29	Un_7297439	7_2755478
		9	12.954	9_3027635	3.05	16.1	1.75 - 3.05 - 2.56	7.90 - 15.72	9_2909561	9_3650890
	bbriz22	9	17.25	9_3851520	8.23	37	5.57 - 8.23 - 5.02	14.18 - 21.49	9_3115478	9_4877122
		9	5.458	9_2430188	3.97	23.3	2.65 - 3.97 - 2.72	1.92 - 22.26	9_553031	9_4957537
		1	46.018	lb_1_14453117	3.08	15.9	2.06 - 3.08 - 2.01	39.84 - 59.49	1_10848183	1_21146880
		7	4.958	Un_7596383	4.04	20.5	3.84 - 4.04 - 2.08	0 - 6.49	Un_7444939	Un_7297439
	bbriz21	-	-	-	-	-	-	-	-	-

* = closest marker

Table 8: List of QTLs detected for Budburst from both vineyards from 2020 to 2022. The QTLs found reproducible are highlighted with red and blue colors.

Similarly, 12 QTLs putatively controlling flowering time, were identified on LGs 4, 7, 9, 10, 11 and 18, where 5 QTLs were found on LG 7, 2 QTLs each for LG 4 and LG 18 and 1 QTL each for LG 9, 10 and 11 were detected. The maximum LOD peak score i.e., 4.02, was found for the QTL on LG 7 positioning at 60.56 cM on chromosome with 18.6 % of variance, from Verona's vineyard for the year 2022. The overall confidence interval was observed as ranging 0.76 cM – 67.10 cM. Among the identified QTLs, the reproducibility was observed in case of LGs 7, 2 and 18. Furthermore, No QTLs for flowering trait were detected on any LG from Negrar's vineyard for the year 2021 (Table 9).

List of QTLs regions observed through IM for Flowering.

		Peak Position					Confidence Interval		Misc. Information	
Trait	Dataset	LG	Position (cM)	Marker	LOD Score	% Variance	LOD	Position (cM)	Flanking Markers	
Flowering	flgoz20	7	48.17	Un_27163990	3.18	16.5	1.66 - 3.18 - 2.12	41.62 - 52.04	Un_13514306	Un_11102886
		9	18.41	9_4142017	3.06	16	2.97 - 3.06 - 1.84	15.74 - 24.57	9_3666399	9_5608664
	flgoz21	7	29.29	Ib_7_8065852	3.87	20	2.59 - 3.87 - 2.56	19.05 - 32.37	7_3630235	7_11129686
		18	18.334	18_4080564*	3.33	18.8	1.75 - 3.33 - 2.22	13.87 - 26.59	18_3515072	18_7747093
		7	40.085	Un_6907125	3.25	17.1	1.97 - 3.25 - 2.02	16.84 - 47.40	7_3040069	Un_32014798
		4	7.693	4_2366119	3.03	18.4	1.01 - 3.03 - 1.88	6.15 - 14.14	4_1827376	4_4410575
	flgoz22	7	60.56	7_16208123	4.02	18.6	2.79 - 4.02 - 2.72	55.88 - 67.58	Un_12799741	be_7_18319099
		18	28.52	18_8441492	3.76	17.5	2.75 - 3.76 - 2.72	27.36 - 31.73	18_8036083	18_9650232
		10	3.47	Un_42927734	3.18	15	2.76 - 3.18 - 2.14	0 - 14.27	10_157322	Un_29987300
		7	46.634	Un_32009174	3.63	16.9	2.16 - 3.63 - 2.56	43.16 - 69.71	Un_12388826	7_18812031
	flriz22	11	11.22	11_4202072	3.1	18.2	2 - 3.1 - 1.53	3.46 - 27.40	11_1699474	11_74271
		4	26.207	4_7707960	2.96	17.5	1.79 - 2.96 - 1.63	21.58 - 32.37	4_6920786	4_10404817
	flriz21	-	-	-	-	-	-	-	-	-

* = closest marker

Table 9: List of QTLs detected for Flowering trait from both vineyards from 2020 to 2022. The QTLs found reproducible are highlighted with red color.

Likewise, for veraison trait, a total of 22 QTLs were identified on LG 1, 6, 9, 14, 16, 17 and 19 (4 QTLs each on LG 14, 16 and 17, 2 QTLs each on LG 1 and 6 and 1 QTLs each for LG 9 and 19). The maximum LOD peak score i.e., 11.44 was found for LG 16 positioning at 24.12 cM with 56.1 % variance from Negrar's vineyard in 2021. The overall confidence interval for this trait for all QTLs was 0.55 – 63.72 cM. Reproducible QTLs were detected on LGs 14, 16 and 17 (Table 10).

List of QTLs regions observed through IM for Veraison.

		Peak Position					Confidence Interval		Misc. Information	
Trait	Dataset	LG	Position (cM)	Marker	LOD Score	% Variance	LOD	Position (cM)	Flanking Markers	
Veraison	vergoz20	16	27.18	16_15483543	9.57	42.8	8.29 - 9.57 - 8.19	21.12 - 35.20	9_35881	16_165957
		16	14.61	16_6384402	6.48	31.5	5.32 - 6.48 - 5.03	9.53 - 37.47	16_2777528	16_17920465
		14	27.01	14_16792373	3.69	19.3	2.08 - 3.69 - 2.87	23.55 - 30.03	lb_14_11854632	bc_5_10489883
		16	4.199	16_974734	3.62	19	2.95 - 3.62 - 2.38	0 - 42.10	16_81198	16_18403941
		6	6.54	6_1881353	3.21	17.1	2.36 - 3.21 - 1.86	0 - 11.53	6_240015	6_3223205
	vergoz21	16	26.83	16_14948240	4.33	22.3	3.26 - 4.33 - 3.04	21.12 - 31.77	16_11988588	16_16713653
		14	27.018	lb_19_18379258	3.87	20.2	2.83 - 2.87 - 2.76	24.70 - 32.43	14_12840882	lb_17_15393076
		14	44.78	14_25735396	3.61	19	2.85 - 3.61 - 2.18	33.60 - 54.50	14_21441912	14_29637771
		1	59.87	1_21.503298	3.5	18.5	2.22 - 3.5 - 3.03	57.18 - 63.72	1_19975589	1_23000434
		19	4.9	19_669060	3.45	18.8	3.05 - 3.45 - 2.33	0 - 11.56	19_17827	19_1303294
	vergoz22	16	20.49	16_1149691	7.78	32.3	6.44 - 7.78 - 6.74	18.48 - 26.83	16_8343864	16_14904922
		9	19.953	9_4457964	3.87	17.6	2.6 - 3.87 - 2.2	15.33 - 23.80	9_3604022	9_5511405
		17	34.43	17_5817251	4.58	20.6	3.42 - 4.58 - 3.5	32.19 - 39.54	17_5136536	17_6896348
		16	37.479	16_17920465	3.65	16.8	2.58 - 3.65 - 2.39	9.53 - 42.10	16_2777528	16_18403941
		1	48.71	1_16694690	3.59	16.4	2.54 - 3.59 - 2.58	47.55 - 57.18	1_15889332	1_19975589
		16	10.693	16_3076923	3.53	16.2	2.07 - 3.53 - 2.39	3.44 - 42.1	16_866206	16_18403941
	verriz21	16	24.12	16_13056359	11.44	56.1	9.97 - 11.44 - 10.34	21.12 - 25.66	ae_13_17736241	16_14670631
		17	34.43	17_5817251	3.74	23.7	2.48 - 3.74 - 2.6	32.19 - 40.70	17_5136536	cn_17_7093829
		6	6.54	6_1881353	3.33	21.3	2.52 - 3.33 - 1.6	0 - 13.19	6_240015	6_3498314
	verriz22	17	50.68	17_8541983	3.99	23.7	2.68 - 3.99 - 2.9	47.38 - 59.92	17_8048717	17_13977638
		14	33.6	14_21441912	3.75	22.4	2.54 - 3.75 - 2.72	30.51 - 36.31	14_20025917	lb_14_22419624
		17	34.434	17_5817251	3.67	22.3	2.15 - 3.67 - 2.48	27.974 - 39.54	17_4462484	17_6896348

Table 10: List of QTLs detected for Veraison trait from both vineyards from 2020 to 2022. The QTLs found reproducible are highlighted with different colors.

Finally, the analysis of ripening trait revealed identification of 12 QTLs on CP population from both years. We detected 4 QTLs on LG 16, 2 QTLs on LG 6 and 1 QTL each for LGs 1, 7, 9, 11, 12 and 15. The maximum LOD threshold peak was observed as 6.18 in case of LG 16, positioning on 31.77 cM with a total variance of 34.6 %, from Verona's vineyard from 2020. The overall confidence interval was observed as 0.76 – 63.72 cM. The QTLs found on LGs 16 were attributed as reproducible QTLs. No QTL was detected from Negrar's vineyard for the year 2022 (Table 11). Interestingly 2 new QTLs at LGs 6 and 1 were also observed putatively controlling veraison time.

List of QTLs regions observed through IM for Ripening.

		Peak Position					Confidence Interval		Misc. Information	
Trait	Dataset	LG	Position (cM)	Marker	LOD Score	% Variance	LOD	Position (cM)	Flanking Markers	
Ripening	brixgoz20	16	31.77	16_16713653	6.18	34.6	4.98 - 6.18 - 4.41	23.20 - 36.71	18_2321518	16_17855245
		9	25.961	9_6203869 *	3.33	39.1	1.93 - 3.25 - 2.1	23.80 - 32.65	9_5511405	9_8876348
		16	6.83	16_1707323	3.22	19.8	3.22 - 1.92 - 2.21	0 - 42.1	16_81198	16_18403941
	brixgoz21	6	1.77	6_487780 *	4.67	24.5	4.58 - 4.67 - 3.26	0 - 5	6_240015	6_1190182
		16	35.2	16_165957	4.22	22.3	3.14 - 4.22 - 2.68	17.49 - 36.71	ae_16_7472812	16_17855245
		6	20.163	6_7078376	4.11	21.8	2.97 - 4.11 - 2.97	15.89 - 23.27	6_5045983	6_7891767
		7	42	Un_14236003	3.77	20.2	2.33 - 3.77 - 2.64	37.38 - 43.93	Un_33724725	Un_12454323
		12	24.8	12_3909546	3.54	19.1	2.43 - 3.54 - 2.26	17.73 - 32.99	12_2085828	12_6768979
		1	52.94	1_18083420	3.14	17.1	2 - 3.14 - 2.31	47.94 - 63.72	1_16444162	1_23000434
	Brixgoz22	11	48.96	11_17926031	3.62	16.1	2.46 - 3.62 - 2.58	39.04 - 58.86	11_13089931	Vvi_10353
		16	31.77	16_16713653	3.4	15.2	2.19 - 3.4 - 2.37	17.49 - 36.71	ae_16_7472812	16_17855245
		15	5.8	ae_15_19543571	3.25	14.6	2.88 - 3.25 - 1.88	0 - 16.85	15_100219	15_13445497
	Brixriz21	16	31.77	16_16713653	4.8	29.2	3.69 - 4.8 - 3.48	22.27 - 36.71	16_12052777	16_17855245
	brixriz22	-	-	-	-	-	-	-	-	-

Table 11: List of QTLs detected for Ripening trait from both vineyards from 2020 to 2022. The QTLs found reproducible are highlighted with white color.

3.7 Identification of Candidate Genes Through Gene Annotation

The genetic regions discovered through QTL analysis were, further explored to identify potential candidate genes putatively controlling phenological traits. The flaking markers of identified QTLs were used to locate the specific genomic regions to reveal their functions from grapevine genome assembly 12XV2 (Appendix Table 4). The left and right coordinates of flanking markers of each reproducible QTL within each trait were used to locate the genomic regions in the assembly scaffolds and underlying genes were extracted to explore their functions (Table 12). For budburst, a total number of 475 candidate genes were observed within the confidence interval (461 genes for LG 9 and 14 genes for LG 7). Similarly, a total of 1740 candidate genes were observed on a single LG i.e., 7. In case of veraison, since 5 reproducible QTLs were observed, therefore it harbors a huge number (4148) of candidate genes within the confidence interval of each QTL (494 genes for LG 1, 300 genes for LG 6, 1475 genes for LG 14, 1346 genes for LG 16 and 533 genes for LG 17). Furthermore, for ripening a set of 1346 candidate genes were observed on LG 16, similar to veraison thus resulting in altogether 6363 candidate genes for all four traits (Table 12).

The genes were then selected based on gene ontology (GO) to report their specific functions. Initially, for each phenological trait, a large number of genes were observed against each QTL however, the group of genes were then short listed based on their putative involvement in controlling the grapevine phenology related traits. The list of gene annotation was filtered through

Gene Ontology options viz., “plant development”, “signal transduction”, “transcription factors” and “response to stress signals”. The potential gene candidates identified for all reproducible QTLs through IM are listed below (Appendix Table 4). Most of the genes found for respective QTLs, were observed to be controlling functions like, plant growth and development, signal transduction and transcription factors for the focused phenology.

Table 12: List of reproducible QTLs detected for budburst, flowering, veraison and ripening with their potential candidate genes.

Phenotypic Trait	LG	No. of Candidate Genes
Budburst	9	461
	7	14
Flowering	7	1740
Veraison	1	494
	6	300
	14	1475
	16	1346
	17	533
Ripening	16	1346
Total		**6363**

4 DISCUSSION

The main goal of this study was to explore the grapevine genome to identify the genomic regions controlling the major phenological stages i.e., budburst, flowering, veraison and ripening. This is particularly important for the ripening because its anticipation related to the climate change has a negative impact on some berry quality traits. The ultimate goal is the production novel grapevine varieties adapted to the future climatic conditions. Quantitative Trait Locus (QTL) analysis approach of a segregating population (CP-F1) derived from a cross between a local variety "Corvina" and a divergent variety "Solaris", was conducted with Interval Mapping (IM). The mapping population propagated in three replicates (two adjacent replicates at one location i.e., Verona, and one replicate at another location, approximately 17 km distant apart, i.e., Negrar) was observed for three years and analyzed for phenology data for four main traits viz., the time of budburst, flowering, veraison and ripening. Since the mapping population propagated at Negrar's vineyard started producing measurable data after a year so both phenotypic and genotypic data from Negrar's vineyard were analyzed only for two years i.e., 2021 and 2022. Although some quality maturity-related traits (berry weight, pH, total acidity and sugar level) were also measured, they were not included in QTL analysis. A set of 150 individuals was evaluated for phenology whereas, 130 individuals were selected for genotypic evaluation (SNP genotyping) and QTL analysis with 6790 total SNPs including 4 SSRs. The construction of high density consensus genetic maps and linkage analysis provide important steps for map-based gene cloning and marker assisted breeding. An accurate estimation of recombination frequencies is the base for shaping the correct linkage maps in different segregating populations (Wu et al., 2002a; van Ooijen 2011, Zhang H. Li, and Wang 2015). The accuracy in genetic maps is highly dependent on correct genotyping as missing values and typing errors greatly affect the final resolution of genetic maps (Hackett and Broadfoot, 2003). An efficient estimation of recombination frequency by exploiting 12 bi-parental populations revealed that higher LOD score is achieved with relatively larger population size and smaller recombination frequency values (Sun et al., 2012).

The phenotypic evaluation of average budburst data indicates a normal trend in growth as highlighted by the distribution curve for all three years. Most of the plants fell in same range of Julian days with a clear anticipation in each successive year. The missing data for some of the plants in separately analyzed dataset for left and right side (2 replicates at Verona's vineyard) were however shown as averaged data. A similar growth pattern was observed in the second vineyard

(Negrar) where most of the plant genotypes exhibited normal distribution with maximum number of plants falling in 90-110 Julian days period over two successive years. The budburst exhibits a reproducible behavior in case of Verona's vineyard for all three years whereas, a slight unexpected opposite growth pattern was observed in Negrar's vineyard for the year 2022, where Solaris seemed to complete budbreak slightly after Corvina's budbreak time period. This might be due to the different climate in Negrar and Verona vineyards. A slight anticipation has been observed in budburst growth at both locations as compared to each passing year over a period of three years, which actually fits relevant to the main concern of this study (i.e., anticipation of phenology related to climate change). Similarly, in case of budburst, some progeny individuals showed transgressive behavior with some genotypes falling in a quite wider range as compared to majority of the genotypes and parents. Since, the both locations harbor slightly different environment, the effect of temperature might interfere with normal distribution of most of the genotypes. The correlation between budburst data for the year 2021 and 2022 from Negrar's vineyard and between both locations for the year 2021 was found to be relatively low as compared to other years and locations. Likewise, the averaged data collected for flowering time highlights a clear anticipation for all three years at both locations. The parental growth usually falls within the range where majority of the plants fall for the year 2020. In case of Negrar's vineyard, though both parents fall in a close range from each other however, they showed a normal growth behavior in both 2021 and 2022 year. Unexpectedly, flowering time exhibited a very early start in 2022 and this developmental stage was completed in less than 30 days. For this reason, the early flowering events remained unnoticed for many genotypes and only a few observations were made at both vineyards. This probably affected the correlation coefficient for flowering data between 2021 and 2022 especially from Negrar's vineyard, that was quite low. Similarly, the veraison time was measured at both vineyards and the analysis over three years of averaged data has expressed anticipated growth in the year 2022 as compared to 2021. However, in case of veraison's gradual appearance, the completion of this stage lasted for the longest time period as compared to any other phenology traits measured during this study over three years. It lasted for more than a month, which indicates its variability and underlying genetic mechanism involved in its control. The behavior of both parental lines is also normal as expected in both locations for most of the time except for the 2022 year from Negrar's vineyard where the completion stage of this trait seemed to be quite closer to each other in terms of Julian days. The vineyard from Negrar exhibited a very transgressive behavior for

several progeny individuals. The measurements of °Brix data has shown reproducibility over three years in both vintages. The majority of the genotypes reached the sugar accumulation level (19 °Brix) that was arbitrary decided as the ripening stage, in the range of 210-230 Julian days with parental's transgressive growth behavior particularly in Verona's vineyard as compared to Negrar's vineyard. Considering the ripening time of parentals, Solaris showed an early maturation falling between the end of July and the beginning of August at both vintages, while in Corvina the ripening time was much later than Solaris.

The behavior of progeny genotypes for ripening in Verona's vineyard, was in most cases falling in between parentals whereas in Negrar's vineyard the more cases of transgressive behavior were noted among progeny individuals. The level of correlation between both replicates at Verona's vineyard was quite high over different vintages, confirming the strong genetic control of this trait. Since the plants are still relatively young, the data show high variability, which is predicted to become more stable over next few years. In general, the plants expresses reproducibility in both vintages over different years with few exceptions in case of Negrar's vineyard in 2022, perhaps due to rapid environmental fluctuation. The overall correlation measured for the whole phenology seems reproducible over different years for all traits, however a relatively low correlation was observed for budburst and flowering for the year 2021 and 2022 from Negrar's vineyard. The variability in correlation between two vintages over different years is explained by the rapid rise in temperature which affected the late-winter/early spring growth period for both traits. The data of maturity time showed a reproducible normal distribution of the genotypes, where most of the genotypes in Negrar's vineyard reached an average berry weight 0.93 g and 0.66 g for 2021 and 2022 respectively whereas the progeny individuals showed a little higher transgressive behavior in Verona's vineyard. The ripening data measured in the field showed a wide interval for harvest time, when each genotype reached the level of 19 °Brix and the sugar measurements of sampled berries in the lab generally confirmed that the grapes in the field were harvested at the required level of sugar. This could be explained by the analysis of different berries from the same cluster used for the field measurement evidencing high variability in sugar accumulation in berries of the same cluster due to environmental influence, or a little delay in harvesting time. The graphical data indicates the homogeneous distribution of all four maturity-related traits (average berry weight, pH, total acidity and °Brix level in laboratory) except for some outliers for sugar level, pH and total acidity, from Negrar's vineyard only. Total acidity and sugar levels are controlled by different

genetic determinants that's why they show a little divergent pattern. The average pH values (distributed in the range 2.9-3.2) of progeny genotypes expresses a relatively different behavior as compared to parental lines, since some individuals showed transgressive pH levels in case of Negrar's vineyard for 2022 and for both years in Verona's vineyard. The observed variability both in phenology- and maturity-related traits highlights the fact that these cross genotypes are at their early stage of growth and they are more vulnerable when exposed to the rapid change in climate, requiring more time to get stable over future years. Such normal trends in phenology also highlights the strong genetic control of some traits, particularly the veraison, resulting less influenced by the environmental interaction. The transgressive growth pattern in phenology accounts for gene mapping of phenological traits, despite some divergent trends in both parental lines. The observed phenology data from this cross population propagated in two different climates provides insight about genotype and environment interaction (G x E) referring the different climatic characteristics. This effect of such interaction is visible in case of low correlation for budburst and flowering for 2021 and 2022 from both vineyards despite the higher correlation for other traits in the same years. The climate of Negrar's vineyard seems better suited for the cultivation and this would result in even better behavior (i.e., higher phenological stability) of the population if cultivation will be continued for further few years. Since missing data often creates biased results, therefore a deeper analysis is only possible when we have many years data from many different locations. For example in case of wheat, the authors used ~ 20 years data to locate stable QTLs (Arif et al., 2021, The plant journal). In addition, we need to look at the environmental data for deeper analysis to look for clues that caused significant variations (Table 4 B-D) in our phenotypes over the period of three years. In addition, each trait must be accompanied by environmental data. The significant differences in our data from both vineyards might highlight the differences in temperatures (during day and night), sunshine hours, sowing dates, rainfall, humidity levels etc. So inclusion of weather data might help us in analyzing the traits more deeply. Genomic regions harboring reproducible QTLs with significant LOD threshold value, within each trait in subsets from both vineyards have been observed in all four traits. In this study, budburst analysis resulted in two reproducible QTLs i.e., on LG 7 with 16.3 % variance, for both vineyards for the year 2022 and on LG 9 with 44.3 % variance from both vineyards for same both years, however no QTL was detected from either of the vineyards for 2020. Likewise both QTLs (LGs 7 and 9) were also observed in case of flowering and ripening.

Some of the identified QTLs have also been reported being involved in controlling phenology related traits, in previous studies, thus endorsing the reproducibility in our results. In case of flowering time a reproducible QTL identified on chromosome 7 with 16.9 % of variance has also been reported in the work of Duchene et al., 2012 and Grzeskowiak et al., 2013. Likewise QTLs for veraison time were identified on chromosomes 1, 6, 14, 16 and 17, which have already been described by Delfino et al., 2019, Zyprian et al., 2016, Duchene et al, 2012, Grzeskowiak et al., 2013 and Costantini et al., 2008 respectively. During this study 2 new QTLs for veraison time were also identified, a QTL on chromosome 1 with a LOD threshold of 3.59 and total variance of 16.4% in the region of 17085231 bp and 24196333 bp and another QTL for veraison time on chromosome 6 with LOD value of 3.33 and variance of 21.3 % in the region between 240015 bp and 3498314 bp.

In general, several QTLs were found reproducible both within each trait and across the traits however, some of them were not found to be reproducible with previous literature. This might be explained by the young age of these genotypes since the mapping population has been set and propagated just for few years. The stability in being reproducible might take few more years when the traits become more stable and consistent in growth. The presence of *Myb* gene family in several QTLs for veraison endorses the involvement of transcription factors (TFs) in controlling the veraison time. Gene ontology helps identification of potential candidate genes underlying the genomic regions harboring putative QTLs. The identified QTLs were annotated after anchoring to the grapevine genome assembly 12XV2 (https://urgi.versailles.inra.fr/Species/Vitis/Genome-Browser) through functional annotation V1 considering the Gene Ontology (GO) like developmental process, transcription factor activity and signal transduction. Functional annotation of budburst trait revealed various genes involved in developmental process of regulation of Phytochrome-associated protein 1 (PAP1) on chromosome 9 (VIT_09s0002g03410) and controlling FLK (flowering locus KH domain) on chromosome 7 (VIT_07s0141g00800). Interestingly Phytochrome-associated protein 1 (PAP1) belonging to AUX/IAA family members, has been reported to be involved in from early developmental stages of leaf to flower development stage in Arabidopsis (Klepikova et al., 2016; Kim et al., 2002). For budburst, other genes found in the region of QTL on chromosome 9, TIFY gene family (VvJAZ4) encoded by VIT_09s0002g00890, involved in response to hormonal stimulus, somehow linked with abscisic acid (ABA) and jasmonic acid (JA). Similarly, genes (VIT_09s0002g01330 and

VIT_09s0002g01340) encoding Auxin-binding protein ABP19, were also observed to be involved in potential control of budburst trait. Among transcription factors, identified in case of budburst trait, include genes (VIT_09s0002g01380 and VIT_09s0002g01400) encoding transcription factors like ATMYB66/WER/WER1 (WEREWOLF 1) and *myb* domain protein 7, potentially involved in controlling budburst. *Myb* protein family regulated by transcription factors involved in plant developmental process also in maturity related traits (Fasoli et al., 2012 and D'Incà et al., 2021). Despite these promising findings, a strong and reproducible evidence of candidate genes controlling budbreak is yet missing. The involvement of another gene VIT_09s0002g04460 has been found encoding Peroxidase 48 (Atperox P48) related to stress response, perhaps relevant to response against oxidative stress. The transcription factors MYR1 (MYB-related protein 1), *VvMYB5b*, MYB domain protein 83, *NAC* domain-containing protein (*VvNAC43*), *NAC* domain-containing protein 25 and another MYB family member (encoded by genes VIT_06s0004g00150, VIT_06s0004g00570, VIT_06s0004g02110, VIT_06s0004g02340, VIT_06s0004g02350 and VIT_06s0004g02460, respectively) involved in controlling veraison time have been identified on chromosome 6. The *VvMYB5b* transcription factor has been already reported to be involved in berry ripening process (Cavallini et al., 2015; Amato et al., 2019). Moreover the involvement of *VvMYB5b* in controlling grapevine early phenology has been reported (Deluc et al., 2006) together with its role in regulating flavonoid synthesis.

A member of *NAC* transcription factors family, *VviNAC60* has been reported to be involved in organ senescence and fruit ripening. It has also been involved in chlorophyll degradation and anthocyanin accumulation by upregulating STAY GREEN PROTEIN 1 (*VviSGR1*) and *VviMYBA1*, respectively (D'Inca et al., 2023). We identified *VvNAC43* and VvNAC05 on LG 14 and 17, respectively, whereas MYB domain protein 24 was also detected on LG 14 as previously found by Zyprian et al. (2016), Grzeskowiak et al. (2013) and Delfino et al. (2019). Likewise, other notable genes like VIT_01s0010g01420 (encoding auxin response factor 1), VIT_01s0146g00180 (encoding Auxin responsive SAUR protein), VIT_01s0146g00210 (response to hormone stimulus), VIT_01s0150g00440 (respiratory burst oxidase protein D) and VIT_01s0150g00450 (stress response) have been found on LG 1 when analyzed for veraison time. The TFs controlling genes encoding MADS-box proteins (putative MADS-box Fruitfull 1 (*VviFUL1*)) have been found on chromosome 17, whose putative function has been reported as master regulator in tomato fruit ripening. The MADX-box genes related FUL1 protein start

accumulating in ripening specific stage whereas FUL2 protein accumulate at pre ripening stage respectively, during tomato fruit development. However they express divergent role in transcriptional regulation (Yoko Shima et al., 2013). Likewise, another grapevine SEPALLATA 2 (*VviSEP2*) related MADS-box gene viz. *VvMADS39*, detected on chromosome 17, has been shown to be involved in regulation of ovule development and seedlessness in grape (Zhang et al., 2022). However, its down regulation stimulates histone H3 lysine 27 trimethylation restoring normal fruit development.

Moreover, co-action between *VvMADS39* and related proteins play a vital role in normal fruit and ovule development (Zhang et al., 2022). Genome wide analysis of TFs of MADS-box gene family and some of the newly identified members of MADS-box genes have been reported as regulating flower development not only in grapevine but also in other plant species. They have been involved in the development of male gametophytes (Grimplet et al., 2016). In case of ripening trait, several QTLs were identified on different chromosomes, however the reproducible QTLs were observed at chromosome 16 (Costantini et al. 2008), overlapping the genomic regions at 5 physical positions. The highest LOD value amongst these reproducible QTLs was observed as 6.18 with % variance of 34.6 in case of Verona's vineyard from the year 2020. The same QTL has been reported to be regulating resistance against downy mildew (Zyprian et al., 2016), which works together with a minor QTL on chromosome 18. Likewise, we also identified a QTL on chromosome 15 which is described in the work of Zyprian et al. (2016). Among the notable genes identifies for this trait, include, APETALA2/Ethylene-Responsive Factor (ERF/AP2), gene family (VvERF022) and "Dehydration Responsive Element-Binding Transcription Factor (*VvDREB23*)". AP2/ERF gene family is a plant specific TF, playing vital role which is reportedly involved in grapevine ripening process (Licausi et al., 2010), in development process, tolerance against biotic and abiotic factors, and responses to plant hormones (Licausi et al., 2013 and Guo et al., 2016). Other transcription factor activity identified in ripening trait includes genes (VIT_16s0050g01100) for Zinc finger (C2H2 type) family, involved in differential expression in grapevine flower development (Arrey-Salaset al., 2021).

In our results, approximately 35 genes have been identified under "secondary metabolic processes" annotation, encoding the stilbene synthase genes, which has been reported to be controlling basal immunity in grapevine, against downy mildew (Ciaffi et al., 2019). Stilbene synthase (STS) is involved in resveratrol biosynthesis. STS s are expressed in stress conditions. Functional genomics

data of STS gene revealed its correlation with WRKY TFs (*VviWRKY03*, *VviWRKY24*, *VviWRKY43* and *VviWRKY53*), both interacting at protein level with other homologs (Vannozzi et al., 2018). A constitutive transformation of stilbene synthase and resveratrol with grapevine pVst1 induced resistance against Phytophthora palmivora (Zhu et al., 2004). presence of these genes within a QTL confidence interval is probably a meaningless fortuity.

SNP genotyping tool (*Vitis*18KSNP chip) assay used in this study produced high-throughput genotyping results. A pool of 6786 SNPs were approved for the final genotyping after removal of distorted, failed and null-allelic SNPs. The *Vitis*18KSNP chip assay identifies SNPs from grapevine genome sequence based on certain criteria. The high percentage of reproducible results highlights a reasonable data size consisting of 130 individuals. Similarly, low error rate also endorses the selection of *Vitis*18KSNP chip assay since higher genotyping error rates have been observed in the results of other assays (Marrano et al. 2018). The authenticity of using *Vitis*18KSNP ChiP has been evident being used in studying genetic diversity and marker trait association in several species (Mercati et al., 2021). However, error rate in *Vitis*18KSNP chip are also observed on account of roughly 25 % genes inherited form other *Vitis* species (Le Paslier et al., 2013) thus resulting in failed SNPs as genotyping output. The number of SNPs gained after SNP genotyping were then projected over 19 chromosomes in order to build high density consensus genetic map with 130 genotypes. In recent past, high density resolution genetic maps built (Duchene et al., 2009, Marrao et al., 2018, Mamani et al., 2021 and Vervalle et al., 2022) by using *Vitis*18kSNP ChiP, have patronaged its application in current study. The types of molecular markers used in this study are same (SNPs) closer to the study proposed by Mamani et al. (2021), where both maps are consensus genetic maps and markers used belong to similar segregation types. This study support the successful application of *Vitis*18ksnp ChiP for the construction of high density resolution maps both for parental and consensus data.

Additionally, by restricting the confidence interval for each QTL and targeting only fewer genes might help us pointing the specific gene that is putatively involved in controlling the phenological traits, particularly phenotypic trait viz., veraison is controlled by many genes however refining the single QTL might end up at single desired gene. The restriction of the confidence intervals needs to be addressed in future in order to know how this developmental machinery works and this information could be used to modify the progression of grapevine whether to delay or anticipate the phenology. Similarly one may proceed to perform the composite interval mapping because

Interval Mapping is the basic form of QTL mapping. Composite interval mapping takes into account neighboring markers to define the QTL intervals. Moreover, collection of phenotypic data for few more years, use of different bioinformatic tools and new analysis of another population can help us in future, finding stable QTLs.

These finding emphasize the importance of tuning more than just phenology to understand the climate impact on viticulture in general. These results might lead the future research in grapevine improvement by addressing few key questions like:

- how does the molecular-level regulation of phenology vary among different grapevine cultivars or varieties?
- what are the key genes and molecular pathways involved in the regulation of grapevine phenology?
- how do environmental factors, such as temperature, light, and water availability, interact with molecular-level regulators to influence grapevine phenology?
- are there specific regulatory mechanisms or feedback loops that control the transition between different phenological stages in grapevines?
- can we manipulate or modulate the molecular-level regulation of grapevine phenology
- how can our understanding of the molecular regulation of grapevine phenology be translated into practical applications for viticulture, such as the development of new cultivars or management strategies to optimize production and mitigate the impact of climate change?.

5 CONCLUSIONS

The current research work is the part of a multi-year project, aimed at exploring the segregation pattern of grapevine phenological traits, under different climatic conditions, with an ultimate goal of creating new genetic resources in local region, potentially yielding high quality grape and wine production with reduced amount of phytosanitary treatments. Rapid change in global environment knocks at modern challenges to maintain the sustainable worldwide crop production. Improved adaptability of local grape cultivars to diverse climates is the potential strategy to introgress desired traits and to ensure distinctive performance of local cultivars.

Continuous high temperature is affecting grapevine phenology with gradual anticipation in development events every year. The annual anticipation in phenological events trigger ripening stage with advanced harvesting time despite of insufficient accumulation of flavor components of other secondary metabolites. Global rise in annual temperature also despair polyphenols and grape ‘s berry texture. This immature ripening results in higher sugar concentration and alcohol contents and ultimately poor wine quality. Grapevine has widely been exploited under breeding programs to ensure high yields and quality in cultivated grapevines region through studying its phenology and genetics under diverse climatic conditions.

A deep understanding of grapevine genetic architecture is required for better adaptation to the changing climate and for its consistent performance over the future years. Therefore, assessment of genetic basis of phenology and quality related traits is needed to be further explored. Harnessing intra-specific genetic architecture for wild alleles using high throughput genetic approaches would however help understanding its genetic mechanism thus making it improvable. The current study addresses similar approach, allowing dissection of local grapevine genetic resources, with the help of SNP genotyping assay i.e., *Vitis*18KSNP ChiP. Through a QTL analysis approach, a huge set of SNP markers were obtained by SNP ChiP hybridization assay helping construction of a high-resolution consensus genetic map and the identification of several genomic regions with the help of phenotypic data collected from two distant vineyards over three years from a biparental cross mapping population.

Our results highlight the analytic association between phenotypic and genotypic data however, a further exploration with extended years of propagation of the same population might help detection of unique genomic regions controlling diverse phenology, once the cross genotypes

become more stable in developmental events and tested under multiple-environments as the mapping population expressed high level of heterogeneity. Likewise, genotypic tools with higher resolution and refined mapping approaches (MQM mapping) would also help identification of candidate genes.

Finally, application of *Vitis*18KSNP assay not only helped identification of several QTLs harboring interesting candidate genes but also endorsed the previous reports which evidenced the phenology and maturity related QTLs on different chromosomes (Delfino et al., 2019, Zyprian et al., 2016, Duchene et al., 2012, Grzeskowiak et al., 2013 and Costantini et al., 2008 etc.). Concludingly, it can be postulated that the strategy used in the current research work highlights ingenious approach to dissect grapevine genetic architecture of quantitative traits to understand their complex inheritance.

6 REFERENCES

Arias LA, Berli F, Fontana A, Bottini R and Piccoli P. 2022. Climate Change Effects on Grapevine Physiology and Biochemistry: Benefits and Challenges of High Altitude as an Adaptation Strategy. Front. Plant Sci. 13:835425. doi: 10.3389/fpls.835425.

Arif MA, Shokat S, Plieske J, Ganal M, Lohwasser U, Chesnokov YV, Kocherina NV, Kulwal P, Kumar N, McGuire PE, Sorrells ME, Qualset CO and Borner A. 2021. A SNP-based genetic dissection of versatile traits in bread wheat (Triticum aestivum L.). The Plant Journal, (2021), 108, 960–976.

Arnold C, F. Gillet, J.M. Gobat. 1998. Situation de la vigne sauvage Vitis vinifera ssp. silvestris en Europe Vitis, 37 (4), pp. 159-170.

Arrey-Salas O, Caris-Maldonado JC, Hernández-Rojas B, Gonzalez E. 2021. Comprehensive Genome-Wide Exploration of C2H2 Zinc Finger Family in Grapevine (Vitis vinifera L.): Insights into the Roles in the Pollen Development Regulation. Genes (Basel). 20;12(2):302. doi: 10.3390/genes12020302. PMID: 33672655; PMCID: PMC7924211.

Barba P, Cadle-Davidson L, Harriman J, Glaubitz JC, Brooks S, Hyma K. 2014. Grapevine powdery mildew resistance and susceptibility loci identified on a high-resolution SNP map. Theor Appl Genet.127:73–84.

Begna T and Yesuf H. 2021. Genetic mapping in crop plants. Open journal of plant science. https://www.peertechzpublications.com.

Bernath S, Paulen O, Siska B, Kusa Z, Toth F. 2021. Influence of Climate Warming on Grapevine (Vitis vinifera L.) Phenology in Conditions of Central Europe (Slovakia). Plants, 10, 1020. https://doi.org/10.3390/ plants10051020.

Bigard A, Berhe DT, Maoddi E, Sire Y, Boursiquot JM, Ojeda H, Peros JP, Doligez A, Romieu C, Torregrosa L. Vitis vinifera L. 2018. Fruit Diversity to Breed Varieties Anticipating Climate Changes. Front Plant Sci.;9:455.

Blasi P, Blanc S, Wiedemann-Merdinoglu S, Prado E, Rühl EH, Mestre P and Merdinoglu D. 2011. Construction of a reference linkage map of Vitis amurensis and genetic mapping of Rpv8, a locus conferring resistance to grapevine downy mildew. Theor Appl Genet. 123:43–53 DOI 10.1007/s00122-011-1565-0.

Bocquet-Appel JP. 2011. When the world's population took off: the springboard of the Neolithic Demographic Transition. Science. 29;333(6042):560-1. doi: 10.1126/science.1208880. PMID: 21798934.

Brighenti A, Allebrandt R, Cipriani R, Malinovski L, de Bem, B, Feldberg N, Silva A. 2017. Using delayed winter pruning to prevent spring frost damage in ‘Chardonnay’ cultivar. Acta Hortic. 1157, 389–392. [CrossRef].

Cabre M F and Nunez M. 2020. Impacts of climate change on viticulture in Argentina. Reg. Environ. Chang. 20, 1–12. doi: 10.1007/s10113-020-01607-8.

Carbonell-Bejerano P, Diago MP, Martínez-Abaigar, J. 2014. Solar ultraviolet radiation I necessary to enhance grapevine fruit ripening transcriptional and phenolic responses.BMC Plant Biol 14, 183. https://doi.org/10.1186/1471-2229-14-183.

Cardell M F, Amengual A and Romero R. 2019. Future effects of climate change on the suitability of wine grape production across Europe. Reg. Environ. Chang. 19, 2299–2310. doi: 10.1007/s10113-019-01502-x.

Cavallini E, Matus JT, Finezzo L. 2015. The phenylpropanoid pathway is controlled at different branches by a set of R2R3-MYB C2 repressors in grapevine. Plant Physiol.,167(4):1448-1470. doi:10.1104/pp.114.256172.

Churchill GA, Doerge RW. 1994. Empirical threshold values for quantitative trait mapping. Genetics. Nov;138(3):963-71. doi: 10.1093/genetics/138.3.963. PMID: 7851788; PMCID: PMC1206241.

Ciaffi M, Paolacci A.R, Paolocci M. 2019. Transcriptional regulation of stilbene synthases in grapevine germplasm differentially susceptible to downy mildew. BMC Plant Biol 19, 404. https://doi.org/10.1186/s12870-019-2014-5.

Conde C, Silva P, Fontes N, Dias A, Tavares R, Sousa M, Agasse A, Delrot S, Gerós H. 2006. Biochemical Changes throughout Grape Berry Developmentand Fruit and Wine Quality. Food 1(1), 1-22, 2007 Global Science Books.

Coombe BG. 1987. Influence of temperature on composition and quality of grapes. Acta Horticulturae, 206, 23–36. https://doi.org/10.17660/ actahortic.1987.206.1.

Coombe BG. 1995. Growth Stages of the Grapevine: Adoption of a system for identifying grapevine growth stages. https://doi.org/10.1111/j.1755-0238.1995.tb00086.x.

Correa J, Mamani M, Munoz-Espinoza C, Laborie D, Muñoz C, Pinto M. 2014. Heritability and identification of QTLs and underlying candidate genes associated with the architecture of the grapevine cluster (Vitis vinifera L.). Theor Appl Genet.;127:1143–62. 35.

Costantini L, Battilana J, Lamaj F, Fanizza G, Grando M. 2008. Berry and phenology-related traits in grapevine (Vitis viniferaL.): From Quantitative Trait Loci to underlying genes. BMC Plant Biol.;8(1):38.

Crespan M, Migliaro D, Larger S, Pindo M, Palmisano M, Manni A, Manni E, Polidori E, Sbaffi F, Silvestri Q, Silvestroni O, Velasco R, Virgili S and Camilli G. 2021. Grapevine (Vitis vinifera L.) varietal assortment and evolution in the Marche region (central Italy). OENO One, 55(3), 17–37. https://doi.org/10.20870/oeno-one.2021.55.3.4628

D'Inca E, Foresti C, Orduna L, Amato A, Vandelle E, Santiago A, Botton A, Cazzaniga S, Bertini E, Pezzotti M, Giovannoni J, Vrebalov J, Matus JT, Tornielli GB and Zenoni S. 2023. The transcription factor VviNAC60 regulates senescence- and ripening-related 2 processes in grapevine. Article/doi/10.1093/plphys/kiad050/7013738 by guest. https://academic.oup.com/plphys/advance.

Delfino P, Zenoni S, Imanifard Z, Tornielli G B and Bellin D. 2019. Selection of candidate genes controlling veraison time in grapevine through integration of meta-QTL and transcriptomic data. BMC Genomics. 20:739.

Deluc L, Barrieu F, Marchive C, Lauvergeat V, Decendit A, Richard T, Carde JP, Merillon JM, Hamdi S. 2006. Characterization of a grapevine R2R3-MYB transcription factor that regulates the phenylpropanoid pathway. Plant Physiol 140: 499–511 Dixon RA, Lamb CJ, Masoud S, Sewal.

Deluc L, Bogs J, Walker AR, Ferrier T, Decendit A, Merillon JM, Robinson SP, Barrieu F. 2008. The transcription factor VvMYB5b contributes to the regulation of anthocyanin and proanthocyanidin biosynthesis in developing grape berries. Plant Physiol. Aug;147(4):2041-53. doi: 10.1104/pp.108.118919. Epub Jun 6. PMID: 18539781; PMCID: PMC2492604.

D'Incà E, Cazzaniga S, Foresti C, Vitulo N, Bertini E, Galli M, Gallavotti A, Pezzotti M, Battista Tornielli G, Zenoni S. 2021. VviNAC33 promotes organ de-greening and represses vegetative growth during the vegetative-to-mature phase transition in grapevine. New Phytol. Jul;231(2):726-746. doi: 10.1111/nph.17263. Epub Mar 16. PMID: 33567124; PMCID: PMC8251598.

Dinu DG, Ricciardi V, Demarco C, Zingarofalo G, De Lorenzis G, Buccolieri R, Cola G, Rustioni L. 2021. Climate Change Impacts on Plant Phenology: Grapevine (Vitis vinifera) Bud Break in Wintertime in Southern Italy. Foods, 10, 2769. https://doi.org/10.3390/foods10112769.

Doligez A, Bertrand Y, Farnos M, Grolier M, Romieu C, Esnault F, Dias S, Berger G, François P, Pons T, Ortigosa P, Roux C, Houel C, Laucou V, Bacilieri R, Peros JP and This P. 2013. New stable QTLs for berry weight do not colocalize with QTLs for seed traits in cultivated grapevine (Vitis vinifera L.). BMC Plant Biology, 13:217 http://www.biomedcentral.com/1471-2229/13/217.

Doligez A, Bertrand Y, Farnos M, Grolier M, Romieu C, Esnault F. 2013. New stable QTLs for berry weight do not colocalize with QTLs for seed traits in cultivated grapevine (Vitis vinifera L.). BMC Plant Biol.;13:217.

Duchene E, Butterlin G, Dumas V, Merdinoglu D. 2012. Towards the adaptation of grapevine varieties to climate change: QTLs and candidate genes for developmental stages. Theoretical and Applied Genetics 124: 623–635: 22052019.

Duchene E, Dumas V, Butterlin G, Jaegli N, Rustenholz C, Chauveau A, Berard A, Paslier MCL, Gaillard I. Merdinoglu D. 2020. Genetic variations of acidity in grape berries are controlled by the interplay between organic acids and potassium. Theoretical and Applied Genetics. 133:993–1008.

Duchene E, Huard F, Dumas V, Schneider C, Merdinoglu D. 2010 The challenge of adapting grapevine varieties to climate change. Clim Res.;41(3):193–204.

Dunn M, Rounsevell MD, Boberg F, Clarke E, Christensen J and Madsen MS. 2019. The future potential for wine production in Scotland under high-end climate change. Reg. Environ. Chang. 19, 723–732. doi: 10.1007/s10113-017-1240-3.

Fasoli M, et al 2012. The grapevine expression atlas reveals a deep transcriptome shift driving the entire plant into a maturation program. Plant Cell. 24(9):3489-3505. Plant Cell. 24(9):3489-3505. doi:10.1105/tpc.112.100230.

Fasoli M, Richter CL, Zenoni S, Bertini E, Vitulo N, Dal Santo S, Dokoozlian N, Pezzotti M, Tornielli GB. 2018. The timing and order of the molecular events that mark the onset of berry ripening in grapevine. Plant Physiology. Volume 178, Issue 3, Pages 1187–1206, https://doi.org/10.1104/pp.18.00559.

Fortes AM, Teixeira RT and Agudelo-Romero P. 2015. Complex Interplay of Hormonal Signals during Grape Berry Ripening. Molecules. Vol. 20: 9326-9343.

Fournier-Level A, Le Cunff L, Gomez C, Doligez A, Ageorges A, Roux C. 2009. Quantitative genetic bases of anthocyanin variation in grape (Vitis vinifera L. ssp. sativa) berry: a quantitative trait locus to quantitative trait nucleotide integrated study. Genetics;183:1127–39. 32.

Friend A, Trought M, Stushnoff C, Wells G. 2011. Effect of delaying budburst on shoot development and yield of Vitis vinifera L. Chardonnay 'Mendoza' after a spring freeze event. Aust. J. Grape Wine Res., 17, 378–382. CrossRef.

Fuller MP, Telli, G. 1999. An investigation of the frost hardiness of grapevine (Vitis vinfera L.) during bud break. Ann. Appl. Biol, 135, 135589–135595. (CrossRef) Genet. Res. 79: 85–96.

Galet P. 2000. Dictionnaire encyclopédique des cépages Hachette, Paris, 936 pp.

Gladstones J. 2011. Wine, Terroir and Climate Change. Adelaide, Australia: Wakefield Press.

Grzeskowiak L, Costantini L, Lorenzi S, Grando MS. 2013. Candidate loci for phenology and fruitfulness contributing to the phenotypic variability observed in grapevine. Theor Appl Genet.;126:2763–76.

Guo B, Wei Y, Xu R, Lin S, Luan H, Lv C. 2016. Genome-Wide Analysis of APETALA2/ Ethylene-Responsive Factor (AP2/ERF) Gene Family in Barley (Hordeum vulgare L.). PLoS ONE 11(9): e0161322. doi:10.1371/journal.pone.0161322.

Hackett CA, Broadfoot L. B. 2003. Effects of genotyping errors, missing values and segregation distortion in molecular marker data on the construction of linkage maps. Heredity 90: 33–38. 10.1038/sj.hdy.6800173.

He GQ, Huang XX, Pei PS, Jin HY, Cheng YZ, Wei T, Liu, Yu YH and Gu DL. 2022. Dissection of the Pearl of Csaba pedigree identifies key genomic segments related to early-ripening in grape. American Society of Plant Biologists.

Houel C, Chatbanyong R, Doligez A, Rienth M, Foria S, Luchaire N, Roux C, Adiveze A, Lopez G, Farnos M, Pellegrino A, This P, Romieu C and Torregrosa L. 2015. Identification of stable QTLs for vegetative and reproductive traits in the microvine (Vitis vinifera L.) using the 18 K Infinium chip. Houel et al. BMC Plant Biology. 15:205 DOI 10.1186/s12870-015-0588-0.

Huang YF, Doligez A, Fournier-Level A, Le Cunff L, Bertrand Y, Canaguier A. 2012. Dissecting genetic architecture of grape proanthocyanidin composition through quantitative trait locus mapping. BMC Plant Biol.;12:30.

Jackson R. S. 2014. Grapevine Structure and Function. In: Wine Science - Principles and Applications. Chapter 3, 4th edn. Elsevier Inc.

Jaillon O, Aury JM, Noel B, Policriti A, Clepet C, Casagrande A, Choisne N, Aubourg S, Vitulo N, Jubin C, Vezzi A, Legeai F, Hugueney P, Dasilva C, Horner D, Mica E, Jublot D, Poulain J, Bruyère C, Billault A, Segurens B, Gouyvenoux M, Ugarte E, Cattonaro F, Anthouard V, Vico V, Del Fabbro C, Alaux M, Di Gaspero G, Dumas V, Felice N, Paillard S, Juman I, Moroldo M, Scalabrin S, Canaguier A, Le Clainche I, Malacrida G, Durand E, Pesole G, Laucou V, Chatelet P, Merdinoglu D, Delledonne M, Pezzotti M, Lecharny A, Scarpelli C, Artiguenave F, Pè ME, Valle G, Morgante M, Caboche M, Adam-Blondon AF, Weissenbach J, Quétier F, Wincker P. 2007. French-Italian Public Consortium for Grapevine Genome Characterization. The grapevine genome sequence suggests ancestral hexaploidization in major angiosperm phyla. Nature. Sep 27;449(7161):463-7. doi: 10.1038/nature06148. Epub, Aug 26. PMID: 17721507.

Jones GV, Davis RE. 2000. Climate influences on grapevine phenology, grape composition, and wine production and quality for Bordeaux, France. Am J Enol Vitic.;51(3):249–61.

Jones VG, White MA, Cooper OR, Storchmann K. 2005. Climate change and global wine quality. Clim Chang.;73(3):319–43.

Kamal N, Ochßner I, Schwandner A, Viehover P, Hausmann L, Topfer R. 2019. Characterization of genes and alleles involved in the control of flowering time in grapevine. PLoS ONE 14(7): e0214703. pone.0214703.

Keller M. 2010. Managing grapevines to optimise fruit development in a challenging environment: A climate change primer for viticulturists. Australian Journal of Grape and Wine Research, 16(SUPPL. 1), 56–69. https://doi.org/10.1111/j.1755-0238.2009.00077.x.

Keller M. 2010. The Science of Grapevines: Anatomy and Physiology. Academic Press, Burlington, Massachusetts.
Kim DH, Kang JG, Yang SS, Chung KS, Song PS, Park CM. A phytochrome-associated protein phosphatase 2A modulates light signals in flowering time control in Arabidopsis. Plant Cell. Dec;14(12):3043-56. doi: 10.1105/tpc.005306. PMID: 12468726; PMCID: PMC151201.

Klepikova AV, Kasianov AS, Gerasimov ES, Logacheva MD, Penin AA. 2016. A high resolution map of the Arabidopsis thaliana developmental transcriptome based on RNA-seq profiling. Plant J. Dec;88(6):1058-1070. doi: 10.1111/tpj.13312. Epub Nov 19. PMID: 27549386.

Kuhn N, Guan L, Wu Dai Z., Wu B. H., Lauvergeat V., Gomès E., Li S. H., Godoy F., Arce-Johnson P. and Serge Delrot S.. 2014. Berry ripening: recently heard through the grapevine. Journal of Experimental Botany. Vol. 65 (16): 4543–4559.

Lewin CR. 2009. “The origin of agriculture and the first villagers”. Human Evolution: An Illustrated Introduction (5 ed.). Malden, Massachusetts: John Wiley & Sons. p. 250. ISBN 978-1-4051-5614-1.

Lewin HA. 2009. It's a bull's market. Science. 324:478–9. doi: 10.1126/science.1173880.

Licausi F, Giorgi FM, Zenoni S. et al. 2010. Genomic and transcriptomic analysis of the AP2/ERF superfamily in Vitis vinifera. BMC Genomics 11, 719. https://doi.org/10.1186/1471-2164-11-719.

Licausi F, Ohme-Takagi M and Perata P. 2013. APETALA2/Ethylene Responsive Factor (AP2/ERF) transcription factors: mediators of stress responses and developmental programs. New Phytol. 199, 639–649. doi: 10.1111/nph.12291.

Limier B, Sarah Ivorra, Laurent Bouby, Isabel Figueiral, Lucie Chabal, Manon Cabanis, Mohammed Ater, Thierry Lacombe, Jérôme Ros, Laurent Brémond, Jean-Frédéric Terral. 2018. Documenting the history of the grapevine and viticulture: A quantitative eco-anatomical perspective applied to modern and archaeological charcoal, Journal of Archaeological Science, Volume 100, Pages 45-61, ISSN 0305-4403, https://doi.org/10.1016/j.jas.10.001.

Lorenzo MN, Ramos AM and Brands S. 2016. Present and future climate conditions for winegrowing in Spain. Reg. Environ. Chang. 16, 617–627. doi: 10.1007/s10113-015-0883-1.

Margarido GR, Souza AP, Garcia AA. 2007. OneMap: software for genetic mapping in outcrossing species. Hereditas. Jul;144(3):78-9. doi: 10.1111/j.2007.0018-0661.02000.x. PMID: 17663699.

Marrano A, Micheletti D, Lorenzi S, Neale D, Grando MS. 2018. Genomic signatures of different adaptations to environmental stimuli between wild and cultivated Vitis vinifera L. Hortic Res. Jul 1;5:34. doi: 10.1038/s41438-018-0041-2. PMID: 29977570; PMCID: PMC6026492.

Massonnet M, Fasoli M, Tornielli G.B., Altieri M, Sandri M, Zuccolotto P, Paci P, Gardiman M, Zenoni S. and Pezzotti M. 2017. Ripening Transcriptomic Program in Red and White Grapevine Varieties Correlates with Berry Skin Anthocyanin Accumulation. Plant Physiology. Vol. 174: 2376–2396.

Mercati F, De Lorenzis G, Mauceri A, Zerbo M, Brancadoro L, D'Onofrio C, Morcia C, Barbagallo MG, Bignami C, Gardiman M, de Palma L, Ruffa P, Novello V, Crespan M and Sunseri F. 2021. Integrated Bayesian Approaches Shed Light on the Dissemination Routes of the Eurasian Grapevine Germplasm. Front. Plant Sci. 12:692661. doi: 10.3389/fpls.2021.692661.

Morales-Castilla, I., García de Cortázar-Atauri, I., Cook, B. I., Lacombe, T., Parker, A., van Leeuwen, C., Nicholas, K. A., & Wolkovich, E. M. 2020. Diversity buffers winegrowing regions from climate change losses. Proceedings of the National Academy of Sciences of the United States of America, 117(6), 2864– 2869. https://doi.org/10.1073/pnas.1906731117.

Mori K, Goto-Yamamoto N, Kitayama M, Hashizume K. 2007. Loss of anthocyanins in red-wine grape under high temperature. J Exp Bot.;58(8):1935–45.

Mosedale JR., Wilson RJ and Maclean IM. 2015. Climate change and crop exposure to adverse weather: changes to frost risk and grapevine flowering conditions. PLoS One 10:e0141218. doi: 10.1371/journal.pone.0141218.

Naulleau A, Gary C, Prevot L and Hossard L. 2021. Evaluating strategies for adaptation to climate change in grapevine production—a systematic review. Front. Plant Sci. 11:2154. doi: 10.3389/fpls.2020.607859.

Palumbo MC, Zenoni S, Fasoli M, Massonnet M, Farina L, Castiglione F, Pezzotti M, Paci P. 2014. Integrated network analysis identifies fight-club nodes as a class of hubs encompassing key putative switch genes that induce major transcriptome reprogramming during grapevine development. Plant Cell. 2014 Dec;26(12):4617-35. doi: 10.1105/tpc.114.133710. Epub 2014 Dec 9. PMID: 25490918; PMCID: PMC4311215.

Parker, A. K., García de Cortázar-Atauri, I., Gény, L., Spring, J.-L., Destrac, A., Schultz, H., Molitor, D., Lacombe, T., Graça, A., Monamy, C., Stoll, M., Storchi, P., Trought, M. C. T., Hofmann, R. W., & van Leeuwen, C. 2020. Temperature-based grapevine sugar ripeness modelling for a wide range of Vitis vinifera L. cultivars. Agricultural and Forest Meteorology, 285–286, 107902. https://doi. org/10.1016/J.AGRFORMET.2020.107902.

Paslier MC, Choisne N, Bacilieri R, Bounon R, Boursiquot J-MB, Brunel D, Di Gaspero G, Hausmann L, Lacombe T, Laucou V LA, Martinez-Zapater J, Morgante M, Raj P, PonnaiahM Q, Scalabrin S, Torres-Perez R. 2013. The

GrapeReSeq 18k Vitis genotyping chip. In: IX International Symposium on Grapevine Physiology and Biotechnology. International Society for Horticultural Science, Abstr. Book p. 123.

Pollard E, Rosenberg C and Robert T. 2015. Worlds together, worlds apart. Vol. 1 (concise ed.). New York: W.W. Norton & Company. p. 23. ISBN 978-0-393-25093-0.

Possamai T and Wiedemann-Merdinoglu S 2022. Phenotyping for QTL identification: A case study of resistance to Plasmopara viticola and Erysiphe necator in grapevine. Front. Plant Sci. 13:930954. doi: 10.3389/fpls.2022.930954

Reshef N, Karn A, Manns DC, Mansfield AK, Cadle-Davidson L, Reisch B and Sacks GL. 2022. Stable QTL for malate levels in ripe fruit and their transferability across Vitis species. Horticulture Research, 9: uhac009 https://doi.org/10.1093/hr/uhac009.

Rogiers SY, Greer DH, Liu Y, Baby T and Xiao Z. 2022. Impact of climate change on grape berry ripening: An assessment of adaptation strategies for the Australian vineyard. Front. Plant Sci. 13:1094633. doi: 10.3389/fpls.2022.1094633.

Sapkota S, Chen LL, Yang S, Hyma KE, Cadle Davidson L, Hwang CF. 2019. Construction of a high density linkage map and QTL detection of downy mildew resistance in Vitis aestivalis derived 'Norton'. Theoretical and Applied Genetics. 132:137–147 https://doi.org/10.1007/s00122-018-3203-6.

Schultz HR. and Hofmann M. 2016. The Ups and Downs of Environmental Impact on Grapevines: Future Challenges in Temperate Viticulture. Grapevine and Environmental Stress. eds. H. Géros, H. Medrano, S. Delrot and M. M. Chaves, (Chichester, UK: John Wiley & Sons Ltd.), 18–37.

Shima Y, Kitagawa M, Fujisawa M, Nakano T, Kato H, Kimbara J, Kasumi T, Ito Y. 2013. Tomato FRUITFULL homologues act in fruit ripening via forming MADS-box transcription factor complexes with RIN. Plant Mol Biol. Jul;82(4-5):427-38. doi: 10.1007/s11103-013-0071-y. Epub May 16. PMID: 23677393.

Signorelli S, Shaw J, Hermawaty D, Wang Z, Verboven P, Considine JA and Considine MJ. 2020. The initiation of bud burst in grapevine features dynamic regulation of the apoplastic pore size, Journal of Experimental Botany, Volume 71, Issue 2, 7, Pages 719–729, https://doi.org/10.1093/jxb/erz200

Stafne E. 2019. Stages of Grape Berry Development. Mississippi State University and Tim Martinson, Cornell University

Teslic N, Vujadinovic M, Ruml M, Ricci A, Vukovic A, Parpinello GP. 2019. Future climatic suitability of the Emilia-Romagna (Italy) region for grape production. Reg. Environ. Chang. 19, 599–614. doi: 10.1007/ s10113-018-1431-6.

This T. Lacombe, M.R. Thomas. 2006. Historical origins and genetic diversity of wine grapes. Trends Genet., 22, pp. 511-519.

Torres N, Martínez-Luscher J, Porte E, Yu R and Kurtural, SK. 2021. Impacts of leaf removal and shoot thinning on cumulative daily light intensity and thermal time and their cascading effects of grapevine (Vitis vinifera L.) berry and wine chemistry in warm climates. Food Chemistry, 343, 1284.

van Leeuwen C. van Destrac-Irvine A, Dubernet M, Duchene E, Gowdy M, Marguerit E, Pieri P, Parker A, de Resseguier L de and Ollat N. 2019. An Update on the Impact of Climate Change in Viticulture and Potential Adaptations. Agronomy, 9(9), 514. https:// doi.org/10.3390/agronomy9090514.

Van Ooigen J. W. 2004. MapQTL-5, Software for the mapping of quantitative trait loci in experimental populations. Kyazma B. V., Wageningen, Netherlands.

Van Ooijen J. W. 2011. Multipoint maximum likelihood mapping in a fullsib family of an outbreeding species. Genet. Res. 93: 343–349.

Vannozzi A, Dry I.B, Fasoli M. 2012. Genome-wide analysis of the grapevine stilbene synthase multigenic family: genomic organization and expression profiles upon biotic and abiotic stresses. BMC Plant Biol 12, 130. https://doi.org/10.1186/1471-2229-12-130

Vannozzi A, Wong DC, Höll J, Hmmam I, Matus JT, Bogs J, Ziegler T, Dry I, Barcaccia G, Lucchin M. 2018. Combinatorial Regulation of Stilbene Synthase Genes by WRKY and MYB Transcription Factors in Grapevine (Vitis vinifera L.), Plant and Cell Physiology, Volume 59, Issue 5, Pages 1043–1059, https://doi.org/10.1093/pcp/pcy045.

Venuti S, Copetti D, Foria S, Falginella L, Hoffmann S, Bellin D. 2013. Historical introgression of the downy mildew resistance gene Rpv12 from the Asian species Vitis amurensis into grapevine varieties. PLoS One.;8, e61228. 36.

Vezzulli S, Doligez A, Bellin D. 2019. Molecular Mapping of Grapevine Genes. In: Cantu, D., Walker, M. (eds) The Grape Genome. Compendium of Plant Genomes. Springer, Cham. https://doi.org/10.1007/978-3-030-18601-2_7.

Wu RL, Ma CX, Painter I and Z. B. Zeng. 2002. A Simultaneous maximum likelihood estimation of linkage and linkage phases in outcrossing species. Theor. Popul. Biol. 61: 349–363.

Wu RL, Ma CX, Wu SS and Zeng ZB, 2002b. Linkage mapping of sex-specific differences.

Zhang L, Li H and Wang J. 2015. Linkage Analysis and Map Construction in Genetic Populations of Clonal F1 and Double Cross. Genes I Genomics I Genetics, Volume 5.

Zhang S, Yao J, Wang L, Wu N, van Nocker S, Li Z, Gao M, Wang X. 2022. Role of grapevine SEPALLATA-related MADS-box gene VvMADS39 in flower and ovule development. Plant J. 111(6):1565-1579. doi: 10.1111/tpj.15907. Epub 2022 Jul 30. PMID: 35830211.

Zhu YJ, Agbayani R, Jackson MC, Tang CS, Moore PH. 2004. Expression of the grapevine stilbene synthase gene VST1 in papaya provides increased resistance against diseases caused by Phytophthora palmivora. Planta. 2004 Dec;220(2):241-50. doi: 10.1007/s00425-004-1343-1. Epub Aug 12. PMID: 15309535.

7 SUPPLEMENTARY DATA (Appendix)

Figure 1. Graphic representation of correlation for phenological data from both vineyards for 2022.

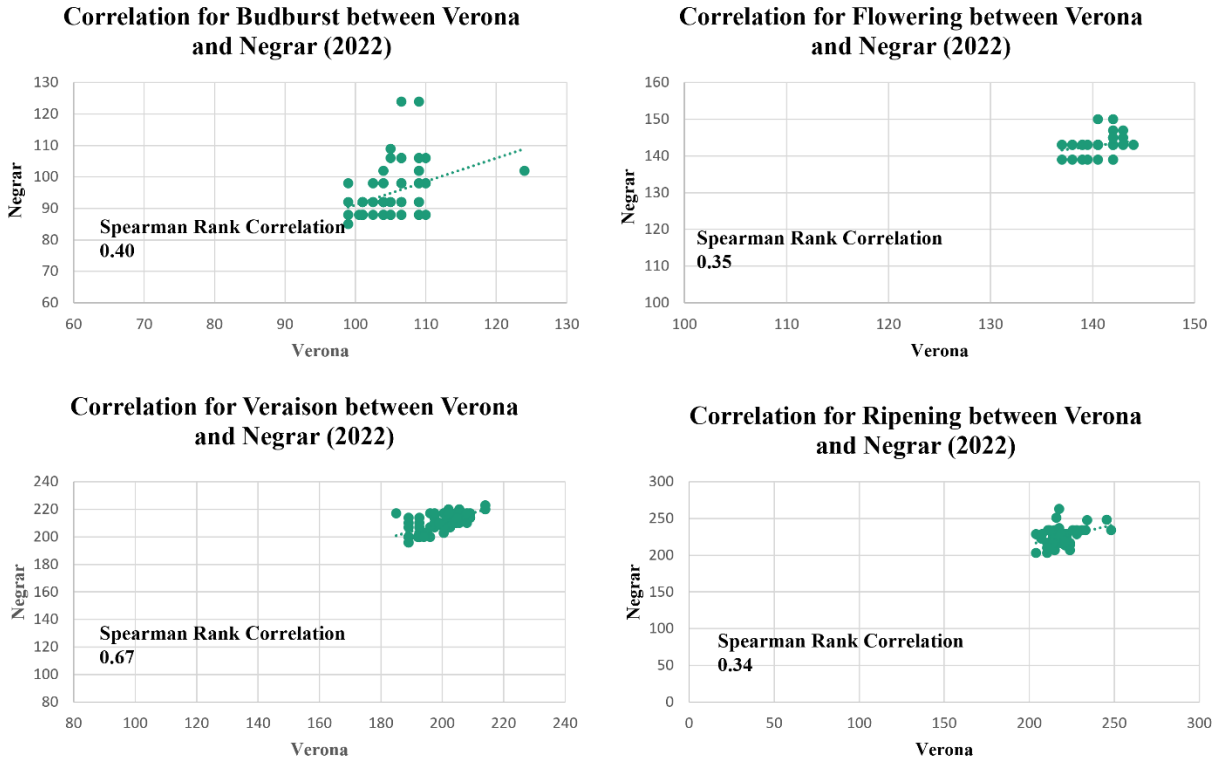

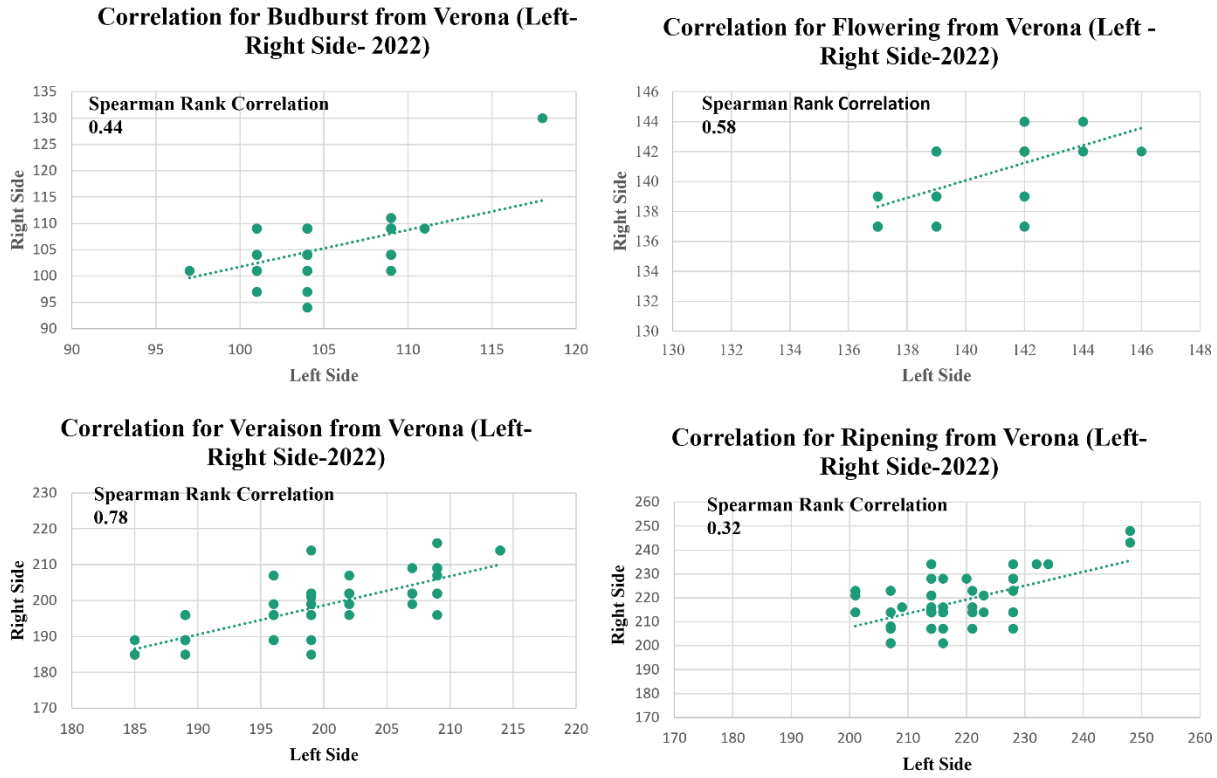

Figure 2. Genetic maps built through OneMap for all 19 chromosomes

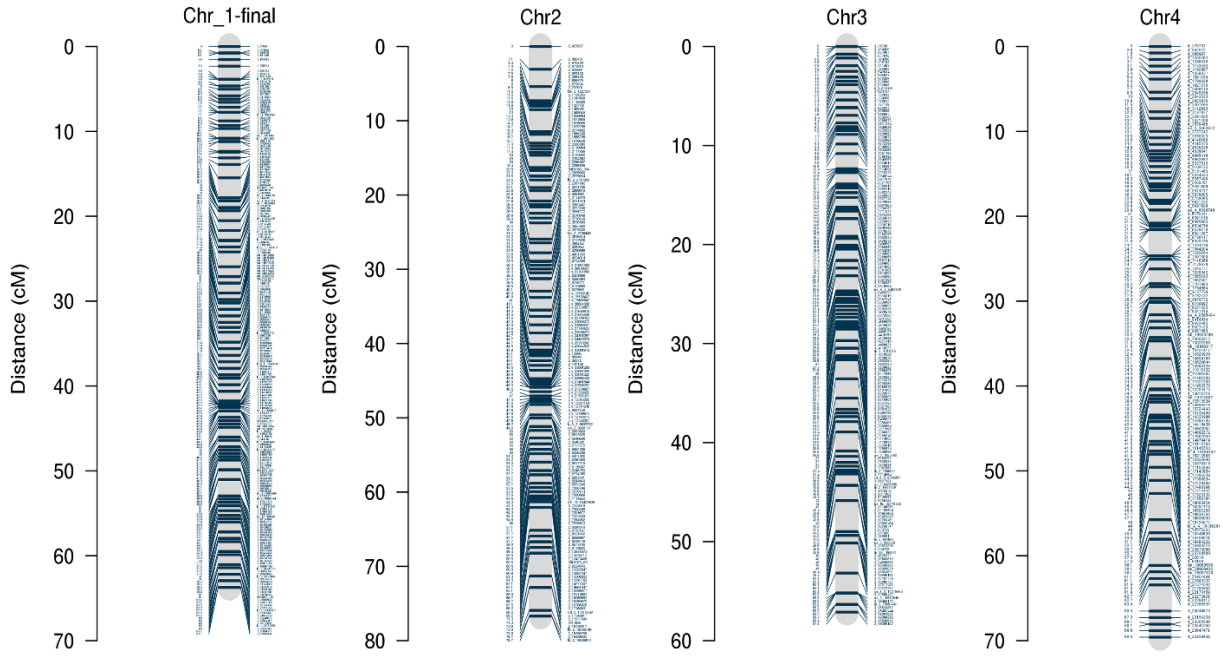

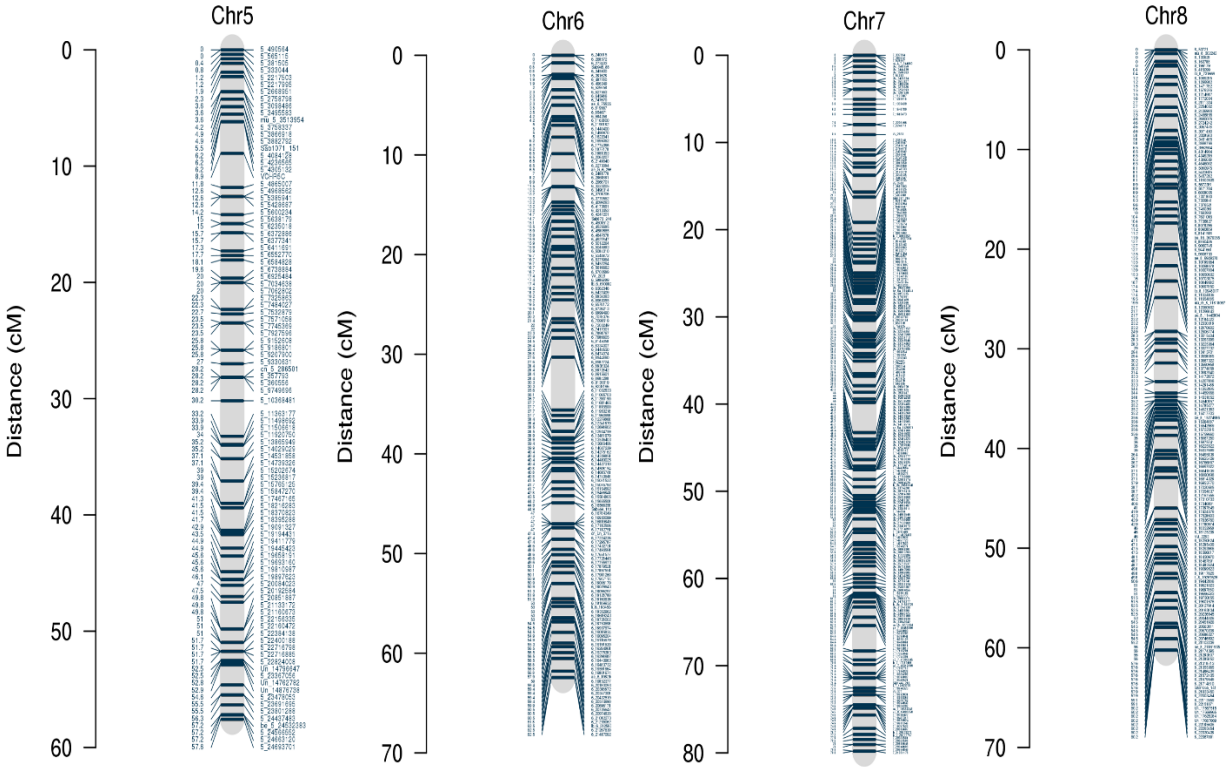
Chr5
Chr6
Chr7
Chr8
Distance (cM)
Distance (cM)
Distance (cM)
Distance (cM)

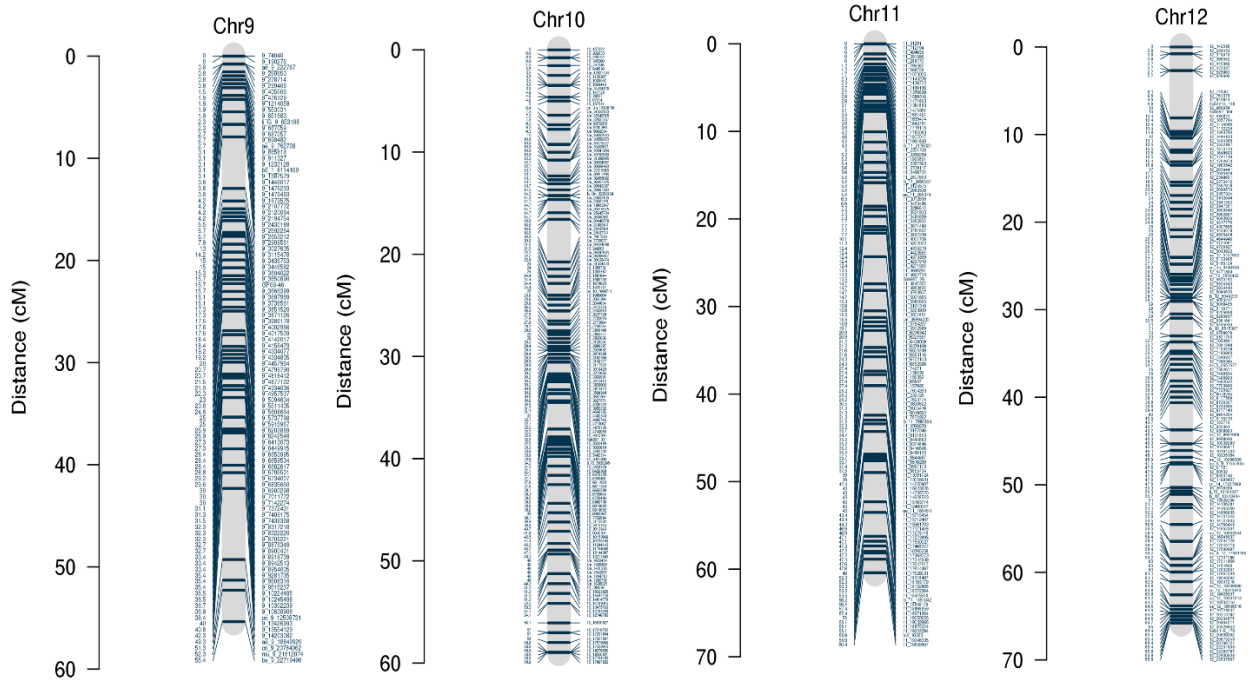
Chr9
Chr10
Chr11
Chr12
Distance (cM)

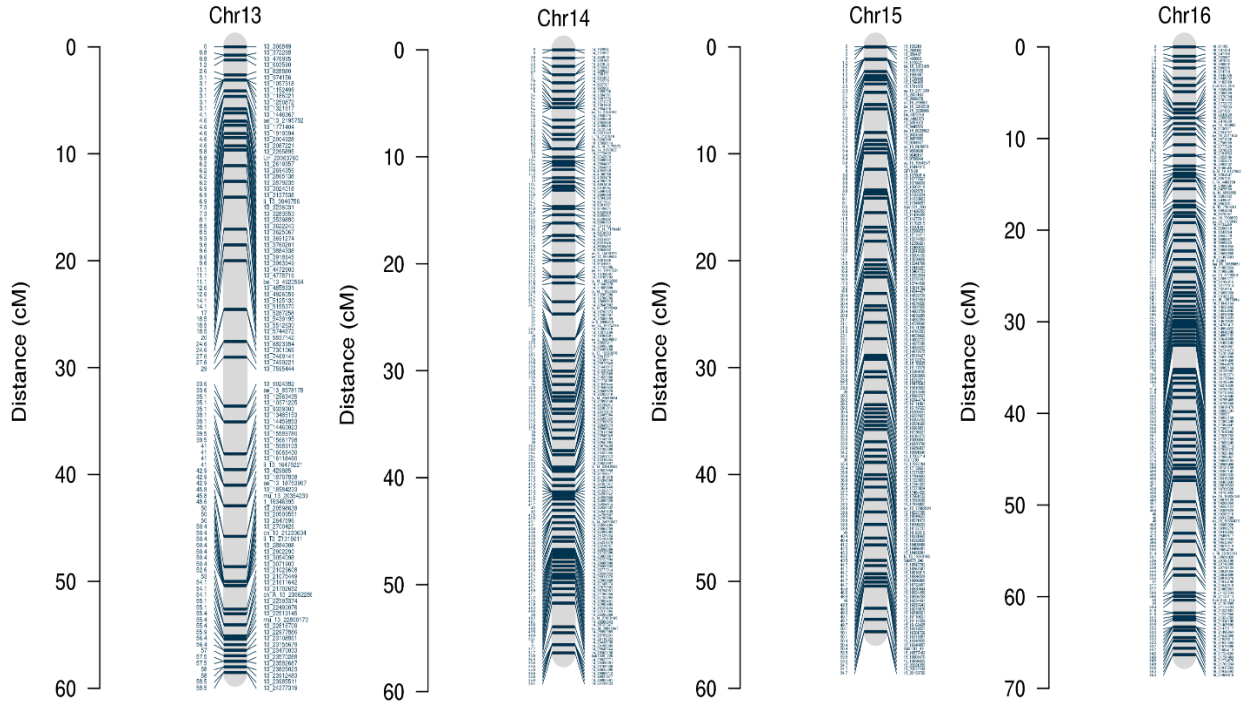
Chr13
Chr14
Chr15
Chr16
Distance (cM)

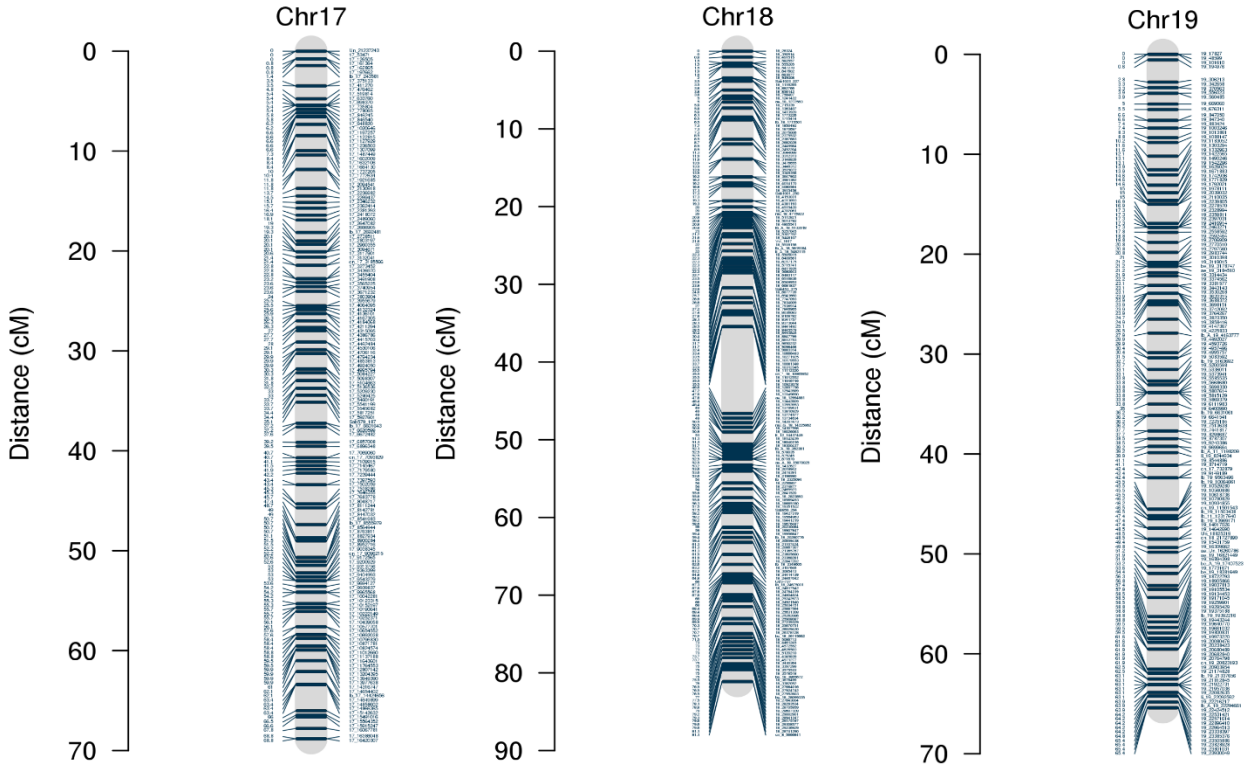
Chr17
Chr18
Chr19
Distance (cM)
0
10
20
30
40
50
60
70
80
90

Table 1. List of genotypes propagated at both vineyards with DNA quantifications used for SNY genotyping.

Plants	DNA(ng/µl)	A260/A280	A260/A230	Plants	DNA(ng/µl)	A260/A280	A260/A230
Corvina (C)	131.2	1.84	2.09	78	169.3	1.84	2.24
Corvina (C)	51.1	1.81	1.81	79	133.8	1.83	2.13
Solaris (S)	135.9	1.78	1.41	80	160.1	1.85	2.18
Solaris (S)	140.5	1.77	1.42	81	77.9	1.78	1.84
1	119.4	1.81	1.91	82	82.1	1.76	1.27
2	34.5	1.88	1.2	83	137.2	1.83	1.91
3	133.2	1.8	1.76	84	154	1.78	1.5
4	83	1.85	2.16	85	131.7	1.82	2.03
5	67.6	1.82	1.88	86	78.8	1.85	1.73
6	53	1.84	1.68	87	61.2	1.86	1
7	145.7	1.83	1.84	88	43.2	1.75	1.19
8	65.2	1.88	1.48	89	64.3	1.8	1.21
9	107	1.78	1.45	90	51.6	1.77	1.33
10	142.9	1.79	1.78	91	202.1	1.81	2.01
11	151.8	1.81	1.82	92	73.3	1.79	1.48
12	161.8	1.83	1.92	93	205.9	1.8	1.56
13	102	1.81	1.78	94	57.6	1.8	1.21
14	125.4	1.79	2	95	95.2	1.83	1.98
15	68.7	1.74	1.4	96	60.4	1.8	1.76
16	108.6	1.81	1.93	97	61.7	1.82	1.68
17	119	1.79	1.88	98	116.7	1.84	2.05
18	33	1.82	1.39	99	125.9	1.8	1.52
19	91.2	1.82	2.03	100	87.7	1.76	1.08
20	132	1.81	1.72	101	44.1	1.94	0.82
21	88.4	1.81	1.82	102	49.8	1.84	1.11
22	134.1	1.8	1.82	103	83.9	1.76	1.21
23	98.6	1.81	2.15	104	187.2	1.81	2.05
24	107.2	1.79	1.83	105	130	1.79	1.69
25	50.3	1.85	1.63	106	95	1.82	1.83
26	126.8	1.79	1.77	107	37.2	1.78	1.11
27	79.6	1.83	1.7	108	135.7	1.81	1.98
28	77.5	1.86	2.06	109	97.7	1.83	2.16
29	M	M	M	111	130	1.8	1.85
30	114.8	1.82	1.62	112	173.8	1.82	2.03
31	72.8	1.83	1.86	113	67.7	1.76	1.65
32	134	1.83	1.88	114	124.3	1.83	1.95
33	127.7	1.84	2.11	115	124.5	1.82	1.94

34	116.2	1.79	1.62	116	63.2	1.71	1.02
36	102.6	1.8	1.54	118	128.7	1.82	1.88
37	170.9	1.83	1.93	120	133.9	1.79	1.93
38	98.5	1.86	2.01	C	N	N	N
39	108.7	1.82	1.57	C	51.1	1.81	1.81
40	71.7	1.76	1.1	S			
41	151.1	1.81	1.72	S	140.5	1.77	1.42
42	105.9	1.82	2.08	132	137	1.8	171
43	128.6	1.82	1.94	133	184	1.83	2.04
44	82.3	1.78	1.37	134	199	1.82	1.95
45	63.9	1.78	1.37	135	109.2	1.82	1.94
46	70.5	1.78	1.18	136	207	1.85	2.09
47	194.2	1.82	1.9	137	423.7	1.84	2.02
48	M	M	M	138	41.5	1.88	1.98
49	103.3	1.79	1.71	139	91	1.87	1.61
50	110.4	1.84	1.81	140	87.2	1.83	1.57
51	69.4	1.81	1.94	141	351.9	1.85	2.21
52	49.6	1.81	1.48	142	71	1.87	1.74
53	111.4	1.77	1.62	143	92.3	1.83	1.68
54	67	1.91	1.12	144	221.3	1.87	2.07
55	93.1	1.8	1.8	148	66.3	1.85	1.66
56	36.5	1.7	0.89	153	72	1.87	1.9
58	30.3	1.74	1.01	154	128.2	1.86	1.74
59	43	1.8	1.33	157	203	1.86	2.12
60	57.7	1.79	1.49	159	86.9	1.86	1.75
61	47.7	1.81	1.18	160	132.2	1.85	1.89
62	57.3	1.74	1.1	161	70.2	1.92	2.07
63	43	1.75	1.26	164	58.9	1.84	1.82
64	58.8	1.79	1.23	165	31.8	1.76	1.52
65	63.6	1.73	1.28	168	63.5	1.79	1.51
66	47.6	1.76	1.21	169	97.9	1.75	1.65
67	60.8	1.77	1.82	171	58	1.76	1.69
68	123.9	1.82	1.86	172	98.8	1.72	1.45
69	33.7	1.69	1.04	178	151.6	1.81	1.83
70	67.9	1.74	1.34	180	54.9	1.84	1.51
71	98.6	1.83	1.55	181	83.6	1.76	1.47
72	84.8	1.85	2.19	182	29.2	1.84	1.33
73	123	1.82	1.9	183	80.8	1.83	1.92
74	M	M	M	189	77.8	1.84	1.84
75	84.1	1.84	2.12	190	61.1	1.83	1.72

76	74.7	1.78	1.4
77	54.2	1.82	1.45

Table 2. Layout of 96 well plate designed for SNP genotyping

	1	2	3	4	5	6	7	8	9	10	11	12
a	C-1 / 7.6	6 / 18.9	14 / 8	22 / 7.5	31 / 13.7	40 / 13.9	49 / 9.7	58 / 33	66 / 21	75 / 11.9	83 / 7.3	91 / 4.9
b	S-1 / 7.4	7 / 6.9	15 / 14.6	23 / 10.1	32 / 7.5	41 / 6.6	50 / 9.1	59 / 23.3	67 / 16.4	76 / 13.4	84 / 6.5	92 / 13.6
c	S-2 / 7.1	8 / 15.3	16 / 9.2	24 / 9.3	33 / 7.8	42 / 9.4	51 / 14.4	60 / 17.3	68 / 8.1	77 / 18.5	85 / 7.6	93 / 4.9
d	1 / 8.4	9 / 9.3	17 / 8.4	25 / 19.9	34 / 8.6	43 / 7.8	52 / 20.2	61 / 21	69 / 29.7	78 / 5.9	86 / 12.7	94 / 17.4
e	B / 29	10/ 7.0	18 / 30.3	26 /7.9	36 / 9.7	44 / 12.2	53 / 9	62 / 17.5	70 / 14.7	79 / 7.5	87 / 16.3	95 / 10.5
f	3 / 7.5	11 / 6.6	19 / 11	27 / 12.6	37 / 5.9	45 / 15.6	54 / 14.9	63 / 23.3	71 / 10.1	80 / 6.2	88 / 23.1	96 / 16.6
g	4/ 12.0	12 / 6.2	20 / 7.6	28 / 12.9	38 / 10.2	46 / 14.2	55 / 10.7	64 / 17	72 / 11.8	81 / 12.8	89 / 15.6	97 / 16.2
h	5 / 14.8	13 / 9.8	21 / 11.3	30 / 8.7	39 / 9.2	47 / 5.1	56 / 27.4	65 / 15.7	73 / 8.1	82 / 12.2	90 / 19.4	98 / 8.6

	1	2	3	4	5	6
a	99 / 7.9	107 /26.9	116 /15.8	137 /2.4	148 /15.1	165 /31.4
b	100 /11.4	108 /7.4	118 /7.8	138 /24.1	153 /13.9	168 /15.7
c	101 /22.7	109 /10.2	120 /7.5	139 /11	154 /7.8	169 /10.2
d	102 /20.1	111 /7.7	132 /7.3	140 /11.5	157 /4.9	171 /17.2
e	103 /11.9	112 /5.8	133 /5.4	141 /2.8	159 /11.5	182 /36
f	104 /5.3	113 /14.8	134 /5	142 /14.1	160 /7.6	183 /17.3
g	105 /7.7	114 /8	135 /9.2	143 /10.8	161 /14.2	189 /17.5
h	106 /10.5	115 /8	136 /4.8	144 /4.5	164 /17	190 /20

Table 3. Complete list of QTLs detected in all 4 phenological traits from both vineyards from 2020-2022.

Table: List of QTLs regions observed through IM for phenological data.

	Peak Position						Confidence Interval		Misc. Information			
Trait	Data set	LG	Position (cM)	Marker	LOD Score	% Variance	LOD	Position (cM)	Flanking Markers		Physical Positions of Fl. Markers (bp) for GO	
Budburst	bbgoz20	-	-	-	-	-	-	-	-	-	-	-
	bbgoz21	9	12.95	9_30277635	7.17	44.4	5.68 -7.17-4.34	7.9 - 14.182	9_2909561	9_3115478	2909561	3115478
		11	57.96	11_19350926	3.4	16.3	2.2 - 3.4 - 4.85	56.80 - 60.406	11_18848178	11_19559507	19148072	19859401
	bbgoz22	10	7.3	Un_31022123	4.42	21.8	3.7 - 4.42 - 3.23	0 - 12.34	10_157322	Un_31396095	157322	16797233
		10	13.114	Un_30911496	4.31	21.3	3.23 - 4.31 - 3.22	12.72 - 14.27	Un_30664097	Un_25602155	2686223	12235420
		4	20.26	4_5758095*	3.57	18.8	2.5 - 3.57 - 2.25	16.56 - 24.66	4_5108722	4_7034738	5108722	7034738
		10	16.588	Un_25187741	3.33	16.8	3.7 - 3.33 - 1.78	0 - 20.76	10_157322	Un_7917520	157322	3954375
		7	11.883	7_2241711	3.11	16.3	1.46 - 3.11 - 1.74	6.49 - 16.29	Un_7297439	7_2755478	1035927	3137454
		9	12.954	9_3027635	3.05	16.1	1.75 - 3.05 - 2.56	7.90 - 15.72	9_2909561	9_3650890	2909561	3650890
	bbriz22	9	17.25	9_3851520	8.23	37	5.57 - 8.23 - 5.02	14.18 - 21.49	9_3115478	9_4877122	3115478	4877122
		9	5.458	9_2430188	3.97	23.3	2.65 - 3.97 - 2.72	1.92 - 22.26	9_553031	9_4957537	553031	4957537
		1	46.018	lb_1_14453117	3.08	15.9	2.06 - 3.08 - 2.01	39.84 - 59.49	1_10848183	1_21146880	11241199	22342779
		7	4.958	Un_7596383	4.04	20.5	3.84 - 4.04 - 2.08	0 - 6.49	Un_7444939	Un_7297439	888427	1035927
	bbriz21	-	-	-	-	-	-	-	-	-	-	-
Flowering	flgoz20	7	48.17	Un_27163990	3.18	16.5	1.66 - 3.18 - 2.12	41.62 - 52.04	Un_13514306	Un_11102886	17612637	20104239
		9	18.41	9_4142017	3.06	16	2.97 - 3.06 - 1.84	15.74 - 24.57	9_3666399	9_5608664	3666399	5608664
	flgoz21	7	29.29	Ib 7 8065852	3.87	20	2.59 - 3.87 - 2.56	19.05 - 32.37	7_3630235	7 1112968 6	4012211	11511662
		18	18.334	18_4080564*	3.33	18.8	1.75 - 3.33 - 2.22	13.87 - 26.59	18_3515072	18_7747093	3515072	7747093
		7	40.085	Un 6907125	3.25	17.1	1.97 - 3.25 - 2.02	16.84 - 47.40	7_3040069	Un 32014798	3422045	18760284
		4	7.693	4_2366119	3.03	18.4	1.01 - 3.03 - 1.88	6.15 - 14.14	4_1827376	4_4410575	1827376	4410575
	flgoz22	7	60.56	7_16208123	4.02	18.6	2.79 - 4.02 - 2.72	55.88 - 67.58	Un_12799741	be_7_18319099	20674252	24648226
		18	28.52	18_8441492	3.76	17.5	2.75 - 3.76 - 2.72	27.36 - 31.73	18_8036083	18_9650232	8036083	9650232
		10	3.47	Un_42927734	3.18	15	2.76 - 3.18 - 2.14	0 - 14.27	10_157322	Un_29987300	157322	3080888
		7	46.634	Un_32009174	3.63	16.9	2.16 - 3.63 - 2.56	43.16 - 69.71	Un_12388826	7_18812031	17937394	25141158
		11	11.22	11_4202072	3.1	18.2	2 - 3.1 - 1.53	3.46 - 27.40	11_1699474	11_74271	1699474	7657591

	flriz 22	4	26.207	4_7707960	2.96	17.5	1.79 - 2.96 - 1.63	21.58 - 32.37	4_6920786	4_10404817	6920786	10551067
	flriz 21	-	-	-	-	-	-	-	-	-	-	-
Veraison	**verg oz20**	16	27.18	16_15483543	9.57	42.8	8.29 - 9.57 - 8.19	21.12 - 35.20	9_35881	16_165957	35881	165957
		16	14.61	16_6384402	6.48	31.5	5.32 - 6.48 - 5.03	9.53 - 37.47	16_2777528	16_17920465	2777528	19431415
		14	27.01	14_16792373	3.69	19.3	2.08 - 3.69 - 2.87	23.55 - 30.03	lb_14_11854632	be_5_10489883	11854632	10911620
		16	4.199	16_974734	3.62	19	2.95 - 3.62 - 2.38	0 - 42.10	16_81198	16_18403941	81198	19914891
		6	6.54	6_1881353	3.21	17.1	2.36 - 3.21 - 1.86	0 - 11.53	6_240015	6_3223205	240015	3223205
	verg oz21	16	26.83	16_14948240	4.33	22.3	3.26 - 4.33 - 3.04	21.12 - 31.77	16_11988588	16_16713653	13499538	18224603
		14	27.018	lb_19_18379258	3.87	20.2	2.83 - 2.87 - 2.76	24.70 - 32.43	14_12840882	lb_17_15393076	12840882	16354939
		14	44.78	14_25735396	3.61	19	2.85 - 3.61 - 2.18	33.60 - 54.50	14_21441912	14_29637771	21441912	29637771
		1	59.87	1_21.503298	3.5	18.5	2.22 - 3.5 - 3.03	57.18 - 63.72	1_19975589	1_23000434	21171488	24196333
		19	4.9	19_669060	3.45	18.8	3.05 - 3.45 - 2.33	0 - 11.56	19_17827	19_1303294	17827	1303294
	verg oz22	16	20.49	16_1149691	7.78	32.3	6.44 - 7.78 - 6.74	18.48 - 26.83	16_8343864	16_14904922	7991617	16415872
		9	19.953	9_4457964	3.87	17.6	2.6 - 3.87 - 2.2	15.33 - 23.80	9_3604022	9_5511405	3604022	5511405
		17	34.43	17_5817251	4.58	20.6	3.42 - 4.58 - 3.5	32.19 - 39.54	17_5136536	17_6896348	5268164	7027976
		16	37.479	16_17920465	3.65	16.8	2.58 - 3.65 - 2.39	9.53 - 42.10	16_2777528	16_18403941	2777528	19914891
		1	48.71	1_16694690	3.59	16.4	2.54 - 3.59 - 2.58	47.55 - 57.18	1_15889332	1_19975589	17085231	21171488
		16	10.693	16_3076923	3.53	16.2	2.07 - 3.53 - 2.39	3.44 - 42.1	16_866206	16_18403941	866206	19914891
	verri z21	16	24.12	16_13056359	11.44	56.1	9.97 - 11.44 - 10.34	21.12 - 25.66	ae_13_17736241	16_14670631	17846164	16181581
		17	34.43	17_5817251	3.74	23.7	2.48 - 3.74 - 2.6	32.19 - 40.70	17_5136536	cn_17_7093829	5268164	7225457
		6	6.54	6_1881353	3.33	21.3	2.52 - 3.33 - 1.6	0 - 13.19	6_240015	6_3498314	240015	3498314
	verri z22	17	50.68	17_8541983	3.99	23.7	2.68 - 3.99 - 2.9	47.38 - 59.92	17_8048717	17_13977638	8180345	14939501
		14	33.6	14_21441912	3.75	22.4	2.54 - 3.75 - 2.72	30.51 - 36.31	14_20025917	lb_14_22419624	20025917	22419624
		17	34.434	17_5817251	3.67	22.3	2.15 - 3.67 - 2.48	27.974 - 39.54	17_4462484	17_6896348	4594112	7027976
Ripening	**brix goz20**	16	31.77	16_16713653	6.18	34.6	4.98 - 6.18 - 4.41	23.20 - 36.71	18_2321518	16_17855245	20282405	19366195
		9	25.961	9_6203869*	3.33	39.1	1.93 - 3.25 - 2.1	23.80 - 32.65	9_5511405	9_8876348	5511405	8876348
		16	6.83	16_1707323	3.22	19.8	3.22 - 1.92 - 2.21	0 - 42.1	16_81198	16_18403941	81198	19914891
	brix goz21	6	1.77	6_487780*	4.67	24.5	4.58 - 4.67 - 3.26	0 - 5	6_240015	6_1190182	240015	1190182
		16	35.2	16_165957	4.22	22.3	3.14 - 4.22 - 2.68	17.49 - 36.71	ae_16_7472812	16_17855245	7120565	19366195
		6	20.163	6_7078376	4.11	21.8	2.97 - 4.11 - 2.97	15.89 - 23.27	6_5045983	6_7891767	5045983	7891767

		7	42	Un_14236003	3.77	20.2	2.33 - 3.77 - 2.64	37.38 - 43.93	Un_33724725	Un_12454323	18672497	18002891
		12	24.8	12_3909546	3.54	19.1	2.43 - 3.54 - 2.26	17.73 - 32.99	12_2085828	12_6768979	2085828	6768979
		1	52.94	1_18083420	3.14	17.1	2 - 3.14 - 2.31	47.94 - 63.72	1_16444162	1_23000434	17640061	24196333
	brix goz22	11	48.96	11_17926031	3.62	16.1	2.46 - 3.62 - 2.58	39.04 - 58.86	11_13089931	Vvi_10353	11481870	19690200
		16	31.77	16_16713653	3.4	15.2	2.19 - 3.4 - 2.37	17.49 - 36.71	ae_16_7472812	16_17855245	7120565	19366195
		15	5.8	ae_15_19543571	3.25	14.6	2.88 - 3.25 - 1.88	0 - 16.85	15_100219	15_13445497	100219	13445497
	brix riz21	16	31.77	16_16713653	4.8	29.2	3.69 - 4.8 - 3.48	22.27 - 36.71	16_12052777	16_17855245	13563727	19366195
	brix riz22	-	-	-	-	-	-	-	-	-	-	-

Table 4: List of reproducible QTLs detected for budburst, flowering, veraison and ripening from both vineyards from 2020 to 2022, in different colors.

Trait	Gene ID	Chr	Start Position (bp)	End Position (bp)	Functional Annotation	Gene Ontology (GO)
Budburst	VIT_09s0002g03410	9	3075730	3079091	Phytochrome-associated protein 1 (PAP1)	Developmental Process
	VIT_07s0141g00800	7	236157	254126	FLK (flowering locus KH domain)	Developmental Process
Flowering	VIT_07s0005g01730	7	4586079	4600718	flowering time control protein fca-like	Developmental Process
	VIT_07s0005g02510	7	5248913	5249812	phytochrome-interacting factor	Developmental Process
	VIT_07s0005g05100	7	9415521	9419944	transcription factor pif1-like	Developmental Process
	VIT_07s0005g05100	7	9415521	9419944	transcription factor pif1	Developmental Process
	VIT_07s0005g05100	7	9415521	9419944	transcription factor pif3	Developmental Process
	VIT_07s0031g01460	7	23877795	23878421	heading date 5	Transcription Factor Activity
Veraison	VIT_06s0004g00150	6	290507	291228	MYR1 (MYB-related protein 1)	Transcription Factor Activity

	VIT_06s0004g00570	6	744515	745967	VvMyb5b	Transcription Factor Activity
	VIT_06s0004g02110	6	2573382	2575343	myb domain protein 83	Transcription Factor Activity
	VIT_06s0004g02340	6	2766401	2773290	NAC domain-containing protein (VvNAC43)	Transcription Factor Activity
	VIT_06s0004g02350	6	2787445	2788412	NAC domain-containing protein 25	Transcription Factor Activity
	VIT_01s0010g01420	1	18619879	18620552	Auxin response factor 1	Response to Hormone Stimulus
	VIT_01s0146g00180	1	22986065	22987155	Auxin responsive SAUR protein	Response to Hormone Stimulus
	VIT_01s0146g00210	1	23042231	23042737	Auxin responsive SAUR protein	Response to Hormone Stimulus
	VIT_01s0150g00440	1	23994498	23998855	Respiratory burst oxidase protein D (RBOHD)	Response to Stress
	VIT_01s0150g00450	1	24010975	24015108	Respiratory burst oxidase protein D (RBOHD)	Response to Stress
	VIT_14s0108g00830	14	29512172	29513717	myb domain protein 94	Transcription Factor Activity
	VIT_17s0000g04990	17	5565646	5584353	putative MADS-box Fruitfull 1 (VviFUL1)	Transcription Factor Activity
	VIT_17s0000g04990	17	5565646	5584353	putative MADS-box Fruitfull 1 (VviFUL1)	Transcription Factor Activity
	VIT_17s0000g05000	17	5589362	5596096	putative MADS-box sepallata 2 (VviSEP2)	Transcription Factor Activity
	VIT_17s0000g05000	17	5589362	5596096	putative MADS-box sepallata 2 (VviSEP2)	Transcription Factor Activity
	VIT_17s0000g05020	17	5637669	5644801	Squamosa promoter-binding protein 6 (SPL6)	Transcription Factor Activity
	VIT_17s0000g05020	17	5637669	5644801	Squamosa promoter-binding protein 6 (SPL6)	Transcription Factor Activity

	VIT_17s0000g06400	17	7109000	7110825	NAC domain-containing protein (VvNAC05)	Transcription Factor Activity
	VIT_16s0100g00380	16	17324775	17325867	ERF/AP2 Gene Family (VvERF022),Dehydration Responsive Element-Binding Transcription Factor (VvDREB23)	Response to Hormone Stimulus
	VIT_16s0100g00390	16	17343424	17343918	Dehydration Responsive Element-Binding Transcription Factor (VvDREB24)	Response to Hormone Stimulus
	VIT_16s0100g00400	16	17348903	17349881	ERF/AP2 Gene Family (VvERF019),Dehydration Responsive Element-Binding Transcription Factor (VvDREB25)	Response to Hormone Stimulus
Ripening	VIT_16s0022g00690	16	13598310	13600451	NAC domain-containing protein (VvNAC22)	Transcription Factor Activity
	VIT_16s0100g00380	16	17324775	17325867	ERF/AP2 Gene Family (VvERF022),Dehydration Responsive Element-Binding Transcription Factor (VvDREB23)	Response to Hormone Stimulus
	VIT_16s0100g00390	16	17343424	17343918	Dehydration Responsive Element-Binding Transcription Factor (VvDREB24)	Response to Hormone Stimulus
	VIT_16s0100g00400	16	17348903	17349881	ERF/AP2 Gene Family (VvERF019),Dehydration Responsive Element-Binding Transcription Factor (VvDREB25)	Response to Hormone Stimulus

Table 5. List of maturity traits measured at Verona's vineyard (left replicate).

CxS Verona (Left)	Plant Status	Ave Berry Wt.	°Brix (Ave)	Total Acidity (TA)	pH (Ave)	Color	Cluster Shape
Corvina1	1	1.9265	19.05	7.227585598	3.11	2	compact
Corvina2	1	2.503333333	18.85	9.080744794	3.035	2	compact
Solaris1	1	1.3135	22.55	8.816007766	3.06	B	fragile
Solaris2	1	1.429166667	19.25	12.38995764	2.835	B	medium
1	dead						
4Bita	dead						
3	1	1.8865	20	10.66916696	3.085		compact
4	1	1.877333333	18.65	9.080744794	3.195	B	medium
5	1	2.350833333	18.7	10.31618426	2.93	B	compact
6	1	1.245666667	20.2	9.786710201	2.955	2	fragile

7	1	1.934333333	19.35	9.610218849	3.09	2	compact
8	dead						
9	1	2.014833333	18.7	8.110042358	3.08	B	medium
10	1						
11	dead						
12	1	1.980166667	18.85	5.639163431	3.165	B	compact
13	1	1.833833333	18.65	12.08109778	2.96	3	fragile
14	1						
15		2.165833333	18.8	4.227232616	3.44	B	compact
183	dead						
144	NG						
18	1	2.006666667	18.6	7.668813978	3.045	B	compact
134	SBS						
20	1	1.665333333	19.9	10.75741264	2.985	B	medium
21	1	1.457666667	19.4	9.257236145	3.075	B	fragile
22	1	2.012333333	19	8.28653371	3.105	1	fragile
23	1	1.699666667	18.7	9.433727497	3.13	2	compact
24	NG						
25	1	1.7345	20.3	11.37513237	3	2	medium
26	1						
27	1	1.542333333	19.1	13.71364278	2.87	2	medium
28	1						
164	NG						
189	1						
31	1	1.984833333	20.1	6.874602894	3.2	B	medium
32	1	1.2865	19.35	8.72776209	3.16	B	fragile
33	1	1.408	19.6	5.021443699	3.39	1	compact
34	1	2.0295	19.85	8.904253442	3.155	B	medium
36	1	1.904	19.1	11.28688669	2.905	2	fragile
37	1	2.096666667	18.7	7.227585598	3.065	B	compact
38	1	1.475666667	18.75	11.46337804	3.065	2	compact
39	1	1.927166667	19.8	7.668813978	3.1	2	medium
40	1	1.326	18.75	7.227585598	3.06	B	medium
41	1	1.042166667	19.35	8.904253442	2.975	B	fragile
42	1	1.640666667	18.85	10.84565831	2.91	1	compact
192	NG						
44	1	1.524	21.25	8.639516414	3.135	2	compact
45	1	1.3765	18.65	9.521973173	2.955	B	compact
192	NG						
47	1	1.613833333	19	9.521973173	3.09	B	medium
169	NG						
49	1	1.791166667	18.75	8.198288034	3.045	B	fragile
50	1	1.736833333	20.1	8.904253442	3.155	B	fragile
51	1	1.039833333	18.75	9.345481821	3.135	1	fragile
52	1	1.788666667	18.6	4.403723968	3.245	1	medium
53	1	1.889333333	19.1	9.874955877	3	2	compact
182	NG						
55	1	1.897	19	10.84565831	3.02	B	compact
56	1	1.6445	20.2	7.580568302	3.195	3	medium
58	1	1.6945	19.6	9.433727497	3.015	2	fragile
59	1	1.494666667	19.1	7.933551006	3.08	2	fragile
60	1	1.6745	19	8.904253442	3.02	B	medium
61	NG						
62	1	1.6395	21.75	9.345481821	18.085	B	medium
63	1	1.545333333	20.2	9.874955877	3.05	B	medium
64	1	1.655	18.55	6.96284857	3.2	3	medium
65	NG						
66	NG						

67	1	1.518666667	19.2	10.97802683	3.06	3	fragile
68	1						
69	1	1.572666667	18.75	11.19864102	3.045	1	medium
70	1	1.661333333	18.7	6.609865867	3.195	B	medium
71	1	1.263333333	19.05	9.168990469	3.01	2	medium
72	1						
73	NG						
169	NG						
141	SBS	1.938333333	18.6	9.168990469	2.965	3	fragile
76	1	1.759	19.35	6.786357218	3.255	2	fragile
77	NG						
78	1	1.8225	19.15	11.6398694	3.045	1	fragile
79	1	2.007166667	19.25	10.31618426	3.15	2	medium
80	1	1.592833333	19.3	9.168990469	3.135	2	fragile
81	1	1.4725	18.7	6.698111543	3.135	2	medium
82	1	1.702833333	20.6	10.49267561	2.99	2	fragile
83	NG						
84	1	1.5065	18.6	8.639516414	2.935	2	medium
85	1	1.426333333	19.95	7.051094246	3.22	3	compact
86	1	1.321333333	18.8	8.72776209	3.06	3	compact
87	1	1.648666667	18.75	7.051094246	3.16	3	medium
88	NG						
89	1	1.325	20.95	8.904253442	3.07	B	compact
90	1	1.622666667	18.7	9.521973173	3.16	2	medium
91	1	2.027	19.85	11.46337804	3.045	B	compact
92	1	1.109333333	19.3	9.345481821	3.08	B	compact
93	1	1.724166667	18.5	11.37513237	3.04	1	compact
94	NG						
95	1	1.871166667	21.85	8.816007766	3.075	2	fragile
96	1	1.425	18.65	9.080744794	3.095	B	medium
97	1	1.341	19.6	8.198288034	3.03	2	fragile
98	1	1.690333333	19.3	10.66916696	3.07	3	fragile
99	NG						
100	1	1.738666667	19.55	9.168990469	3.045	2	medium
101	1	2.124833333	18.9	5.992146135	3.23	2	medium
182	NG						
103	1	1.9215	20.15	7.757059654	3.135	B	medium
104	1	1.912	19.6	11.46337804	3.015	3	medium
105	1	2.146833333	18.85	6.345128839	3.145	B	compact
106	1						
107	1	1.349666667	20.85	11.28688669	2.995	B	compact
108	1	1.517666667	18.6	5.109689375	3.325	3	compact
109	1	1.460833333	20.4	10.13969291	3.02	3	medium
111	1	1.7435	19.55	8.198288034	3.15	3	medium
112	1	1.257333333	19.1	7.668813978	3.14	b	fragile
113	1	1.3435	18.8	6.168637487	3.21	2	compact
114	1	1.4315	20.9	8.639516414	3.02	1	compact
115	1						
116	NG						
118	NG						
120	1	1.916333333	19.95	11.19864102	2.915	2	medium
Corvina 3	dead						
183	NG						
Solaris 3	1	1.199	23.2	9.963201553	2.975	B	fragile
CxS ?	1						
164		1.476666667	18.95	5.286180727	3.285	B	fragile
159							
136							

CxS 139	xx	1.107666667	18.9	8.28653371	3	2	medium
CxS 168	xx	0.995833333	19	8.28653371	3.215	B	compact
CxS 143	xx	1.476666667	21.3	7.84530533	3.245	3	medium
CxS 182	xx	1.197833333	20.7	9.433727497	2.95	2	compact
CxS 133	xx	1.261666667	18.6	8.904253442	3.115	B	compact
CxS 190	NG						
CxS 148	xx	1.234666667	21.2	5.992146135	2.885	2	medium
CxS 138	xx	1.416833333	20.3	6.698111543	3.07	2	fragile
CxS 154	xx	1.221166667	19	9.257236145	3.015	B	compact
CxS 140	xx	1.039166667	21.4	6.698111543	3.165	2	fragile
CxS 142	xx	1.781833333	18.6	9.168990469	2.995	3	medium
CxS 153	xx	1.532333333	18.7	6.609865867	3.13	B	compact
CxS 4Bita	NG						

* NG = no grapes, NF = no flowers, SBS = small berry size

Table 6. List of maturity traits measured at Verona's vineyard (Right replicate).

CxS Verona (Right)	Plant Status	Ave Berry Wt.	°Brix (Ave)	Total Acidity (TA)	pH (Ave)	Color	Cluster Shape
Corvina1	1	2.716666667	18.65	6.96284857	3.17	2	compact
Corvina2	1	2.825	18.65	7.315831274	3.275	2	compact
Solaris1	1	1.244333333	22.5	12.16934345	2.905	B	fragile
Solaris2	dead						
1	1	1.74	22	9.963201553	2.975	B	medium
4Bita	NG						
3	dead						
4	1	2.152666667	18.4	10.22793858	2.93	B	compact
5	1	2.701	18.7	10.58092128	2.98	B	medium
6	1	1.007166667	19.95	9.874955877	2.89	3	fragile
7	1	1.644	18.55	6.786357218	3.175	1	compact
8	SBS						
9	1	1.908833333	19.9	10.58092128	3.035	B	medium
10	1						
11	NG						
12	1	1.9675	18.7	8.110042358	3	B	compact
13	1	1.603666667	18.9	8.816007766	3.17	3	compact
14	1						
15	1	2.353	18.75	6.874602894	3.345	B	compact
16	SBS						
17	SBS	1.362833333	18.55	7.933551006	3.095	B	fragile
18	1	2.629166667	19.75	8.72776209	3.165	B	compact
19	NG						
20	1	1.598666667	18.5	9.345481821	3.03	B	medium
21	1	1.8995	18.4	8.816007766	2.995	B	compact
22	1	1.6705	18.7	6.874602894	3.175	2	fragile
23	1	1.604333333	18.1	9.698464525	3.055	2	compact
24	NG						
141		1.9615	19.2	8.463025062	2.98	3	fragile
26	SBS						
27	1	1.3475	18.6	13.71364278	2.85	2	medium
28	1						
165	NG						
30	NG						
31	1	2.001	19.25	6.874602894	3.135	B	medium

32	1	1.197666667	18.6	9.168990469	3.025	B	medium
33	1	1.214	18.65	7.315831274	3.115	1	medium
34	1	1.850833333	19.2	10.58092128	3.015	B	fragile
36	1	1.7735	19.1	10.22793858	3.055	2	fragile
37	1	1.91	19.05	8.28653371	2.985	B	compact
38	1	1.798833333	20.15	6.609865867	3.25	3	medium
39	1	1.761	18.7	7.315831274	3.01	3	medium
40	1	1.261166667	21.6	6.256883163	3.18	B	fragile
41	1	1.208333333	20.1	7.933551006	2.96	B	fragile
42	1	1.57	20.4	6.521620191	3.07	2	medium
43	1	1.623333333	21	8.551270738	2.93	2	fragile
44	1	1.213333333	18.7	5.286180727	3.055	3	compact
45	1	1.381333333	18.6	10.31618426	2.955	B	compact
46	1	1.787833333	19.65	6.874602894	3.005	B	compact
47	1	1.661166667	20.95	6.874602894	3.21	B	medium
160	NG						
49	1	1.548166667	19.35	8.198288034	3.065	B	medium
50	1	1.748166667	20.8	8.110042358	3.06	B	medium
51	1	2.020833333	20	7.139339922	3.165	2	medium
52	1	1.559833333	19.75	5.550917755	3.33	2	medium
53	1	1.752166667	19.7	10.36030709	2.89	2	compact
54	1	1.3045	20	5.903900459	3.305	2	medium
55	1	1.9045	18.7	12.52232616	2.8	B	medium
56	1	1.190166667	18.4	11.86048359	2.815	2	fragile
58	1	1.898666667	18.8	7.757059654	3.035	3	fragile
59	1	1.232	18.8	8.551270738	3.095	2	compact
60	1	1.833	18.6	8.639516414	2.945	B	compact
61	NG						
62	1	1.4605	18.55	13.49302859	2.81	B	medium
63	1	1.380166667	18.55	11.72811507	2.87	B	fragile
64	1	1.733166667	18.4	6.874602894	3.1	3	compact
65	SBS	1.563833333	18.55	7.84530533	3.05	B	medium
66	SBS						
67	1	1.5695	19.95	8.749823509	3.08	3	medium
189	SBS						
69	SBS	1.162	18.6	12.08109778	2.925	2	fragile
70	1	1.543833333	18.7	8.28653371	2.95	B	fragile
71	1	1.189833333	20.9	9.257236145	2.975	3	compact
72	1						
165	SBS						
144	SBS						
75	1						
76	1	1.541	19.05	7.977673844	3.17	1	fragile
77	NG						
78	1	1.525833333	20.2	10.05144723	3.085	2	compact
79	1	1.963833333	18.55	8.639516414	3.045	2	medium
80	1	0.772833333	20.5	13.58127427	2.935	2	fragile
81	1	1.324333333	18.75	10.75741264	2.9	2	medium
82	1	1.7515	18.75	11.72811507	2.91	2	compact
83	NG						
84	1	1.568	19.1	9.874955877	3.02	2	medium
85	1	1.894833333	18.8	8.72776209	3.065	3	fragile
86	1	1.363166667	19.6	11.19864102	2.88	3	medium
87	1	1.519166667	18.65	6.698111543	3.155	3	medium
88	NG						
89	1	1.322166667	20.25	10.13969291	2.93	B	medium
90	1	1.369833333	19.6	8.110042358	3.385	3	fragile
91	1	1.409833333	20.15	11.19864102	2.98	B	medium

92	1	1.194166667	21.75	9.080744794	2.97	B	compact
93	NG						
94	SBS						
95	1	1.739333333	18.7	8.992499118	2.955	2	fragile
96	1	1.322	18.55	10.84565831	3.015	B	medium
97	1	1.508833333	19.15	14.02250265	2.86	3	fragile
98	1	1.620833333	19	11.6398694	2.875	3	fragile
99	NG						
100	1	1.878	18.9	9.521973173	2.925	3	medium
101	1	2.045666667	18.85	7.051094246	3.17	2	medium
102	SBS	1.471	20.15	6.609865867	3.075	B	fragile
103	1	2.089166667	18.75	9.433727497	3.015	B	medium
104	1	1.417666667	20	11.90460642	2.97	3	medium
105	1						
106	SBS						
107	1	1.290833333	21.5	11.28688669	3.035	B	compact
108	1	1.600833333	19.55	5.109689375	3.29	3	compact
109	1	1.156	20.45	10.31618426	2.88	3	medium
111	1	1.403333333	18.6	9.345481821	3.095	3	medium
112	SBS	1.140666667	19.2	6.168637487	3.27	B	compact
113	NG						
114	1	1.587166667	19.75	10.49267561	2.87	2	compact
115	1						
116	SBS						
118	NG						
135	NG						
Corvina 3	NG						
corvina 4	SBS	1.7965	19.3	6.874602894	3.16	3	medium
Solaris 3	1	1.217333333	23	9.830833039	2.595	B	fragile
Solaris 4	1	1.109666667	21.055	12.16934345	2.885	B	fragile
159							
136	NG						
CxS 139	NG						
CxS 168	xx	1.187333333	19.4	9.433727497	3.025	B	fragile
CxS 143	xx	1.406666667	19.3	8.639516414	3.2	3	medium
CxS 182	xx	1.267333333	20.35	9.521973173	2.965	3	compact
CxS 133	NG						
CxS 190	NG						
CxS 148	xx	1.376	21.1	5.286180727	3.47	1	compact
CxS 138	dead						
CxS 154	xx	1.272833333	20.45	7.492322626	3.145	B	compact
CxS 140	xx	1.025	20.8	8.639516414	3.075	2	fragile
CxS 142	xx	1.655	18.8	9.989675256	3.05	3	fragile
CxS 153	xx	1.4875	19.9	6.345128839	3.27	B	medium
CxS 160	NG						

* NG = no grapes, NF = no flowers, SBS = small berry size

Table 7. List of maturity traits measured at Negrar's vineyard.

CxS Negrar	Budburst Data	Flowering Data	Harvest Data (19°)	Ave Berry (30) Wt.	°Brix (Ave)	Total Acidity (TA)	pH (Ave)	Color	Cluster Shape
Corvina	2022/04/16	5/27/2022	9/5/2022	18.85	19.15	4.85	3.51	R3	fragile

Corvina	2022/04/12	5/25/2022	8/22/2022	16.5	20.15	5.75	3.32	R3	fragile
Corvina	2022/04/02	5/23/2022	8/17/2022	24.09	18.75	20.5	3.19	R3	medium
Corvina	2022/04/02	5/23/2022	8/17/2022	23.15	19.35	8.5	3.23	R3	medium
1	2022/04/12	5/23/2022	8/17/2022	30.675	21.55	9.8	3.35	w	fragile
4Bita	2022/05/04	NG							
3	2022/04/02	5/23/2022	8/11/2022	22.03	19.75	11.25	3.04	w3	fragile
4	2022/03/26	5/23/2022						w	fragile
5	2022/04/16	5/30/2022	8/17/2022	21.92	20.4	9	3.08	R1	medium
6	2022/04/02	5/23/2022	8/5/2022	20.075	19.95	11.45	2.96	R3	fragile
7	2022/04/02	5/23/2022	7/26/2022	22.6	18.4	12.5	3.095	R3	medium
8	2022/04/19	NG							
9	2022/04/02	5/23/2022	8/5/2022	22.6	19.5	11	3.085	w	compact
10	2022/04/02	NF							
11	Sprouted late	NG							
12	2022/04/12	5/25/2022	8/22/2022	33.4	19.05	9.25	3.11	w	medium
13	2022/04/02	5/23/2022	9/20/2022	13.8	18.5			R3	fragile
14	2022/03/29	NF							
15	2022/04/02	5/19/2022						W	medium
16	dead	dead							
17	2022/04/05	NG							
18	2022/04/02	5/23/2022	8/22/2022	28.6	18.85	5.15	3.285	w	compact
19	Sprouted late	NG							
20	2022/03/29	5/19/2022	8/2/2022	24	17.45	9	3.3	W	compact
21	2022/03/29	5/23/2022	8/5/2022	14.3	12.5	12.5	3.21	R3	fragile
22	2022/04/08	5/23/2022	8/2/2022	16.4	18.75	12.2	3.19	R3	fragile
23	2022/05/04	NG							
24	Sprouted late	NG							
25	2022/03/29	5/19/2022	8/2/2022	13.7	19.8	17.35	3.49	R3	fragile
26	2022/04/16	NF							
27	2022/04/02	5/27/2022	7/22/2022	26.95	19.8	13.25	2.94	R3	fragile
28	2022/04/02	NF							
29	NF	NF							
C(170322)	2022/04/23	NG							
31	2022/03/29	5/23/2022	7/26/2022	42.2	18.65	8	3.235	W	compact
32	2022/04/08	NG							
33	2022/03/29	5/23/2022	8/5/2022	16.15	18	11.25	3.16	R1	medium
34	2022/04/08	5/23/2022	8/22/2022	18.2	18.85	5.85	3.19	R3	medium
36	2022/04/16	5/23/2022	8/17/2022	24.75	21.9	8.9	3.19	R3	fragile
37	2022/04/02	5/23/2022	8/5/2022	18.73	18.25	9.75	3.065	w	compact
38	2022/03/29	5/19/2022	8/22/2022	19.8	20.6	9.25	3.345	R3	fragile
39	2022/04/16	NG							
40	2022/04/27	NG	8/17/2022	28.87	20.05	13.3	3	R2	medium
41	2022/04/08	5/23/2022	8/5/2022	11.125	20.05	17.75	2.88	w	fragile
42	2022/03/29	5/23/2022	7/29/2022	31.1	18.45	9.55	3.125	R2	medium
43	2022/04/16	5/25/2022	8/5/2022	22.65	21.3	11	3.025	R1	fragile
44	2022/04/08	5/23/2022	8/5/2022	19.1	18.5	8.07	3.18	R3	medium
45	dead	dead							
46	2022/03/29	5/23/2022	8/25/2022	12.3	19.1	6.45	2.94	w	medium
47	2022/04/02	5/23/2022	8/22/2022	19.15	17.65	8.75	3.085	w	fragile
48	2022/04/02	/	9/1/2022	14.05	18.9	7.25	3.06	R3	medium
49	2022/03/29	5/23/2022	8/25/2022	17.1	19.9	4.7	3.205	w	fragile
50	2022/03/29	5/23/2022	8/5/2022	16.48	18.75	16.25	2.965	w	fragile
51	2022/04/08	5/23/2022	8/17/2022	20.065	18.85	9.9	3.18	R2	medium

52	2022/04/16	5/23/2022	8/11/2022	29.845	19.85	7.5	3.185	w2	compact
53	2022/04/19	5/30/2022	NO GRAPES						
54	2022/04/02	5/19/2022	8/17/2022	11.8	18.25	17	3.08	R2	fragile
55	2022/04/02	5/23/2022	8/17/2022	23.7	18.15	14.8	2.97	R2	medium
56	2022/03/29	5/25/2022	8/22/2022	18.75	22.75	11.5	2.985	R3	fragile
58	2022/04/02	5/23/2022	9/8/2022	26.7	19	4.85	3.19	R3	fragile
59	2022/04/08	5/23/2022	8/17/2022	19.46	19.25	9.2	3.09	R3	fragile
60	2022/04/08	5/23/2022	7/29/2022	20.95	18	10.75	3.09	W	medium
61	Sprouted late	NG							
62	2022/04/08	5/23/2022	8/5/2022	12.49	20.2	17.25	2.885	w	fragile
63	2022/03/29	5/23/2022	8/5/2022	19.09	19	14	2.995	w	medium
64	2022/04/16	5/25/2022	8/2/2022	21	19.1	8.53	3.085	R3	medium
65	Sprouted late	NG							
66	Sprouted late	NG							
67	2022/03/29	5/23/2022	8/11/2022	18.365	18.7	8.5	3.015	w3	fragile
68	2022/04/12	NF							
69	2022/04/08	NG							
70	2022/04/02	5/23/2022	8/11/2022	26.11	18.75	8.725	3.025	w1	fragile
71	2022/03/29	5/23/2022	8/11/2022	18.85	18.35	8.3	3.13	w3	fragile
84	dead	dead							
93	2022/03/29	5/23/2022	NO GRAPES						
C(170 322)	dead	dead							
75	2022/04/02	NF							
76	2022/03/29	5/19/2022	8/2/2022	17.8	19.6	10.85	3.18	R3	fragile
77	2022/05/04	NG							
Solaris	2022/04/19	NG							
79	2022/04/02	5/23/2022	8/17/2022	35.83	19.25	6.5	3.37	R3	compact
80	2022/04/08	5/23/2022	8/17/2022	12.95	18.7	13.5	3.14	R3	fragile
81	2022/03/29	5/23/2022	8/5/2022	14.45	19.3	16.65	2.95	R3	fragile
82	2022/03/29	5/23/2022	8/2/2022	11.5	19.3	20.05	2.895	R3	fragile
83	2022/04/19	NG							
85	2022/04/02	5/19/2022	7/29/2022	12	17.3	16.1	2.88	R3	fragile
86	2022/04/08	5/25/2022	8/5/2022	9.84	18	22.6	2.84	R3	fragile
87	2022/04/12	5/23/2022	8/17/2022	20.7	20.55	10.2	3.11	R3	fragile
88	2022/05/04	NG							
89	2022/03/29	5/23/2022	8/5/2022	16	21.95	13.75	2.995	w	fragile
91	2022/04/02	5/23/2022	8/17/2022	15.7	18.9	12.4	3.15	w	medium
92	2022/04/02	5/23/2022	8/22/2022	13.1	18.5	6.75	3.08	w	medium
95	2022/03/29	5/19/2022						R3	medium
96	2022/04/02	5/23/2022	7/29/2022	12.3	18.35	17.5	2.86	W	fragile
97	2022/04/16	5/30/2022	NG						
98	2022/04/08	5/23/2022	8/5/2022	20.9	19.3	10	3.12		
100	2022/04/02	5/23/2022	8/17/2022	18.15	18.6	11.4	3.24	R3	medium
101	2022/04/02	5/25/2022	8/17/2022	17.27	18.9	9.4	3.2	R3	medium
103	2022/03/29	5/19/2022	8/22/2022	17.85	16.7	14.5	3.08	w	fragile
104	2022/04/02	5/23/2022	8/22/2022	16	19	17.25	2.995	R3	fragile
105	2022/05/04	NG							
106	2022/03/29	NF							
107	2022/03/29	5/23/2022	7/22/2022	15.9	18.8	15.5	3.005	W	fragile
108	2022/04/08	5/23/2022	8/22/2022	20.75	18.45	4.5	3.365	R3	medium
111	2022/04/02	5/23/2022	8/25/2022	13.2	18.65	4.75	3.28	R3	medium
113	2022/04/12	5/25/2022	8/5/2022	25.9	18.7	10.25	3.195	R3	fragile
114	2022/04/08	5/23/2022	8/17/2022	19.005	21.5	16.3	3.05	R3	fragile
118	Sprouted late	NG							

94	2022/04/19	NG							
Solaris	2022/04/19	NG							
112	2022/03/29	5/19/2022	7/22/2022	28.35	18.85	11.25	2.99	W	medium
116	2022/04/16	NG							

* NG = no grapes, NF = no flowers, SBS = small berry size